PHYSIOLOGICAL ROLES OF HIRANO BODIES

by

SANGDEUK HA

(Under the Direction of Marcus Fechheimer)

ABSTRACT

Hirano bodies are actin rich, rod-shaped, cytoplasmic, paracrystalline inclusions found predominantly in the central nervous system in association with a variety of conditions including aging and Alzheimer's disease. Since most studies of Hirano bodies have been performed in post-mortem samples from patients, the physiological role of Hirano bodies has not been investigated.

We have developed a cell culture model system for the formation of Hirano bodies in H4 neuroglioma cells using a modified form of a 34 kDa actin bundling protein from *Dictyostelium* named CT-GFP. Using this cell culture system, association of a C-terminal fragment of amyloid-β precursor protein (AICD) and adapter protein Fe65 with model Hirano bodies were investigated. Further, cells with Hirano bodies down-regulate both AICD-dependent caspase activation and cell death. Finally, cells with Hirano bodies show significantly reduced levels of AICD- and Fe65-dependent transcriptional activity. Therefore, association of AICD with Hirano bodies may impede its function in promoting apoptosis and modulating transcription. These results suggest that Hirano bodies may function as adaptive structures in Alzheimer's disease by limiting AICD-dependent neurotoxicity.

We generated a mouse model of Hirano bodies to examine the physiological effects and roles of Hirano bodies in the brain. We used Thy1 promoter to drive tissue specific expression of Cre recombinase to induce expression of the CT-GFP transgene that promotes formation of Hirano bodies in cell cultures. The expression of CT-GFP was detected and largely co-localized with F-actin in hippocampus beginning at P0. The mouse model of Hirano bodies showed paracrystalline F-actin and eosinophilic rod-like structure. These inclusions were first detected in the hippocampus in 6 month $R26CT^{+/+};Cre^{+}$ mice. The number, density, and morphology of neurons in the hippocampus appeared normal. Studies of long term potentiation in hippocampal slice cultures revealed only minor (not significant) differences in synaptic plasticity between Hirano body and littermate control mice, consistent with the interpretation that Hirano bodies are not toxic or deleterious to neuronal function. These mice will be extremely valuable tools for future studies of the physiological function of Hirano bodies in vivo in normal mice, during aging, and in mouse models of diseases including Alzheimer's disease.

INDEX WORDS: Hirano bodies, F-actin, a C-terminal fragment of amyloid-β precursor protein, Fe65, Alzheimer's Disease, apoptosis, transcriptional activity, Cre/loxP recombination system, Mouse model.

PHYSIOLOGICAL ROLES OF HIRANO BODIES

by

SANGDEUK HA

B.S., Hankuk University of Foreign Studies, Rep. of Korea, 1996

M.S., Hankuk University of Foreign Studies, Rep. of Korea, 1998

A Dissertation Submitted to the Graduate Faculty of The University of Georgia in Partial Fulfillment of the Requirements for the Degree

DOCTOR OF PHILOSOPHY

ATHENS, GEORGIA

2008

PHYSIOLOGICAL ROLES OF HIRANO BODIES

by

SANGDEUK HA

Major Professor:	Marcus Fechheimer
Committee:	Charles Keith James Lauderdale Nancy Manley

Electronic Version Approved:

Maureen Grasso
Dean of the Graduate School
The University of Georgia
August 2008

DEDICATION

First of all, my dissertation is dedicated to my family in Korea . Without their encouragement and support, it would be impossible for me to make achievements. My deep gratitude goes to my parents specially. I would not be able to become a scientist without their endless support and love.

Especially, I would like to dedicate my dissertation to my wife Jiha Kim. She always supports and takes care of me around 10 years at the same fields look like friend and adviser. Without her endless love and support, I can not believe I can make the achievement in my doctoral study.

ACKNOWLEDGEMENTS

I would like to give my deep gratitude to my advisor Dr. Marcus Fechheimer for five years of guidance and support. He was always open for any questions and encouraged me in any trouble I might have. Without his support and advice, I would not be able to achieve all these experiences through my graduate study years. I also should thank to Dr. Ruth Furukawa for always there for me and taking care of our lab.

I also would like to address my deep appreciation to my committee members, Dr. Nancy Menley, Dr. Charles Keith, and Dr. James Lauderdale who have been challenging but also supporting me through entire academic training. They helped me to have open mind on my project and were always willing to share all the equipments. Many thanks for Dr. John Shields for teaching and helping me with EM experiments. Without his help, I would have not been able to achieve such results.

I shouldn't forget my wonderful lab mate Paul Griffin. He has always been there for me to support and cheer me up. Also thanks to all the members of Fechheimer Lab. They made my graduate student life an enjoyable experience. I am grateful to all my wonderful friends for supporting me. They have contributed to my study in a very special way.

Of course, my special and heart-felt gratitude goes to Jiha Kim, my wife and colleague. She always gave me strength and endless support through all these years. She was always there for me not only in joyful moment but also hard time. It has been and will be a beautiful journey with her. For the last but not the least, my heart full of love goes to my little angel David. He gave me strength to finish my last journey in graduate school and to go on my life.

TABLE OF CONTENTS

Page

LIST OF TABLES

Page

LIST OF FIGURES

Page

Chapter 1

Introduction and Literature Review

1. Overview of Neurodegenerative disease

Neurodegenerative disease results from dramatic loss of neurons of the brain and spinal cord over time which leads to dysfunction and disabilities of controlling movements, processing sensory information and making decisions. These are characterized by the accumulation of intracellular or extracellular protein aggregation and inclusion body formation in neurons (Maccioni et al., 2001; Muchowski and Wacker, 2005). Among neurodegenerative diseases, Alzheimer's disease, Parkinson's disease, amyotrophic lateral sclerosis, and Huntington's disease are the most common and largely known ones, althought several other related neurological and psychiatric disorders have been characterized. The neuropathological hallmarks of these disorders include the loss of synapses and neurons, formation of neuritic plaques, and different types of inclusions and aggregations. For example, Alzheimer's disease ature , the most common chronic neurodegenerative disorder and the leading cause of dementia, is neuropathologically characterized by neuronal and synaptic loss, neurofibrillary tangles (NTF), and senile plaque. The amyloid precursor protein (APP) is a type I transmembrane glycoprotein

that is preteolytically processed by α, β, or γ secretases to produce secreted derivatives. Extracellular senile plaques are the 40-42 amino acid Aβ peptide deposits within amyloid plaques which are associated with activated microglial cells and surrounded by abnormal neuronal processes known as dystrophic neurites in the brains (Masliah et al., 1993; Selkoe, 1998; Selkoe, 2001; Wegiel et al., 2001). Intracellular neurofibrillary tangles (NFT) are neuronal inclusions of highly phosphorylated forms of the microtubule-associated protein tau found in neurons and in dystrophic neuritis associated with Aβ deposits, which lead to the degeneration of neurons (Kosik et al., 1986; Garcia and Cleveland, 2001; Augustinack et al., 2002). Parkinson's disease is a degenerative movement disorder of the central nerve system (CNS) characterized by the degeneration of dopaminergic neurons; their neurons often have Lewy bodies (van der Putten et al., 2000; Giasson and Lee, 2001). The presynaptic protein α-Synuclein is the major component of Lewy bodies induced by A53T mutation in the α-synuclein gene (Spillantini et al., 1997). α-Synuclein aggregations are larger electron-dense cytoplasmic inclusions of 2 to 5 μm in diameter composed of fine granular material, leading to neuronal dysfunction in the substantia nigra (Masliah et al., 2000; van der Putten et al., 2000). Huntington disease (HD) is an inherited genetic disorder caused by an abnormal polyglutamine (polyQ ; CAG repeat) expansion within the protein huntingtin (Htt). Intracellular inclusion bodies are formed by the aggregation of Htt in which the normal 6-34 glutamine repeat size expands to 37 or more. Huntington is characterized

by abnormal motor function due to the degeneration of striatal and cortical neurons (Michalik and Van Broeckhoven, 2003; Arrasate et al., 2004; Obrietan and Hoyt, 2004). Amyotrophic lateral sclerosis (ALS), called Lou Gehrig's disease is a motor neuron disease caused by mutations in the superoxide dismutase (SOD1) gene. ALS is characterized by the gradual degeneration and death of motor neurons in the brainstem and spinal cord. In summary, many neurodegerative disorders are related to dysfunction of cytoskeleton proteins which act together to form intracellular inclusions such as tau, α-synuclein or extracellular inclusions such as Aβ. Remarkably, although amyloid fibrils associated with neurodegerative diseases are unrelated in size or primary amino acid sequence, they show common structural features such as β-sheet with a width of ~10 nm and a length of 0.1-10 μm and are able to bind lipophilic dyes such as Congo red, suggesting that a conserved mechanism might contribute to early stages in a variety of disease processes (Eanes and Glenner, 1968; Sunde and Blake, 1998; Dobson, 2003) and also may provide targets for therapeutic drug development (Skovronsky et al., 2006). Hirano bodies are cytoplasmic inclusions composed of filamentous actin-rich aggregates found in many of the neurodegenerative diseases mentioned above (Goldman, 1983; Hirano, 1994; Fechheimer et al., 2002). However, the physiological roles of Hirano bodies on disease progression are still unknown. Therefore, it is essential to understand the role of aggregates in neurodegerative

disease, the mechanism of how protein aggregations form, and their effects on cells and development of pathology.

2. Overview of Hirano Bodies

Hirano bodies are intracellular, rod-shaped, eosinophilic, paracrystalline structures that were initially described in patients with amyotrophic lateral sclerosis or parkinsonism-dementia complex on Guam (Hirano et al., 1968). These cytoplasmic inclusions are observed more frequently in the elderly and in post-mortem samples obtained from patients with a variety of neurodegenrative diseases and other conditions that produce persistent injury or stress including Alzheimer's disease (Gibson, 1978; Mori et al., 1986), Parkinson's disease and amyotrophic lateral sclerosis (Hirano et al., 1968), Pick's disease (Schochet et al., 1968), ataxic Creuzfeldt-Jakob disease (Cartier et al., 1985), chronic alcoholism (Laas and Hagel, 1994), diabetes (Sima and Hinton, 1983), degenerating muscle (Fisher et al., 1972), and neuronal degeneration associated with abnormal copper homeostasis (Peterson et al., 1986). Hirano bodies are stained by heavy metal stains for electron microscopy and by immunohistochemistry. Hirano bodies are often found in degenerating neurons of the central nervous system, particularly the Ammon's horn (CA1) in the hippocampus in AD (Schochet et al., 1968; Gibson and Tomlinson, 1977; Yamamoto and Hirano, 1985; Hirano, 1994; Mitake et al., 1997). However, they have also been

reported in other cells and tissues including glial cells (Field and Narang, 1972; Gessaga and Anzil, 1975; Gibson, 1978), peripheral nerve axons (Laas and Hagel, 1994), extraocular muscles of eyes (Tomonaga, 1983), skeletal muscle (Fernandez et al., 1999), and canine testicular interstitial cells (Setoguti et al., 1974). Hirano bodies are observed in normal brains of elderly individuals without obvious underlying neurodegeration (Ogata et al., 1972; Gibson and Tomlinson, 1977). A summary of a variety of conditions associated with Hirano bodies is shown in Table 1.

Some animal models for Hirano bodies have been reported. Hirano bodies are found in the dendrites of cerebellum Perkinje cells of the brindled mouse (Nagara et al., 1980), in nerve cell bodies and neurites of the lumbosacral region of the squirrel monkey spinal cord (Beal, 2001), and in several neural regions of Wistar Rats (Yagishita et al., 1979). In addition, ultrastructural studies in transgenic (Tg) mice models of AD revealed that some inclusions are structurally reminiscent of Hirano bodies in the synapse of APPsw (Tg2576) tg mouse (Wegiel et al., 2001), in the neuritic plaques of PDAPP (V717F) tg mouse (Masliah et al., 1996), and in the dystrophic neurites of tau/PS1/APP tg mouse (Boutajangout et al., 2004). In all of these animal model systems, the intracellular aggregations have been discovered as Hirano bodies or Hirano-type bodies, but a common relationship or a single causal determinant has yet to be discovered.

A. Structure and molecular composition of Hirano bodies

Analysis of Hirano bodies is largely restricted to immunohistochemical and ultrastructural studies. Hirano bodies are well-organized, elliptical and filamentous inclusions composed predominantly of filamentous actin (Schochet et al., 1968; Goldman, 1983). Ultastructural examination reveals that Hirano bodies are paracrystalline inclusions composed of parallel filaments in orthogonal sheets, which contain highly ordered interlacing parallel filaments of 8-10 nm in diameter with 20-25 nm center to center spacing between filaments The inclusions appear rod-shaped, elliptical, or herringbone patterned depending on the plane of sectioning through an individual Hirano body (Fig. 1.1) (Schochet and McCormick, 1972; Tomonaga, 1974; Hirano, 1994). Freeze-etching electron microscopy further shows that the basic structure of Hirano bodies is arranged in a folded, waved or concentric manner and is connected or supported by cross-linking filaments suggesting electron dense "cross-links" between parallel filaments (Izumiyama et al., 1991). Immunohistochemical studies show that the shape of Hirano bodies in the CA1 area of hippocampal neurons varies from small ovoid structures to longer, narrow bodies and often located adjacent to pyramidal cells (Maciver and Harrington, 1995). Hirano bodies consist mostly of F-actin and actin-associated proteins such as α-actinin, tropomyosin and vinculin (Goldman, 1983; Peterson et al., 1986; Galloway et al., 1987), ADF/cofilin (Maciver and Harrington, 1995), but not myosin (Galloway et al., 1987). Since actin

is one of the major cytoskeletal proteins present in neurons and actin dynamics are essential for nerve cell function, a possible relationship between Hirano bodies and their perturbations to the cytoskeleton may prove to be important. For example, actin is involved in cell motility, vesicle transport, membrane turnover (Kuhn et al., 2000) and provides the framework for neurite growth and retraction (Matus, 2000; Luo, 2002; Vale, 2003). Hirano bodies also contain neurofilament proteins (Schmidt et al., 1989) and microtubule associated proteins such as MAP1, MAP2, and tau, but not microtubules (Galloway et al., 1987; Peterson et al., 1988). Stress related proteins such as inducible nitric oxide synthase (iNOS) (Lee et al., 1999), and small heatshock protein 27 (Renkawek et al., 1994) are also found in these inclusions. The presence of other proteins including C-terminal fragments of β-amyloid (Munoz et al., 1993), caspase-cleaved actin (Fractin) (Rossiter et al., 2000), hippocampal cholinergic neurostimulating peptide (HCNP)(Mitake et al., 1995), transforming growth factor-β3 (TGF-β3) (Peress and Perillo, 1995), and FAC1 (Jordan-Sciutto et al., 1998) suggests that Hirano bodies may modulate the pathology of a cell through perturbation of normal cellular process as transcriptional regulation and cell signaling. Although epitopes from the C-terminal fragments of APP (AICD) is found to be enriched in Hirano bodies (Munoz et al., 1993), significance of this association with Hirano bodies is unknown. Recently, some groups have reported that AICD can function as a transcriptional regulator (Cao and Sudhof, 2001) and stimulates apoptosis (Kinoshita et al.,

2002). Therefore, the sequestration of AICD in Hirano bodies may modulate transcription and apoptosis. A summary of the proteins reported present in Hirano bodies is shown in table 2.

3. Development of a model for formation of Hirano bodies

A. The 34-kDa actin bundling protein

The 34 kDa actin bundling protein is one of eleven actin cross-linking proteins found in the slime mold, *Dictyostelium discoideum* (Furukawa and Fechheimer, 1996). The 34 kDa protein is dynamic *in vivo* and its cellular localization often reflects the dynamic behavior of the actin cytoskeleton. Consequently, it localizes to a number of important actin dependent structures. For example, it can be found at the leading edge and in filopodia (Fechheimer, 1987), at the point of cell - cell contacts (Fechheimer et al., 1994), and phagocytic cups (Furukawa et al., 1992; Okazaki and Yumura, 1995). It is suggested that the 34 kDa protein is involved in many diverse functions. This is further supported by genetic studies in which the cellular function for 34 kDa protein was examined using 34 kDa protein null cells. 34 kDa deficient *Dictyostelium* cells show modest defects in cell motility, morphology, and growth (Rivero et al., 1996). However, double knockout mutants for α-actinin/34 kDa and ABP-120/34 kDa show even more severe phenotypes suggesting that there is some functional redundancy amongst the actin cross-linking proteins (Rivero et al., 1999). The combinatorial effects of actin cross-linking proteins as

illustrated by genetic studies using other actin cross-linking proteins (Fisher et al., 1997; Noegel and Schleicher, 2000; Ponte et al., 2000) clearly show that perturbations in the actin cross-linking proteins present in a cell are coupled to modulation of the actin cytoskeleton. Therefore, actin dynamics of *Dictyostelium* are sensitive to perturbations of the normal functions of the actin binding proteins that regulate it.

B. Model of the 34-kDa protein structure and regulation

Purified 34 kDa protein from the cytosol of *Dictyostelium* is soluble and monomeric in solution (Fig. 1.2). It is a calcium regulated F-actin binding protein whose ability to bundle actin filaments is decreased by micromolar concentrations of Ca^{2+} (Fechheimer and Taylor, 1984). The cDNA of the 34 kDa protein predicts a 295 amino acid protein with two putative EF hand regions (Ca^{2+} binding sites) at amino acids 84-112 (EF1) and amino acids 135-163 (EF2) (Fechheimer et al., 1991). Ca^{2+} binding assays reveal that only 1 mole of Ca^{2+} binds per mole of 34 kDa protein and the site of Ca^{2+} binding is restricted to the second EF hand (Furukawa et al., 2003). In the structural model of 34 kDa protein, it contains three binding sites for actin filaments (Lim et al., 1999): amino acids 1-123, amino acids 193-254, and amino acids 278-295 with the strongest actin binding correlating with the region encompassing amino acids 193-254. Subsequent biochemical studies with a truncated form of 34 kDa protein, CT (aa 124-295), revealed that the CT fragment showed calcium-insensitive activated actin binding and had enhanced actin binding

possibly due to the loss of the putative inhibitory N-terminal region (amino acids 1-71). The 34 kDa protein also contains two interaction zones (IZs) that mediate intramolecular domain-domain interaction and an amino terminal inhibitory site (Lim et al., 1999). In terms of this model, release of bound Ca^{2+} induces a conformational change in the structure of 34 kDa protein so that the Interaction Zone 1 (IZ1) is no longer able to interact with interaction zone 2 (IZ-2) which also contains the strong actin binding site (amino acids 193-254). Therefore, it is predicted that the N-terminal inhibitory region could not interact with the strong actin binding site in the absence of bound Ca^{2+}, thus enabling it to freely bind to F-actin. Additionally, minor mutations in N-terminal portion of 34 kDa protein can also induce the formation of Hirano body like structures. For example, mutations in either EF-hand 1 of 34 kDa protein (residues 84-112) named as 34 kDa ΔEF1, or a point mutation called as 34 kDa E60K, (Dong-Hwan Kim and Paul Griffin, unpublished data) also leads to Hirano body formation in *Dictyostelium*. Taken together, this model can be used to predict why CT (amino acids 124-295) expression might lead to the formation of Hirano bodies in *Dictyostelium*, mammalian cell cultures, and a transgenic mouse model.

C. Formation of Model Hirano bodies in *Dictyostelium* and Cultured Mammalian Cells

We have reported that expression of altered forms of the 34 kD protein (CT and ΔEF1) induces formation of Hirano bodies in *Dictyostelium discoideum* (Maselli et al., 2002; Maselli et

al., 2003), and expression of the CT protein induces F-actin rearrangement in HEK 293, HeLa, Cos7 cells, astrocytoma, astrocytic cells, and primary neurons to induce the formation of Hirano bodies (Davis et al., 2008). In ultrastructural and immunocytochemical characterization, our model Hirano bodies form cytoplasmic inclusions, and reveal features strikingly similar to those of Hirano bodies observed from postmortem neurodegenerative disease brains. First, they have an elliptical shape containing ordered assemblies of F-actin, cofilin, and α-actinin. Second, they contain a paracrystalline array of actin filaments with a diameter between 6-12 nm and a center to center spacing 10-20 nm, Third, they vary in size from 500 nm to 2 μm, and depending on plane of section or tilt feature, a herringbone pattern in oblique sections and parallel filaments in longitudinal and cross sections (Maselli et al., 2002; Maselli et al., 2003; Davis et al., 2008). Model Hirano bodies have slight ultrastructural and immunocytochemical differences from Hirano bodies. For example, the filaments in model Hirano bodies appear to be comprised of small foci of ordered curvilinear filaments and contain ubiquitin and myosin II. The Hirano bodies in the cell culture model are sufficiently similar to native HB to allow more intensive analysis of these poorly understood inclusions.

D. Goals of the dissertation

This dissertation reports two investigations of the physiological function of Hirano bodies. First, the association of a C-terminal fragment of amyloid-β precursor protein (AICD) with

Hirano bodies in a cell culture model system might impede its function in promoting apoptosis and modulating transcription. These results would suggest that Hirano bodies may function as adaptive structures in Alzheimer's disease by limiting AICD-dependent neurotoxicity. Second, a mouse model of Hirano bodies was developed for investigation of the physiological effects and roles of Hirano bodies in the brain *in vivo*. This transgenic mouse model will allow us to determine whether Hirano bodies may either promote development of pathology, or exert a protective effect during disease progression in the brain.

References

Anzil, A. P., H. Herrlinger, K. Blinzinger and A. Heldrich (1974). Ultrastructure of brain and nerve biopsy tissue in Wilson disease. Arch. Neurol. **31**(2): 94-100.

Arrasate, M., S. Mitra, E. S. Schweitzer, M. R. Segal and S. Finkbeiner (2004). Inclusion body formation reduces levels of mutant huntingtin and the risk of neuronal death. Nature **431**(7010): 805-10.

Augustinack, J. C., A. Schneider, E. M. Mandelkow and B. T. Hyman (2002). Specific tau phosphorylation sites correlate with severity of neuronal cytopathology in Alzheimer's disease. Acta Neuropathol **103**(1): 26-35.

Beal, M. F. (2001). Experimental models of Parkinson's disease. Nat Rev Neurosci **2**(5): 325-34.

Boutajangout, A., M. Authelet, V. Blanchard, N. Touchet, G. Tremp, L. Pradier and J. P. Brion (2004). Characterisation of cytoskeletal abnormalities in mice transgenic for wild-type human tau and familial Alzheimer's disease mutants of APP and presenilin-1. Neurobiol Dis **15**(1): 47-60.

Cao, X. and T. C. Sudhof (2001). A transcriptionally [correction of transcriptively] active complex of APP with Fe65 and histone acetyltransferase Tip60. Science **293**(5527): 115-20.

Cartier, L., S. Galvez and D. C. Gajdusek (1985). Familial clustering of the ataxic form of Creutzfeldt-Jakob disease with Hirano bodies. J. Neurol. Neurosurg. Psychiatry **48**(3): 234-8.

Cartier, L., S. Galvez and D. C. Gajdusek (1985). Familial clustering of the ataxic form of Creutzfeldt-Jakob disease with Hirano bodies. J Neurol Neurosurg Psychiatry **48**(3): 234-8.

Davis, R. C., R. Furukawa and M. Fechheimer (2008). A cell culture model for investigation of Hirano bodies. Acta Neuropathol **115**(2): 205-17.

Dobson, C. M. (2003). Protein folding and misfolding. Nature **426**(6968): 884-90.

Eanes, E. D. and G. G. Glenner (1968). X-ray diffraction studies on amyloid filaments. J Histochem Cytochem **16**(11): 673-7.

Fechheimer, M. (1987). The Dictyostelium discoideum 30,000-dalton protein is an actin filament-bundling protein that is selectively present in filopodia. J. Cell Biol. **104**(6): 1539-51.

Fechheimer, M., R. Furukawa, A. Maselli and R. C. Davis (2002). Hirano bodies in health and disease. Trends Mol. Med. **8**(12): 590-1.

Fechheimer, M., H. M. Ingalls, R. Furukawa and E. J. Luna (1994). Association of the Dictyostelium 30 kDa actin bundling protein with contact regions. J. Cell Sci. **107 (Pt 9)**: 2393-401.

Fechheimer, M., D. Murdock, M. Carney and C. V. Glover (1991). Isolation and sequencing of cDNA clones encoding the Dictyostelium discoideum 30,000-dalton actin-bundling protein. J. Biol Chem. **266**(5): 2883-9.

Fechheimer, M. and D. L. Taylor (1984). Isolation and characterization of a 30,000-dalton calcium-sensitive actin cross-linking protein from Dictyostelium discoideum. J. Biol. Chem. **259**(7): 4514-20.

Fernandez, R., J. M. Fernandez, C. Cervera, S. Teijeira, A. Teijeiro, C. Dominguez and C. Navarro (1999). Adult glycogenosis II with paracrystalline mitochondrial inclusions and Hirano bodies in skeletal muscle. Neuromuscul. Disord. **9**(3): 136-43.

Field, E. J., J. D. Mathews and C. S. Raine (1969). Electron microscopic observations on the cerebellar cortex in kuru. J. Neurol. Sci. **8**(2): 209-24.

Field, E. J. and H. K. Narang (1972). An electron-microscopic study of scrapie in the rat: further observations on "inclusion bodies" and virus-like particles. J. Neurol. Sci. **17**(3): 347-64.

Fisher, E. R., A. R. Gonzalez, R. C. Khurana and T. S. Danowski (1972). Unique, concentrically laminated, membranous inclusions in myofibers. Am. J. Clin. Pathol. **58**(3): 239-44.

Fisher, P. R., A. A. Noegel, M. Fechheimer, F. Rivero, J. Prassler and G. Gerisch (1997). Photosensory and thermosensory responses in Dictyostelium slugs are specifically

impaired by absence of the F-actin cross-linking gelation factor (ABP-120). Curr Biol **7**(11): 889-92.

Fu, Y., J. Ward and H. F. Young (1975). Unusual, rod-shaped cytoplasmic inclusions (Hirano bodies) in a cerebellar hemangioblastoma. Acta Neuropathol. (Berl) **31**(2): 129-35.

Furukawa, R., S. Butz, E. Fleischmann and M. Fechheimer (1992). The Dictyostelium discoideum 30,000 dalton protein contributes to phagocytosis. Protoplasma **169**: 18-27.

Furukawa, R. and M. Fechheimer (1996). Role of the Dictyostelium 30 kDa protein in actin bundle formation. Biochemistry **35**(22): 7224-32.

Furukawa, R., A. Maselli, S. A. Thomson, R. W. Lim, J. V. Stokes and M. Fechheimer (2003). Calcium regulation of actin crosslinking is important for function of the actin cytoskeleton in Dictyostelium. J. Cell Sci. **116**(Pt 1): 187-96.

Galloway, P. G., G. Perry and P. Gambetti (1987). Hirano body filaments contain actin and actin-associated proteins. J. Neuropathol. Exp. Neurol. **46**(2): 185-99.

Galloway, P. G., G. Perry, K. S. Kosik and P. Gambetti (1987). Hirano bodies contain tau protein. Brain Res **403**(2): 337-40.

Garcia, M. L. and D. W. Cleveland (2001). Going new places using an old MAP: tau, microtubules and human neurodegenerative disease. Curr Opin Cell Biol **13**(1): 41-8.

Gessaga, E. C. and A. P. Anzil (1975). Rod-shaped filamentous inclusions and other ultrastructural features in a cerebellar astrocytoma. Acta Neuropathol. (Berl) **33**(2): 119-27.

Giasson, B. I. and V. M. Lee (2001). Parkin and the molecular pathways of Parkinson's disease. Neuron **31**(6): 885-8.

Gibson, P. H. (1978). Light and electron microscopic observations on the relationship between Hirano bodies, neuron and glial perikarya in the human hippocampus. Acta Neuropathol **42**(3): 165-71.

Gibson, P. H. and B. E. Tomlinson (1977). Numbers of Hirano bodies in the hippocampus of normal and demented people with Alzheimer's disease. J. Neurol. Sci. **33**(1-2): 199-206.

Goldman, J. E. (1983). The association of actin with Hirano bodies. J. Neuropathol. Exp. Neurol. **42**(2): 146-52.

Hirano, A. (1994). Hirano bodies and related neuronal inclusions. Neuropathol. Appl. Neurobiol. **20**(1): 3-11.

Hirano, A., H. M. Dembitzer, L. T. Kurland and H. M. Zimmerman (1968). The fine structure of some intraganglionic alterations. Neurofibrillary tangles, granulovacuolar bodies and "rod-like" structures as seen in Guam amyotrophic lateral sclerosis and parkinsonism-dementia complex. J. Neuropathol. Exp. Neurol. **27**(2): 167-82.

Izumiyama, N., K. Ohtsubo, T. Tachikawa and H. Nakamura (1991). Elucidation of three-dimensional ultrastructure of Hirano bodies by the quick-freeze, deep-etch and replica method. Acta Neuropathol. (Berl) **81**(3): 248-54.

Jordan-Sciutto, K., J. Dragich, D. Walcott and R. Bowser (1998). The presence of FAC1 protein in Hirano bodies. Neuropathol. Appl. Neurobiol. **24**(5): 359-66.

Kinoshita, A., C. M. Whelan, O. Berezovska and B. T. Hyman (2002). The gamma secretase-generated carboxyl-terminal domain of the amyloid precursor protein induces apoptosis via Tip60 in H4 cells. J. Biol. Chem. **277**(32): 28530-6.

Kosik, K. S., C. L. Joachim and D. J. Selkoe (1986). Microtubule-associated protein tau (Sturchler-Pierrat et al.) is a major antigenic component of paired helical filaments in Alzheimer disease. Proc Natl Acad Sci U S A **83**(11): 4044-8.

Kuhn, T. B., P. J. Meberg, M. D. Brown, B. W. Bernstein, L. S. Minamide, J. R. Jensen, K. Okada, E. A. Soda and J. R. Bamburg (2000). Regulating actin dynamics in neuronal growth cones by ADF/cofilin and rho family GTPases. J Neurobiol **44**(2): 126-44.

Laas, R. and C. Hagel (1994). Hirano bodies and chronic alcoholism. Neuropathol. Appl. Neurobiol. **20**(1): 12-21.

Lee, H. G., M. Ueda, Y. Miyamoto, Y. Yoneda, G. Perry, M. A. Smith and X. Zhu (2006). Aberrant localization of importin alpha1 in hippocampal neurons in Alzheimer disease. Brain Res **1124**(1): 1-4.

Lee, S. C., M. L. Zhao, A. Hirano and D. W. Dickson (1999). Inducible nitric oxide synthase immunoreactivity in the Alzheimer disease hippocampus: association with Hirano bodies, neurofibrillary tangles, and senile plaques. J. Neuropathol. Exp. Neurol. **58**(11): 1163-9.

Lim, R. W., R. Furukawa, S. Eagle, R. C. Cartwright and M. Fechheimer (1999). Three distinct F-actin binding sites in the Dictyostelium discoideum 34,000 dalton actin bundling protein. Biochemistry **38**(2): 800-12.

Lim, R. W., R. Furukawa and M. Fechheimer (1999). Evidence of intramolecular regulation of the Dictyostelium discoideum 34 000 Da F-actin-bundling protein. Biochemistry **38**(49): 16323-32.

Luo, L. (2002). Actin cytoskeleton regulation in neuronal morphogenesis and structural plasticity. Annu Rev Cell Dev Biol **18**: 601-35.

Maccioni, R. B., J. P. Munoz and L. Barbeito (2001). The molecular bases of Alzheimer's disease and other neurodegenerative disorders. Arch Med Res **32**(5): 367-81.

Maciver, S. K. and C. R. Harrington (1995). Two actin binding proteins, actin depolymerizing factor and cofilin, are associated with Hirano bodies. Neuroreport **6**(15): 1985-8.

Maselli, A., R. Furukawa, S. A. Thomson, R. C. Davis and M. Fechheimer (2003). Formation of Hirano bodies induced by expression of an actin cross-linking protein with a gain-of-function mutation. Eukaryot. Cell **2**(4): 778-87.

Maselli, A. G., R. Davis, R. Furukawa and M. Fechheimer (2002). Formation of Hirano bodies in Dictyostelium and mammalian cells induced by expression of a modified form of an actin-crosslinking protein. J. Cell Sci. **115**(Pt 9): 1939-49.

Masliah, E., M. Mallory, T. Deerinck, R. DeTeresa, S. Lamont, A. Miller, R. D. Terry, B. Carragher and M. Ellisman (1993). Re-evaluation of the structural organization of neuritic plaques in Alzheimer's disease. J Neuropathol Exp Neurol **52**(6): 619-32.

Masliah, E., E. Rockenstein, I. Veinbergs, M. Mallory, M. Hashimoto, A. Takeda, Y. Sagara, A. Sisk and L. Mucke (2000). Dopaminergic loss and inclusion body formation in alpha-synuclein mice: implications for neurodegenerative disorders. Science **287**(5456): 1265-9.

Masliah, E., A. Sisk, M. Mallory, L. Mucke, D. Schenk and D. Games (1996). Comparison of neurodegenerative pathology in transgenic mice overexpressing V717F beta-amyloid precursor protein and Alzheimer's disease. J Neurosci **16**(18): 5795-811.

Matus, A. (2000). Actin-based plasticity in dendritic spines. Science **290**(5492): 754-8.

Michalik, A. and C. Van Broeckhoven (2003). Pathogenesis of polyglutamine disorders: aggregation revisited. Hum Mol Genet **12 Spec No 2**: R173-86.

Mitake, S., K. Ojika and A. Hirano (1997). Hirano bodies and Alzheimer's disease. Kaohsiung J. Med. Sci. **13**(1): 10-8.

Mitake, S., K. Ojika, E. Katada, Y. Otsuka, N. Matsukawa and O. Fujimori (1995). Accumulation of hippocampal cholinergic neurostimulating peptide (HCNP)-related components in Hirano bodies. Neuropathol Appl Neurobiol **21**(1): 35-40.

Mori, H., M. Tomonaga, N. Baba and K. Kanaya (1986). The structure analysis of Hirano bodies by digital processing on electron micrographs. Acta Neuropathol. (Berl) **71**(1-2): 32-7.

Muchowski, P. J. and J. L. Wacker (2005). Modulation of neurodegeneration by molecular chaperones. Nat Rev Neurosci **6**(1): 11-22.

Munoz, D. G., D. Wang and B. D. Greenberg (1993). Hirano bodies accumulate C-terminal sequences of beta-amyloid precursor protein (beta-APP) epitopes. J. Neuropathol. Exp. Neurol. **52**(1): 14-21.

Nagara, H., K. Yajima and K. Suzuki (1980). An ultrastructural study on the cerebellum of the brindled mouse. Acta Neuropathol. (Berl) **52**(1): 41-50.

Noegel, A. A. and M. Schleicher (2000). The actin cytoskeleton of Dictyostelium: a story told by mutants. J Cell Sci **113 (Pt 5)**: 759-66.

Obrietan, K. and K. R. Hoyt (2004). CRE-mediated transcription is increased in Huntington's disease transgenic mice. J Neurosci **24**(4): 791-6.

Ogata, J., G. N. Budzilovich and H. Cravioto (1972). A study of rod-like structures (Hirano bodies) in 240 normal and pathological brains. Acta Neuropathol. (Berl) **21**(1): 61-7.

Okamoto, K., S. Hirai and A. Hirano (1982). Hirano bodies in myelinated fibers of hepatic encephalopathy. Acta Neuropathol. (Berl) **58**(4): 307-10.

Okazaki, K. and S. Yumura (1995). Differential association of three actin-bundling proteins with microfilaments in Dictyostelium amoebae. Eur. J. Cell Biol. **66**(1): 75-81.

Peress, N. S. and E. Perillo (1995). Differential expression of TGF-beta 1, 2 and 3 isotypes in Alzheimer's disease: a comparative immunohistochemical study with cerebral infarction, aged human and mouse control brains. J. Neuropathol. Exp. Neurol. **54**(6): 802-11.

Peterson, C., Y. Kress, R. Vallee and J. E. Goldman (1988). High molecular weight microtubule-associated proteins bind to actin lattices (Hirano bodies). Acta Neuropathol. (Berl) **77**(2): 168-74.

Peterson, C., K. Suzuki, Y. Kress and J. E. Goldman (1986). Abnormalities of dendritic actin organization in the brindled mouse. Brain Res. **382**(2): 205-12.

Ponte, E., F. Rivero, M. Fechheimer, A. Noegel and S. Bozzaro (2000). Severe developmental defects in Dictyostelium null mutants for actin-binding proteins. Mech Dev **91**(1-2): 153-61.

Previll, L. A., M. E. Crosby, R. J. Castellani, R. Bowser, G. Perry, M. A. Smith and X. Zhu (2007). Increased expression of p130 in Alzheimer disease. Neurochem Res **32**(4-5): 639-44.

Renkawek, K., G. J. Bosman and W. W. de Jong (1994). Expression of small heat-shock protein hsp 27 in reactive gliosis in Alzheimer disease and other types of dementia. Acta Neuropathol. (Berl) **87**(5): 511-9.

Rivero, F., R. Furukawa, M. Fechheimer and A. A. Noegel (1999). Three actin cross-linking proteins, the 34 kDa actin-bundling protein, alpha-actinin and gelation factor (ABP-120), have both unique and redundant roles in the growth and development of Dictyostelium. J Cell Sci **112 (Pt 16)**: 2737-51.

Rivero, F., R. Furukawa, A. A. Noegel and M. Fechheimer (1996). Dictyostelium discoideum cells lacking the 34,000-dalton actin-binding protein can grow, locomote, and develop, but exhibit defects in regulation of cell structure and movement: a case of partial redundancy. J Cell Biol **135**(4): 965-80.

Rossiter, J. P., L. L. Anderson, F. Yang and G. M. Cole (2000). Caspase-cleaved actin (fractin) immunolabelling of Hirano bodies. Neuropathol. Appl. Neurobiol. **26**(4): 342-6.

Santa-Mara, I., G. Santpere, M. J. MacDonald, E. Gomez de Barreda, F. Hernandez, F. J. Moreno, I. Ferrer and J. Avila (2008). Coenzyme q induces tau aggregation, tau filaments, and Hirano bodies. J Neuropathol Exp Neurol **67**(5): 428-34.

Schmidt, M. L., V. M. Lee and J. Q. Trojanowski (1989). Analysis of epitopes shared by Hirano bodies and neurofilament proteins in normal and Alzheimer's disease hippocampus. Lab Invest. **60**(4): 513-22.

Schochet, S. S., Jr., P. W. Lampert and R. Lindenberg (1968). Fine structure of the Pick and Hirano bodies in a case of Pick's disease. Acta Neuropathol. (Berl) **11**(4): 330-7.

Schochet, S. S., Jr. and W. F. McCormick (1972). Ultrastructure of Hirano bodies. Acta Neuropathol. (Berl) **21**(1): 50-60.

Selkoe, D. J. (1998). The cell biology of beta-amyloid precursor protein and presenilin in Alzheimer's disease. Trends Cell Biol **8**(11): 447-53.

Selkoe, D. J. (2001). Alzheimer's disease: genes, proteins, and therapy. Physiol Rev **81**(2): 741-66.

Setoguti, T., H. Esumi and T. Shimizu (1974). Specific organization of intracytoplasmic filaments in the dog testicular interstitial cell. Cell Tissue Res. **148**(4): 493-7.

Shao, C. Y., J. F. Crary, C. Rao, T. C. Sacktor and S. S. Mirra (2006). Atypical protein kinase C in neurodegenerative disease II: PKCiota/lambda in tauopathies and alpha-synucleinopathies. J. Neuropathol. Exp. Neurol. **65**(4): 327-35.

Sima, A. A. and D. Hinton (1983). Hirano-bodies in the distal symmetric polyneuropathy of the spontaneously diabetic BB-Wistar rat. Acta Neurol. Scand. **68**(2): 107-12.

Skovronsky, D. M., V. M. Lee and J. Q. Trojanowski (2006). Neurodegenerative diseases: new concepts of pathogenesis and their therapeutic implications. Annu Rev Pathol **1**: 151-70.

Spillantini, M. G., M. L. Schmidt, V. M. Lee, J. Q. Trojanowski, R. Jakes and M. Goedert (1997). Alpha-synuclein in Lewy bodies. Nature **388**(6645): 839-40.

Sunde, M. and C. C. Blake (1998). From the globular to the fibrous state: protein structure and structural conversion in amyloid formation. Q Rev Biophys **31**(1): 1-39.

Tomonaga, M. (1974). Ultrastructure of Hirano bodies. Acta Neuropathol. (Berl) **28**(4): 365-6.

Tomonaga, M. (1983). Hirano body in extraocular muscle. Acta Neuropathol. (Berl) **60**(3-4): 309-13.

Vale, R. D. (2003). The molecular motor toolbox for intracellular transport. Cell **112**(4): 467-80.

van der Putten, H., K. H. Wiederhold, A. Probst, S. Barbieri, C. Mistl, S. Danner, S. Kauffmann, K. Hofele, W. P. Spooren, M. A. Ruegg, S. Lin, P. Caroni, B. Sommer, M. Tolnay and G. Bilbe (2000). Neuropathology in mice expressing human alpha-synuclein. J Neurosci **20**(16): 6021-9.

Wegiel, J., K. C. Wang, H. Imaki, R. Rubenstein, A. Wronska, M. Osuchowski, W. J. Lipinski, L. C. Walker and H. LeVine (2001). The role of microglial cells and astrocytes in fibrillar plaque evolution in transgenic APP(Swant and Wagner) mice. Neurobiol Aging **22**(1): 49-61.

Yagishita, S., Y. Itoh, T. Nakano, Y. Ono and N. Amano (1979). Crystalloid inclusions reminiscent of Hirano bodies in autolyzed peripheral nerve of normal wistar rats. Acta Neuropathol **47**(3): 231-6.

Yamamoto, T. and A. Hirano (1985). Hirano bodies in the perikaryon of the Purkinje cell in a case of Alzheimer's disease. Acta Neuropathol. (Berl) **67**(1-2): 167-9.

Table 1.

Association of Hirano bodies with neurodegenerative diseases and conditions

Condition	Tissue or Cell type	Reference
Alzheimer's disease	Hippocampus CA1, Purkinje cells, Oligodendrocytes	(Gibson and Tomlinson, 1977; Yamamoto and Hirano, 1985; Mori et al., 1986; Schmidt et al., 1989; Mitake et al., 1997)
Parkinson's disease	Hippocampus CA1	(Hirano et al., 1968)
Pick's disease	Hippocampus CA1	(Schochet et al., 1968)
Amyotrophic lateral sclerosis (ALS)	Hippocampus CA1	(Hirano et al., 1968)
Creutzfeldt-Jakob disease	Hippocampus CA1	(Cartier et al., 1985)
Scrapie and kuru	Cerebellar cortex	(Field et al., 1969; Field and Narang, 1972)
Chronic alcoholism, Hepatic encephalopathy	Hippocampus CA1, Substantia nigra, Dentate nucleus	(Okamoto et al., 1982; Laas and Hagel, 1994)
Neuroblastoma, Astrocytoma	Stromal cell, Glial cell, Cerebellum	(Fu et al., 1975; Gessaga and Anzil, 1975)
Diabetes (rat model)	Peripheral nerves, Oligodendrocytes	(Sima and Hinton, 1983)
Muscle degeneration	Myofibers	(Fisher et al., 1972; Tomonaga, 1983; Fernandez et al., 1999)
Brindled mice (Menke's); Wilson's Disease	Cerebellum, Neocortex, and Cerebral cortex	(Anzil et al., 1974; Nagara et al., 1980; Peterson et al., 1986)
Aging	Hippocampus CA1	(Ogata et al., 1972; Schmidt et al., 1989)

Table 2.

Protein components of Hirano bodies

Protein	Reference
Actin (F-actin)	(Goldman, 1983; Galloway et al., 1987)
α-Actinin	(Galloway, Perry et al. 1987)
Vinculin	(Galloway, Perry et al. 1987)
Tropomyosin	(Galloway, Perry et al. 1987)
ADF/cofilin	(Maciver and Harrington, 1995)
Tau protein	(Munoz et al., 1993)
MAPs	(Peterson et al., 1988)
Caspase-cleaved actin (Fractin)	(Rossiter et al., 2000)
FAC1	(Jordan-Sciutto et al., 1998)
C-terminal fragment of β-APP (AICD)	(Munoz et al., 1993)
Neurofilament subunits L and M	(Schmidt et al., 1989)
Hippocampus acetylcholine neurostimulating peptide (HCNP)	(Rossiter et al., 2000)
Transforming growth factor β3	(Peress and Perillo, 1995)
Inducible nitric oxide synthase	(Lee et al., 1999)
Small heat shock protein 27 (HSP27)	(Renkawek et al., 1994)
Importin	(Lee et al., 2006)
Protein Kinase C i/λ	(Shao et al., 2006)
P130 (retinoblastoma related protein)	(Previll et al., 2007)
Coenzyme Q (Ubiquinine)	(Santa-Mara et al., 2008)

Figure 1.1. The major hallmarks of Hirano bodies

(A) A large spindle-shaped Hirano body adjacent to the perikaryon of a neuron. (B) A small irregular Hirano body. (C) Various patterns are observed in sections through the Hirano bodies. Views of the strata or subunits, each consisting of two overlapping or intersecting expanses of parallel filaments produce a lattice work pattern *(LW).* Cross sections through the strata appear as rows of punctate densities *(PD)* closely applied to filaments or as broader fibrils (*BF*) depending upon the rotation of the subunits. Uranyl acetate-lead citrate. (D) Light micrograph of the hippocampal cortex illustrating a spindle-shaped juxtaganglionic Hirano body (arrow) stained by hematoxylin and eosin (Schochet and McCormick, 1972).

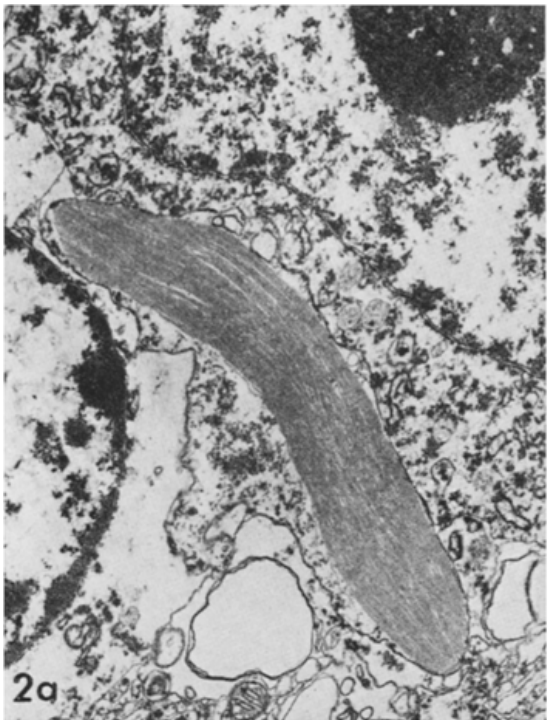
2a

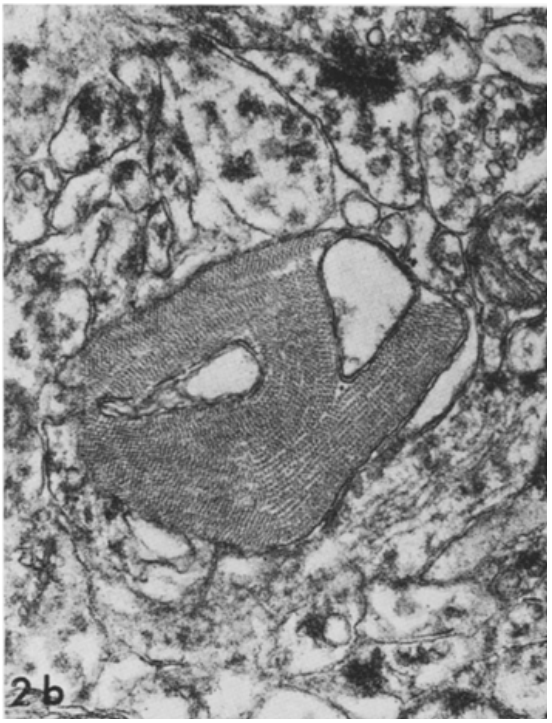
2b

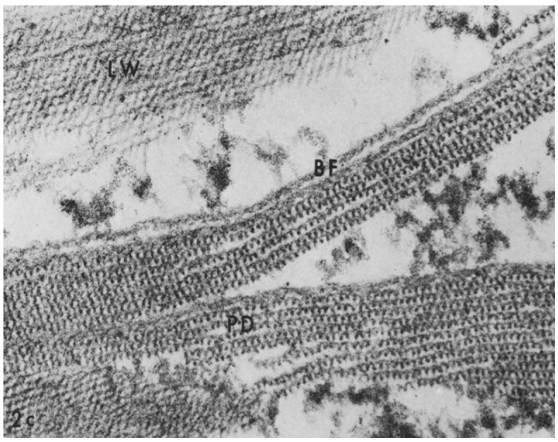
CW
BF
PD
2c

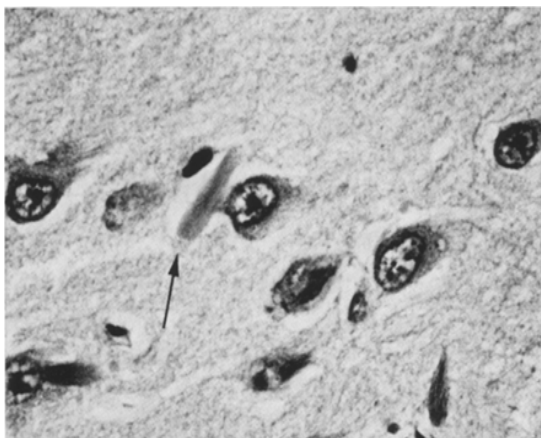

Figure 1.2. Schematic model of the 34 kDa actin-bundling protein.

(A) The structural organization of the 34 kDa protein including the N-terminal inhibitory domain, the intramolecular interaction zones (IZ-1 and IZ-2), the two putative EF-hand calcium-binding motifs (EF1 and EF2), the strong F-actin binding site, and the extreme C-terminal actin-binding site. Proposed folded conformation of 34 kDa protein in the absence (B) and presence of calcium (C). Model of N-terminally truncated 34 kDa protein, 34kDa ΔEF1 (D) and CT (E), which is inaccessible for calcium binding, and the strong actin binding site is exposed, resulting in constitutive elevated actin binding (Lim et al., 1999). Circle in yellow is calcium (C).

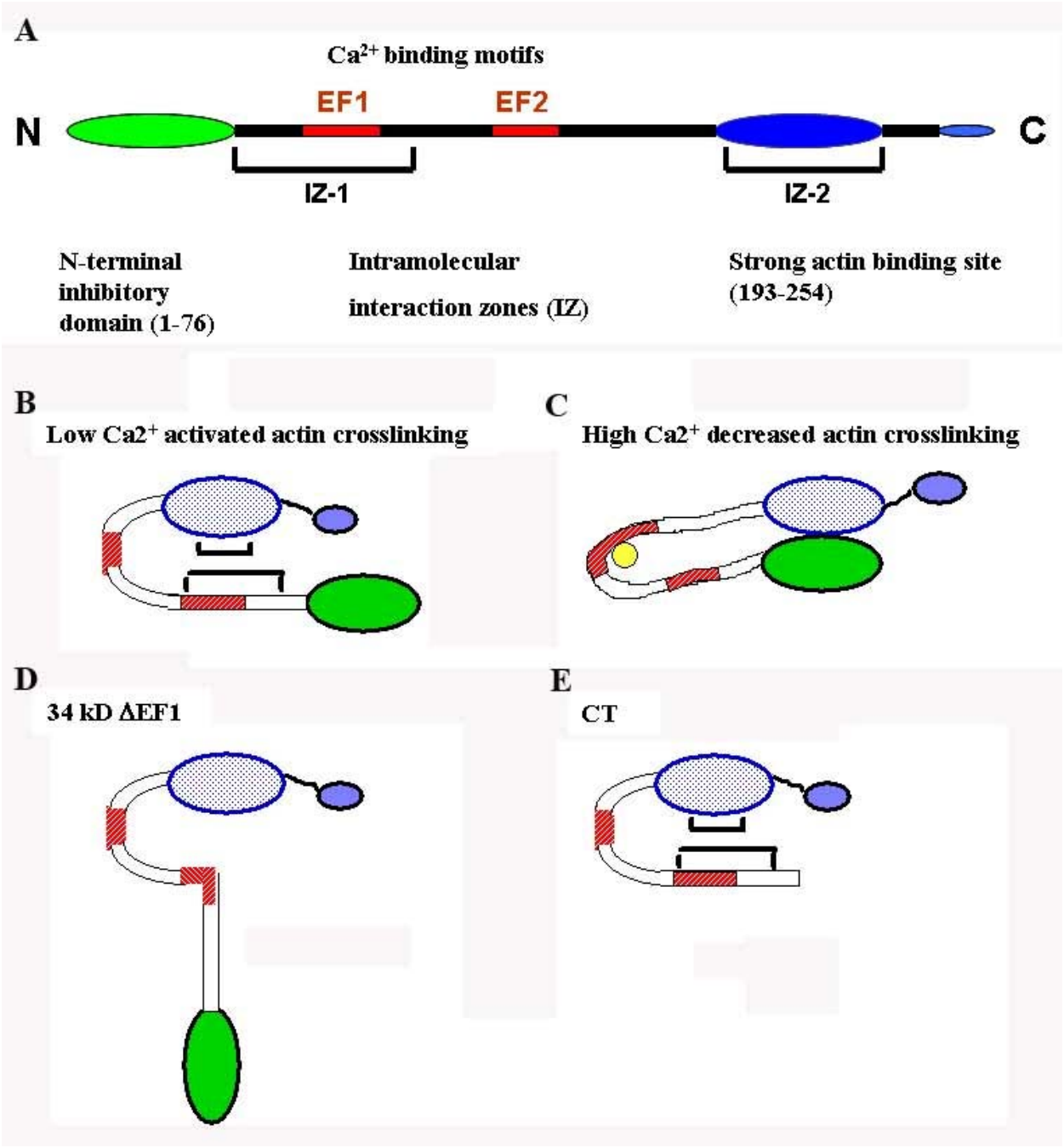
A
Ca2+ binding motifs
EF1
EF2
N
C
IZ-1
IZ-2
N-terminal inhibitory domain (1-76)
Intramolecular interaction zones (IZ)
Strong actin binding site (193-254)
B
Low Ca2+ activated actin crosslinking
C
High Ca2+ decreased actin crosslinking
D
34 kD ΔEF1
E
CT

Chapter 2

Association of AICD to Hirano bodies reduces transcriptional activation and initiation of apoptosis[1]

[1] Sangdeuk Ha, Marcus Fechheimer, and Ruth Furukawa. Submitted to Neurobiology of Aging, 2008

Abstract

Hirano bodies are cytoplasmic inclusions predominantly found in the central nervous system associated with various conditions including aging and Alzheimer's disease (AD). Since most studies of Hirano bodies have been performed in post-mortem samples, the physiological roles of Hirano bodies have not been investigated. Astrocytoma H4 cells were employed to test the hypothesis that Hirano bodies interact with and modulate signaling by the C-terminal fragment of amyloid-β precursor protein (AICD). We demonstrated by immunofluorescence and immunoprecipitation that model Hirano bodies accumulate AICD. Since stimulation of transcription by AICD is dependent on its interaction with the nuclear adaptor protein Fe65, we examined localization of Fe65, and employed a dual luciferase reporter assay to test the effects of Hirano bodies on AICD- and Fe65-dependent modulation of gene expression. We find that both AICD and Fe65 are co-localized in model Hirano bodies. Model Hirano bodies also down-regulate both AICD-dependent apoptosis and AICD- and Fe65-dependent transcriptional activity. Thus, association of AICD with Hirano bodies impedes its function in promoting apoptosis and modulating transcription.

Introduction

Hirano bodies are intracellular inclusions found in a number of neurodegenerative diseases including Alzheimer's disease (AD), Amyotrophic Lateral Sclerosis (ALS), Parkinson's disease, and other conditions in humans and animals producing persistent injury or stress such as diabetes and chronic alcoholism (Gibson and Tomlinson, 1977; Okamoto et al., 1982; Yamamoto and Hirano, 1985; Mori et al., 1986; Schmidt et al., 1989; Hirano, 1994; Laas and Hagel, 1994; Mitake et al., 1997). Although Hirano bodies are often reported in neurons of the central nervous system (CNS), particularly the Ammon's horn (CA1) in the hippocampus, they have been reported in a variety of cells such as glial cells, peripheral nerve axons, and in skeletal muscle (Hirano, 1994). These inclusions are also observed in normal elderly individuals without obvious underlying neurodegeneration (Ogata et al., 1972; Gibson and Tomlinson, 1977). The fundamental organization of Hirano bodies consists of highly ordered, eosinophilic, paracrystalline interlacing arrays of 6-10 nm parallel filaments which show a lattice or herringbone-like arrangement of fibrillary structure (Schochet and McCormick, 1972; Hirano, 1994). They have been reported to contain actin filaments and actin-associated proteins (Goldman, 1983; Galloway et al., 1987; Maciver and Harrington, 1995), microtubule associated proteins including tau (Galloway et al., 1987; Peterson et al., 1988; Davis et al., 2008), and a variety of signaling molecules and transcriptional regulators including protein kinase C (Shao et

al., 2006), inducible nitric oxide synthase (Lee et al., 1999), FAC1 (Jordan-Sciutto et al., 1998), and epitopes from the cytoplasmic region of the amyloid precursor protein (Munoz et al., 1993). The latter observation is particularly interesting, since the carboxy-terminal fragment of the amyloid precursor protein (AICD or γ-CTF) is released by presenilin-dependent gamma secretase cleavage of the amyloid precursor protein. AICD forms multimeric complexes with the nuclear adaptor protein Fe65, the histone acetyltransferase Tip60, or CP2/LSF/LBP1 transcription factor, and these complexes potently stimulate gene expression and induce apoptosis (Cao and Südhof, 2001; Kinoshita et al., 2002; Kinoshita et al., 2002; Kim et al., 2003; Cao and Südhof, 2004; Kim et al., 2004; King and Turner, 2004; von Rotz et al., 2004; Xu et al., 2007).

The physiological roles of Hirano bodies are not understood, because most studies of Hirano bodies have been performed in post-mortem samples from patients with neurodegenerative disease. Model Hirano bodies were first induced in *Dictyostelium* by expression of modified forms of a 34 kDa actin bundling protein with activated actin binding activity (Maselli et al., 2002; Maselli et al., 2003). More recently, we have demonstrated formation of model Hirano bodies in cultured mammalian cells, and compared these model Hirano bodies to authentic Hirano bodies in the brain by rigorous immunohistochemical and ultrastructural criteria providing firm evidence that this system provides a good model for studies

of Hirano bodies (Davis et al., 2008). In this paper, we have utilized this model to test the hypothesis that Hirano bodies interact with and modulate signaling by the C-terminal fragment of amyloid-β precursor protein (AICD). We report that expression in human H4 cells of GFP fused to the carboxy-terminus of a 34 kDa actin binding protein (CT-GFP) with activated actin binding activity induces the formation of model Hirano bodies that contains sites for accumulation of a C-terminal fragment of amyloid-β precursor protein (AICD) and a neuronal adaptor protein Fe65. The model Hirano bodies efficiently decrease AICD-induced apoptotic cell death determined by cell viability and caspase-3 activity. Moreover, we demonstrate that model Hirano bodies down-regulate the transcriptional activity of APP-Gal4 and APPct-Gal4 reporter constructs in the presence of Fe65. Therefore, our results suggest that a physiological effect of Hirano bodies on mammalian cells is to impede and down-regulate AICD-induced gene transactivation, and AICD-mediated apoptosis.

Material and Methods

Generation of expression construct and cell culture conditions

For generation of the expression construct for model Hirano bodies (Lim et al., 1999b; Maselli et al., 2002), truncated CT fragment (amino acids 124-295) encoding 34 kDa actin bundling protein from *Dictyostelium* was subcloned into the BamHI site of the pEGFP-N1

(Clontech, Palo Alto, CA) at the carboxyl-terminus to express a fusion protein of CT with GFP (CT-GFP) (Davis et al., 2008). H4 cells (American Type Culture Collection, Manassas, VA) and HEK293T (CRL-1573, ATCC) cells derived from human embryonic kidney cells were cultured in Dulbecco's modified Eagle's medium (DMEM) supplemented with 100 U/ml penicillin/streptomycin and 10% fetal bovine serum. Transient transfection of cells was performed using FuGene 6 (Roche Applied Science, Nutley, NJ) or LipofectAMINE PLUS (Invitrogen, Carlsbad, CA) according to the manufacturer's instructions. To generate stable cell lines expressing pEGFP-N1 or CT-GFP in H4 and HEK 293 cells, cells were transfected following the manufacturer's instructions with 10 μg of plasmid DNA and either 50 μL of LipofectAMINE PLUS or FuGene 6 per 100 mm culture dish. Stable cell lines were generated through G418 selection (800 μg/ml final concentration) for 14 days, and clones were isolated and sorted by MoFlo cell sorter (DakoCytomation, Ft. Collins, Colorado).

Immunofluorescence

Immunofluorescence of transiently transfected cells was performed 24–48 h post-transfection. The cells were fixed in 3.7% formaldehyde for 10 min, washed three times with PBS, permeabilized with 0.2% Triton X-100 for 5 min, and blocked with PBS containing 5 % bovine serum albumin for 1 h at room temperature. The cells were incubated with appropriate

primary antibodies for 1 h at room temperature: mouse anti-HA.11 monoclonal antibody to label HA-Fe65, rabbit anti-c-Myc A-14 (Santa Cruz Biotechnology, Santa Cruz, CA; 1:200) to label APPc58-myc. The cells were washed three times with PBS and labeled with Cy5-conjugated anti-mouse or anti-rabbit IgG antibody (Jackson Immunoresearch Laboratories, West Grove, PA) or TRITC-conjugated anti-mouse or anti-rabbit IgG antibody (Sigma-Aldrich, St. Louis, MO) and Hoechst 33342 (Sigma-Aldrich, St. Louis, MO) for labeling nuclei for 1 h at room temperature. The cells were washed three times with PBS, mounted with Crystal Mount (Biomeda, Foster City, CA), and examined with a Leica TCS SP2 spectral confocal microscope with coherent Ti:sapphire multiphoton laser (Mira Optima 900-F) (Leica Microsystems Inc, PA).

Assessment of cell viability and caspase-3/7 activity

H4 cells stably expressing CT-GFP or EGFP were plated at 4 x 10^5 cells in 60-mm culture dishes. Cells were transiently transfected with 0, 0.5 or 1.0 μg of APPc58-myc (generously provided by Dr. Bradley T. Hyman, Harvard Medical School, Charlestown, Massachusetts). At 24 h post-transfection, cells were stained directly with a mixture of 10 μg Hoechst 33342 and 10 μg propidium iodide. Stained cells were visualized and counted using the confocal microscope with a 40X water immersion objective in five random fields from each culture dish. More than one hundred cells were counted per field in triplicate for each condition. To calculate the cell

death ratio, the number of propidium iodide stained cells was divided by the total number of Hoechst stained cells. Caspase activity was measured by fluorometric Apo-One Homogeneous Caspase-3/7 assay (Promega, Madison, WI). Cells were transiently co-transfected with APPc58-myc and pCS-βgal constructs in 60-mm culture dishes. At 24 h post-transfection, cells were washed twice with PBS and lysed with 500 μL of 1X reporter lysis buffer at room temperature for 15 min. After centrifugation, protein concentrations in the supernatant were determined by Bradford protein assay (Bio-Rad, Richmond, CA, USA) using BSA as a standard. Cell lysates (20 μg of protein) and caspase-3/7 substrate (Z-DEVD-R110) were added to 96-well clear-bottom plates in triplicate wells and incubated at 37°C for 1 h to measure caspase-3/7 activity. Reporter lysis buffer without cells was used to measure background fluorescence. Fluorescence of the rhodamine 110 leaving group was measured on a fluorescence plate reader (Bio-Tek Synergy HT, Winooski, VT) set at 499 nm excitation and 512 nm emission. Caspase-3/7 activity was calculated as [((mean R110 fluorescence performed in triplicate)-(mean background fluorescence)) divided by μg of protein]. In addition, to normalize transfection efficiency of APPc58-myc in caspase assays, cells were co-transfected with 0.25 μg of pCS-β gal construct. The β-galactosidase product was measured at 420 nm. All measurements were performed in triplicate in three independent experiments. Statistically significant differences were determined using Student’s t-test.

Immunoprecipitation and western blot

HEK293T cells stably expressing EGFP or CT-GFP were plated at a density of 2 x 10^6 cells per 100 mm diameter dish. Cells were transfected with APPc58-myc or co-transfected with HA-Fe65 plasmid (Cao and Südhof, 2001) (generously provided by Dr. Thomas Südhof, Southwestern Medical School, Dallas, TX) using FuGene6 reagent according to manufacturer recommendations. At 48 hr post-transfection, cells were washed twice with ice-cold PBS and lysed with lysis buffer (1% triton-X 100, 0.1% SDS, 0.5% deoxycholic acid, 20 mM Tris-Cl pH 7.5, 10% glycerol, 0.5 M EDTA, 100 mM PMSF, and protease inhibitor cocktail (Roche Applied Science) for 10 min on ice. Cells were scraped, collected, and incubated for 20 min on ice with occasional vortexing. Cell debris was separated from total protein lysates by centrifugation at 13,000g for 20 min at 4°C. Supernatant was stored at -20°C until used. Protein concentrations of the supernatants were determined by Bradford protein assay using BSA as a standard. For immunoblot analysis, samples were loaded with 50 μg of protein from total protein lysates and separated by SDS-PAGE. Blots were probed using anti-34 kDa (B2C) mouse monoclonal antibody at a 1:5000 dilution or anti-GFP mouse monoclonal antibody (Molecular Probes-Invitrogen, Carlsbad, CA) at a 1:3000 dilution. The signals were detected by chemiluminescence (Pierce Biotechnology, Rockford, IL). For immunoprecipitation assays, cell lysates of 500 μg of total protein were immunoprecipitated with either anti-APPct (Sigma-Aldrich, St. Louis, MO),

anti-c-Myc A-14 (Santa Cruz Biotechnology), anti-Fe65 E-20 (Santa Cruz Biotechnology), or anti-HA.11 (Covance) antibody, and collected with protein G-Agarose (Roche Applied Science, Nutley, NJ). The beads were washed 3 times in lysis buffer. Immunoprecipitated proteins were eluted, resolved by SDS-PAGE, and analyzed by immunoblotting with chemiluminescent detection.

Transactivation assays

This assay was performed essentially as described (Cao and Südhof, 2001). For Gal4 transactivation assays, luciferase assays were performed using a Dual-Glo luciferase assay system (Promega, Madison, WI) according to the manufacturer's instructions. Most plasmids for transactivation assays were a generous gift from Dr. T. Südhof (University of Texas Southwestern Medical Center, Dallas, TX); (A) pG5E1B-luc (0.1 μg DNA) which contains five Gal4 binding sites and the E1B minimal promoter in front of the firefly luciferase gene; (B) pMst (Gal4, 0.1 μg DNA), pMst-APP695 (APP-Gal4, 0.1 μg DNA), pMst-APP695* (APP*-Gal4, 0.1 μg DNA), pMst-APPct (APPct-Gal4, 0.1 μg DNA), and pMst-APPct* (APPct*-Gal4, 0.1 μg DNA); Plasmids with * contain NATA mutation instead of NPTY in the C-terminal domain of APP. (C) pRL-TK (kind gift of Dr. J. Lauderdale, University of Georgia, 0.02 μg DNA) which produces *Renilla* luciferase as a control for transfection efficiency; (D) HA-Fe65 (0.1 μg DNA)

which stimulates transcription by binding to the YENPTY sequence of the C-terminal domain of APP. Briefly, HEK293T cells stably expressing EGFP or CT-GFP were co-transfected with three or four plasmids at a density of 1 x 10^4 cells per well in white, opaque 96-well microtiter plates using FuGene6 reagent. At 48 h after transfection, cells were lysed with Glo lysis buffer, and Firefly and Renilla luciferase activities in cell lysates were sequentially measured using the Dual-Glo Luciferase Reporter System and Lmax luminometer (Molecular Devices, Sunnyvale, Calif.). Firefly luciferase activity from reporter plasmid pG5E1B-Luc was produced by adding Dual-Glo luciferase substrate. Renilla luciferase activity from pRL-TK was produced by addition of Dual-Glo Stop&Glo substrate which is a substrate for Renilla luciferase and acts also as the stop solution for firefly luciferase. Firefly luciferase luminescence was normalized by Renilla luciferase luminescence as a control for transfection efficiency and further normalized by beta-galactosidase activity as a control for the transactivation assay. The mean values were obtained from transactivation assays performed in triplicate and repeated in at least three independent experiments. Statistical analyses were performed using Student's t-test.

Results

Localization of the C-terminal domain of amyloid-β precursor protein (AICD) and Fe65 in Hirano bodies

We have developed a cell culture model for the formation of Hirano bodies in *Dictyostelium* and mammalian cells using altered forms of the 34 kDa actin bundling protein (Maselli et al., 2002; Maselli et al., 2003; Davis et al., 2008). We wanted to verify whether the C-terminal fragment of APP is associated with model Hirano bodies in human H4 cells stably expressing CT-GFP fusion protein as predicted by the original study of Hirano bodies in the CA1 region of the hippocampus (Munoz et al., 1993). Immunofluorescence of H4 stable cells expressing either GFP or CT-GFP was performed utilizing an antibody raised against the C-terminal amino acids 676-695 of APP. This antibody recognizes all endogenous forms of APP that contain the COOH-terminus including APP695, C99, C83, and C57-59. This collection of APP isoforms recognized by the antibody to the COOH terminus will be referred to as APPx. APPx is diffusely distributed through the control H4 cells expressing GFP, and co-localizes with Hirano bodies in CT-GFP H4 cells (Fig 2.1A).

Fe65 is a neuronal adaptor protein that interacts with the C-terminal domain of APP through a YENPTY binding motif. The Fe65 is activated by interaction with this YENPTY motif, and the activated form of Fe65 potently activates transcription in the nucleus (Cao and Südhof,

2001; Kinoshita et al., 2002; Kim et al., 2003; Cao and Südhof, 2004). Since APPx is co-localized in model Hirano bodies, we assessed whether Fe65 is also co-localized in model Hirano bodies in H4 stable cells expressing CT-GFP fusion protein. In H4 stable cells expressing GFP, Fe65 was predominantly localized in the nucleus and also diffusely distributed in the cytoplasm (Fig 2.1B). Fe65 was also localized in the nucleus of CT-GFP stable cells (Fig 2.1B), but concentrated in model Hirano bodies in the cytoplasm of CT-GFP stable cells. These results show that Fe65 also associates with model Hirano bodies.

Biochemical confirmation of the localization of APPx and Fe65 in Hirano bodies was obtained through immunoprecipitation using antibody recognizing either the C-terminal fragment of APP or anti-Fe65. Blots were probed with an antibody to GFP that recognizes free GFP and CT-GFP in the control and Hirano body containing cells, respectively (Fig 2.2A). The input obtained with antibody to the C-terminal fragment of APP contained full length APP (not shown), and C99/C83 (Fig 2.2B). The AICD (C57-59) is probably not detectable due to its labile state (Cupers et al., 2001). The 46 kDa CT-GFP fusion protein was detected as a single band in immunoprecipitates prepared with anti-APPx or anti-Fe65, supporting the conclusion that model Hirano bodies expressing CT-GFP fusion protein contain sites for accumulation of endogenous Fe65 (Fig 2.2C) and APPx including at least APP 695 and gamma-secretase cleaved APP (C99/C83) (Fig 2.2B).

To determine directly whether AICD (C58) could also associate with Hirano bodies, H4 stable cell lines expressing GFP or CT-GFP were transiently transfected with APPc58-myc (AICD), and the localization of APPc58-myc was determined by immunofluorescence with anti-c-Myc antibody (Fig 2.3A). The APPc58-myc showed a predominantly nuclear localization with diffuse cytoplasmic staining in GFP stable cells (Fig 2.3B), in agreement with previous reports of the localization of APPc58 in cells lacking Hirano bodies (Kinoshita et al., 2002; Kim et al., 2003; von Rotz et al., 2004). By contrast, the staining with antibody to myc was also partially nuclear in CT-GFP stable cells, but significantly co-localized with model Hirano bodies in the cytoplasm of these cells (Fig 2.3A). Similarly, in cells expressing exogenous HA-Fe65 and APPc58-myc, staining with antibody to the HA epitope reveals that Fe65 is co-localized with AICD in the model Hirano bodies (data not shown). Thus, AICD and Fe65 co-localize with Hirano bodies in cells overexpressing APPc58-myc.

Biochemical confirmation of the molecular interaction of Hirano bodies and AICD was performed by immunoprecipitation from total cell lysates of cells stably expressing GFP or CT-GFP to induce model Hirano bodies, and either APPc58-myc or HA-Fe65 (Fig 2.4). Cell lysates were immunoprecipitated with anti-c-Myc antibody to APPc58-myc (AICD) or anti-HA antibody to HA-Fe65, and western blot analysis was performed with anti-GFP or anti-34 kDa (B2C) antibody. The 46 kDa CT-GFP fusion protein was detected as a single band in

immunoprecipitates prepared from Hirano body containing cells but not from control cells (Fig 2. 4). These results show that model Hirano bodies contain sites for accumulation of AICD (APPc58-myc) and Fe65 (HA-Fe65).

Inhibition of AICD-induced apoptosis by Hirano bodies

AICD and Fe65 associate with Tip60 and other factors in the nucleus to modify transcription, and to promote apoptosis by inducing GSK-3β and p53 (Kinoshita et al., 2002; Kim et al., 2003; Lu et al., 2003; Kim et al., 2004; Alves da Costa et al., 2006). In this study, we investigated the physiological effect of the presence of Hirano bodies on cell death and caspase-3 activity in GFP and CT-GFP expressing H4 cells transfected with different concentrations of APPc58-myc DNA. Immunoblotting was used to verify increases in expression of APPc58-myc with increasing concentration of plasmid used for transformation (Fig 2.5). In cells transfected with 0.5 and 1 μg of APPc58-myc, the percentage of dead cells measured by staining with propidium iodide 24 h after transfection was significantly lower in CT-GFP stable cells (10±0.9% and 25.9±2.5%) than in GFP stable cells (13±1.5% and 41.8±3.6%), respectively (means ± S.E.M; $p < 0.01$) (Fig 2.5A). Thus, AICD-induced cell death is reduced in CT-GFP expressing H4 cells that contain model Hirano bodies.

To confirm the effect of model Hirano bodies on AICD-induced cell death, we assessed the

caspase-3 enzyme activity at the same conditions. H4 stable cells were co-transfected with 0, 0.5, and 1 μg of APPc58-myc containing 0.25 μg of βgal DNA to control for transfection efficiency. Caspase-3 activities in GFP stable cells were significantly increased depending on the concentration of APPc58-myc DNA. By contrast, caspase-3 activities in CT-GFP stable cells were not significantly elevated after expression of APPc58-myc DNA (Fig 2.5B). Further, caspase-3 levels were significantly lower in CT-GFP stable H4 cells as compared to GFP stable H4 cells over the entire range of concentrations of APPc58-myc DNA (Fig 2.5B; $p \leq 0.001$). Taken together, these results show that the presence of model Hirano bodies decreases AICD-induced apoptosis.

Hirano bodies down-regulate Fe65 dependent transcriptional activity of APP-Gal4 and APPct-Gal4 in HEK293T cells

Since AICD and Fe65 accumulated in model Hirano bodies in H4 cells (Fig 2.1-2.4), we hypothesized that Hirano bodies might be able to modulate transcriptional activity. As reported by Cao and Südhof (Cao and Südhof, 2001; Cao and Südhof, 2004), Fe65 interacts with the YENPTY binding motif of the C-terminal domain of APP and activates transactivation of APP-Gal4 and APPct-Gal4. We examined whether model Hirano bodies regulate transcriptional activity of AICD in the presence or absence of Fe65. Transcriptional activity was measured in

HEK293T stable cells using a dual luciferase reporter method and a Gal4/UAS transactivation assay using 4 different APP and APPct constructs fused to Gal4 (Fig 2.6C), and further normalized with control Gal4 transcriptional activity. We measured Gal4 transcriptional activity in the absence (Fig 2.6A) or presence (Fig 2.6B) of exogenous Fe65 in HEK293T cells stably expressing either GFP or CT-GFP. In the absence of exogenous Fe65, there was a >10 fold enhancement of reporter activity in APPct-Gal4 transfected cells as compared to other constructs, and this enhancement was not observed following transfection with the APPct*-Gal4 mutant bearing a mutation in the YENPTY motif that mediates binding to Fe65 (Fig 2.6A). The transcriptional activation in the absence of exogenous Fe65 was consistently less in cells with Hirano bodies as compared to control cells, but the fold activation is relatively small and the differences were not statistically significant (Fig 2.6A). In the presence of exogenous Fe65 expression, transcriptional activation induced by APP and APPct was enhanced by 300- and 700-fold, respectively, in cells expressing GFP (Fig 2.6B). This dramatic enhancement was not observed following transfection with the APP*-Gal4 and APPct*-Gal4 bearing a mutation in the YENPTY motif. These results are consistent with previous reports that Fe65 is required to increase transcriptional activity of APP-Gal4 and APPct-Gal4 (Cao and Südhof, 2001; Zhao and Lee, 2003; Cao and Südhof, 2004; Perkinton et al., 2004; von Rotz et al., 2004). Most importantly, APP-Gal4 and APPct-Gal4 transcriptional activity in the presence of exogenous

Fe65 was significantly decreased in CT-GFP stable cells as compared to GFP stable cells (Fig 2.6B, $p<0.001$). These results indicate that Hirano bodies greatly down-regulated APP-Gal4 and APPct-Gal4 transcriptional activity, suggesting a physiological role of Hirano bodies in regulation of AICD- and Fe65-dependent transcriptional regulation.

Discussion

The amyloid cascade is the most prominent hypothesis proposed to explain the initiation and progression of Alzheimer's disease (Hardy and Selkoe, 2002), while other hypotheses posit important roles of other factors including oxidative stress (Butterfield et al., 2002), axonal transport (Stokin et al., 2005), presenilin (Tu et al., 2006), tau (Lee et al., 2001), and AICD (Galvan et al., 2006; Saganich et al., 2006). AICD is released from APP by the presenilin-dependent gamma-secretase, and interacts with a number of adaptor proteins that function in signal transduction, to modulate the metabolism and internalization of APP, the secretion of Aβ, and to promote gene transactivation (Sastre et al., 1998; Kinoshita et al., 2002; King and Turner, 2004; Raychaudhuri and Mukhopadhyay, 2007; McLoughlin and Miller, 2008). Further, two of these adaptor proteins, CP2 and Fe65, have genetic polymorphisms that are correlated with Alzheimer's disease (Hu et al., 1998; Lambert et al., 2000). Induction of cell death by AICD (Kinoshita et al., 2002) requires Fe65-dependent gene transactivation (Cao and Südhof, 2001),

and is likely mediated by enhanced expression of known neurotoxic agents including GSK3β and p53 (Kim et al., 2003; Alves da Costa et al., 2006; Xu et al., 2007), implying that p53-dependent apoptosis is involved. Furthermore, AICD-induced apoptosis is characterized by nuclear blebbing, TUNEL staining, and blockade by a caspase inhibitor (Kinoshita et al., 2002; Kim et al., 2003).

In addition to its role in initiation of apoptosis, AICD can also lead to changes in calcium signaling, growth factor and NF-kB pathway activation, the production, trafficking, and processing of APP, and neuronal development and differentiation (Raychaudhuri and Mukhopadhyay, 2007).

We initiated this work by revisiting the report (Munoz et al., 1993) that epitopes from the carboxy-terminus, but not the amino-terminus of APP are associated with Hirano bodies. Epitopes from the C-terminus of APP (APPx) and the adapter protein Fe65 have been localized to model Hirano bodies using both immunofluorescence and immunoprecipitation (Fig 2.1 and 2.2). Direct demonstration that AICD itself can associate with model Hirano bodies was obtained in cells transfected with epitope tagged APPc58-myc (Fig 2.3 and 2.4). In addition, cells with model Hirano bodies had reduced susceptibility to AICD-induced programmed cell death as revealed by enhanced survival and reduced activation of caspase 3 following expression of AICD (Fig 2.5). Finally, gene transactivation initiated by expression of APP-Gal4 and APPct-

Gal4 is Fe65-dependent, and is significantly reduced in cells bearing model Hirano bodies (Fig 2.6). These findings have considerable significance with regard to the AICD hypothesis.

First, how could the presence of Hirano bodies modulate AICD-induced apoptosis and gene transactivation? The simplest model is that Hirano bodies sequester AICD and Fe65, and reduce the concentration of these agents available to stimulate transcription. While the mechanism of the regulation of transcription by AICD and Fe65 is controversial, the presence of Fe65 in an active conformation in the nucleus is required for AICD-dependent transcriptional activation (Cao and Südhof, 2004), so the sequestration of Fe65 in Hirano bodies is as significant as the presence of AICD. Fe65 interacts with other nuclear proteins, CP2/LSF/LBP1 and Tip60, and plays a major role in activation of transcription (Zambrano et al., 1998; Cao and Südhof, 2001; Kim et al.). The sequestration of Fe65 in Hirano bodies can also impact the metabolism of APP, and may inhibit production of Aβ and of AICD (King and Turner, 2004), and may also interfere in other cellular functions of Fe65 (McLoughlin and Miller, 2008). In addition, Hirano bodies could impact the course of apoptosis and gene expression by sequestration of other molecules whose presence in Hirano bodies has been reported previously including iNOS (Lee et al., 1999), PKC ι/λ (Shao et al., 2006), and other transcriptional regulators including FAC1 (Jordan-Sciutto et al., 1998), and p130 (Previll et al., 2007). Sequestration of such signaling molecules could impact the results of AICD-induced gene transactivation directly, or indirectly

by affecting the metabolism, trafficking, and interactions of AICD at multiple levels. For example, it has been reported that phosphorylation of AICD at threonine 668 is required for its interaction with Fe65, import to the nucleus, and for stimulation of neurotoxicity (Chang et al., 2006). Other transcriptional modulators such as low density lipoprotein receptor related protein intracellular domain (LRPICD) and NF-κB can inhibit or repress AICD dependent gene transactivation (Kinoshita et al., 2003; Zhao and Lee, 2003). Finally, AICD can be cleaved at aspartate 664 to generate a fragment, APPc31. Expression of an APP with alanine inserted at position 664 suppresses loss of synaptic function in mouse models of AD, even though $A\beta_{42}$ levels increase and plaque deposits at normal levels (Galvan et al., 2006; Saganich et al., 2006). These results highlight the potential significance in the progression of AD of the generation of an APPc31 fragment by cleavage of AICD at aspartate 664. Since the APPc31 fragment contains the YENPTY motif required for interaction with adapter proteins, and induces cell death and promotes gene transactivation with a potency similar to or slightly less than that of APPc59 (Kim et al., 2003; Cao and Südhof, 2004; Kim et al., 2004), it is possible that Hirano bodies could affect either this cleavage event, or the localization and biological activity of APPc31. Finally, in addition to simple sequestration, the degradation of Hirano bodies would permanently remove AICD, Fe65, and other signaling molecules that traffic to these cytoskeletal inclusions. Consistent with this proposal, we have recently found that model Hirano bodies are degraded by

autophagy (Dong-Hwan Kim, R. C. Davis, R. Furukawa, and M. Fechheimer, unpublished results).

A second major question concerns the mechanism of association of AICD and Fe65 with Hirano bodies. The immunofluorescence and immunoprecipitation assays revealed an association of AICD and Fe65 with CT-GFP (Fig 2.3 and 2.4), and our working model is that this interaction is indirect. It has been known for some time that Fe65 binds to the actin associated protein mena (Ermekova et al., 1997). Studies of the localization of Fe65 show nuclear accumulation, or cytoplasmic staining that is frequently punctate rather than diffuse (Cao and Südhof, 2001). It is consistent to propose that these punctate foci arise from Fe65 that is anchored to the actin cytoskeleton through mena. In addition, interactions of APP with Fe65 and mena in lamellipodia have been proposed to modulate cell movement (Sabo et al., 2003). One explanation of this effect is that components of the actin cytoskeleton are major targets of AICD- and Fe65-dependent gene transcription (Muller et al., 2007). It will be exciting to test the proposal that mena is present in Hirano bodies and could mediate the association of Fe65 and AICD with Hirano bodies.

The reported association of tau with Hirano bodies (Galloway et al., 1987; Peterson et al., 1988; Davis et al., 2008) suggests another possible mechanism by which the presence of Hirano bodies in cells could promote cell survival. AICD and Fe65 also induce expression of glycogen

synthase kinase-3β that is involved in the phosphorylation of tau (Kim et al., 2003; Xu et al., 2007). Thus, their sequestration in Hirano bodies might modulate these interactions. In addition, Fe65 is reported to be co-localized with tau proteins in neurofibrillary tangles (Delatour et al., 2001). Finally, a recent study reveals interactions of tau with filamentous actin, and implicates rearrangement of the actin cytoskeleton in tau-induced neurodegeneration (Fulga et al., 2007). These studies focus additional attention on the fact that the actin cytoskeleton can modulate pathological processes that induce neurodegeneration. The molecular basis for such modulation presents an exciting prospect for future study.

In summary, the cultured cell system for formation of model Hirano bodies provides direct evidence that cells with model Hirano bodies grow normally, and are not necessarily involved in a stage of cell death (Maselli et al., 2002; Maselli et al., 2003; Davis et al., 2008). Further, we have shown that model Hirano bodies contain sites for accumulation of AICD as well as Fe65, and that model Hirano bodies suppress apoptosis induced by AICD and Fe65. Finally, Gal4-transactivation assays confirm that Hirano bodies reduce AICD- and Fe65-dependent transcription. Thus, our current results support the hypothesis that the formation of Hirano bodies should be considered an adaptive response involving the actin cytoskeleton that may play a protective role in the progression of neurodegenerative disease like Alzheimer’s disease. Further studies will be required to explore and to critically test this hypothesis.

Acknowledgements

We thank Drs. T. Südhof, Bradley T. Hyman, and James Lauderdale for kindly providing plasmids. This work was supported by awards to RF and MF from NSF (MCB 98-08748), the Alzheimer's Association (IIRG-00-2436), and NIH (1R01-NS04645101).

References

Alves da Costa, C., C. Sunyach, R. Pardossi-Piquard, J. Sevalle, B. Vincent, N. Boyer, T. Kawarai, N. Girardot, P. St George-Hyslop and F. Checler (2006). Presenilin-dependent gamma-secretase-mediated control of p53-associated cell death in Alzheimer's disease. J. Neurosci. **26**: 6377-6385.

Butterfield, D. A., S. Griffin, G. Munch and G. M. Pasinetti (2002). Amyloid beta-peptide and amyloid pathology are central to the oxidative stress and inflammatory cascades under which Alzheimer's disease brain exists. J. Alzheimer's Dis. **4**: 193-201.

Cao, X. and T. C. Südhof (2001). A transcriptionally active complex of APP with Fe65 and histone acetyltransferase Tip60. Science **293**: 115-120.

Cao, X. and T. C. Südhof (2004). Dissection of amyloid-b precursor protein-dependent transcriptional transactivation. J. Biol. Chem. **279**: 24601-14611.

Chang, K. A., H. S. Kim, T. Y. Ha, J. W. Ha, K. Y. Shin, Y. H. Jeong, J. P. Lee, C. H. Park, S. Kim, T. K. Baik and Y. H. Suh (2006). Phosphorylation of amyloid precursor protein (APP) at Thr668 regulates the nuclear translocation of the APP intracellular domain and induces neurodegeneration. Mol. Biol. Cell **26**: 4327-4338.

Cupers, P., I. Orlans, K. Craessarts, W. Annaert and B. De Strooper (2001). The amyloid precursor protein (APP)-cytoplasmic fragment generated by gamma-secretase is rapidly degraded but distributes partially in a nuclear fraction of neurons in culture. J. Neurochem. **78**: 1168-1178.

Davis, R. C., R. Furukawa and M. Fechheimer (2008). A cell culture model for investigation of Hirano bodies. Acta Neuropathol. (Berl) **115**: 205-17.

Delatour, B., L. Mercken, K. H. Hachimi, M. A. Colle, L. Padier and C. Duyckaerts (2001).

FE65 in Alzheimer's disease: neuronal distribution and association with neurofibrillary tangles. Am. J. Clin. Pathol. **158**: 1585-1591.

Ermekova, K. S., N. Zambrano, H. Linn, G. Minopoli, F. Gertler, T. Russo and M. Sudol (1997). The WW domain of neural protein FE65 interacts with proline-rich motifs in mena, the mammalian homolog of Drosophila enabled. J. Biol. Chem. **272**: 32869-32877.

Fulga, T. A., I. Elson-Schwab, V. Khurana, M. L. Steinhib, T. L. Spires, H. B. T. and M. B. Feany (2007). Abnormal bundling and accumulation of F-actin mediates tau-induced neuronal degeneration in vivo. Nat. Cell Biol. **9**: 139-148.

Galloway, P. G., G. Perry and P. Gambetti (1987). Hirano body filaments contain actin and actin-associated proteins. J Neuropathol Exp Neurol **46**(2): 185-99.

Galloway, P. G., G. Perry, K. S. Kosik and P. Gambetti (1987). Hirano bodies contain tau protein. Brain Res **403**(2): 337-40.

Galvan, V., O. F. Gorostiza, S. Banwait, M. Ataie, A. V. Logvinova, S. Sitaraman, E. Carlson, S. A. Sagi, N. Chevallier, K. Jin, D. A. Greenberg and D. E. Bredesen (2006). Reversal of Alzheimer's-like pathology and behavior in human APP transgenic mice by mutation of Asp664. Proc. Natl. Acad. Sci. U. S. A. **103**: 7130-7135.

Gibson, P. H. and B. E. Tomlinson (1977). Numbers of Hirano bodies in the hippocampus of normal and demented people with Alzheimer's disease. J Neurol Sci **33**(1-2): 199-206.

Goldman, J. E. (1983). The association of actin with Hirano bodies. J Neuropathol Exp Neurol **42**(2): 146-52.

Hardy, J. and D. J. Selkoe (2002). The amyloid hypothesis of Alzheimer's disease: Progress and problems on the road to therapeutics. Science **297**: 353-356.

Hirano, A. (1994). Hirano bodies and related neuronal inclusions. Neuropathol Appl Neurobiol **20**(1): 3-11.

Hu, Q., W. A. Kukull, S. L. Bressler, M. D. Gray, J. A. Cam, E. B. Larson, G. M. Martin and S. S. Deeb (1998). The human FE65 gene: genomic structure and an intronic biallelic polymorphism associated with sporadic dementia of the Alzheimer type. Human Mol. Genet. **103**: 295-303.

Jordan-Sciutto, K., J. Dragich, D. Walcott and R. Bowser (1998). The presence of FAC1 protein in Hirano bodies. Neuropathol Appl Neurobiol **24**(5): 359-66.

Kim, H.-S., E.-M. Kim, J.-P. Lee, C. H. Park, S. Kim, J.-H. Seo, K.-A. Chang, E. Yu, S.-J. Jeong, Y. H. Chong and A. Y.-H. Suh (2003). C-terminal fragments of amyloid precursor protein exert neurotoxicity by inducing glycogen synthase kinase-3b expression. FASEB J. **17**: 1951-1954.

Kim, H. S., E. M. Kim, N. J. Kim, K. A. Chang, Y. Choi, K. W. Ahn, J. H. Lee, S. Kim, C. H. Park and Y. H. Suh (2004). Inhibition of histone deacetylation enhances the neurotoxicity

induced by the C-terminal fragments of amyloid precursor protein. J. Neurosci. Res. **75**: 117-124.

Kim, H. S., E. M. Kim, J. P. Lee, C. H. Park, S. Kim, J. H. Seo, K. A. Chang, E. Yu, S. J. Jeong, Y. H. Chong and Y. H. Suh (2003). C-terminal fragments of amyloid precursor protein exert neurotoxicity by inducing glycogen synthase kinase-3beta expression. FASEB J. **17**(13): 1951-3.

Kim, J.-S., L. He and J. J. Lemasters (2003). Mitochondrial permeability transition: a common pathway to necrosis and apoptosis. Biochem. Biophys. Res. Comm. **304**: 463-470.

King, G. D. and R. S. Turner (2004). Adaptor protein interactions: modulators of amyloid precursor protein metabolism and Alzheimer's disease risk? Exp. Neurol. **185**: 208-219.

Kinoshita, A., T. Shah, M. M. Tangredi, D. K. Strickland and B. T. Hyman (2003). The intracellular domain of the low density lipoprotein receptor-related protein modulates transactivation mediated by amyloid precursor protein and Fe65. J. Biol. Chem. **278**: 41182-41188.

Kinoshita, A., C. M. Whelan, O. Berezovska and B. T. Hyman (2002). The gamma secretase-generated carboxyl-terminal domain of the amyloid precursor protein induces apoptosis via Tip60 in H4 cells. J. Biol. Chem. **277**: 28530-28536.

Kinoshita, A., C. M. Whelan, O. Berezovska and B. T. Hyman (2002). The gamma secretase-generated carboxyl-terminal domain of the amyloid precursor protein induces apoptosis via Tip60 in H4 cells. J. Biol. Chem. **277**(32): 28530-6.

Kinoshita, A., C. M. Whelan, C. J. Smith, O. Berezovska and B. T. Hyman (2002). Direct visualization of the gamma secretase-generated carboxyl-terminal domain of the amyloid precursor protein: association with Fe65 and translocation to the nucleus. J. Neurochem. **82**: 839-847.

Laas, R. and C. Hagel (1994). Hirano bodies and chronic alcoholism. Neuropathol Appl Neurobiol **20**(1): 12-21.

Lambert, J. C., L. Goumidi, F. W. Vrieze, B. Frigard, J. M. Harris, A. Cummings, J. Coates, F. Pasquier, D. Cottel, M. Gaillac, D. St. Clair, D. M. Mann, J. Hardy, C. L. Lendon, P. Amouyel and M. C. Chartier-Harlin (2000). The transcription factor LBP-1c/CP2//LSF gene on chromosome 12 is a genetic determinant of Alzheimer's disease. Human Mol. Genet. **9**: 2275-2280.

Lee, S. C., M. L. Zhao, A. Hirano and D. W. Dickson (1999). Inducible nitric oxide synthase immunoreactivity in the Alzheimer disease hippocampus: association with Hirano bodies, neurofibrillary tangles, and senile plaques. J Neuropathol Exp Neurol **58**(11): 1163-9.

Lee, V. M., M. Goedert and J. Q. Trojanowski (2001). Neurodegenerative tauopathies. Ann. Rev. Neurosci. **24**: 1121-1159.

Lim, R. W. L., R. Furukawa and M. Fechheimer (1999b). Evidence of intramolecular regulation of the Dictyostelium discoideum 34,000 dalton F-actin bundling protein. Biochemistry **38**: 16323-16332.

Lu, D. C., S. Soriano, D. E. Bredesen and E. H. Koo (2003). Caspase cleavage of the amyloid precursor protein modulates amyloid beta-protein toxicity. J. Neurochem. **87**: 733-741.

Maciver, S. K. and C. R. Harrington (1995). Two actin binding proteins, actin depolymerizing factor and cofilin, are associated with Hirano bodies. Neuroreport **6**(15): 1985-8.

Maselli, A. G., R. Davis, R. Furukawa and M. Fechheimer (2002). Formation of Hirano bodies in Dictyostelium and mammalian cells induced by expression of a modified form of an actin cross-linking protein. J. Cell Sci. **115**: 1939-1952.

Maselli, A. G., R. Furukawa, S. A. M. Thomson, R. C. Davis and M. Fechheimer (2003). Formation of Hirano bodies induced by expression of an actin cross-linking protein with a gain of function mutation. Eucaryot. Cell **2**: 778-787.

McLoughlin, D. M. and C. C. J. Miller (2008). The Fe65 proteins and Alzheimer's disease. J. Neurosci. Res. **86**: 744-754.

Mitake, S., K. Ojika and A. Hirano (1997). Hirano bodies and Alzheimer's disease. Kao Hsiung I Hsueh Ko Hsueh Tsa Chih **13**(1): 10-8.

Mori, H., M. Tomonaga, N. Baba and K. Kanaya (1986). The structure analysis of Hirano bodies by digital processing on electron micrographs. Acta Neuropathol **71**(1-2): 32-7.

Muller, T., C. G. Concannon, M. W. Ward, C. M. Walsh, A. L. Tirniceriu, F. Tribl, D. Kogel, J. H. M. Prehn and R. Egensperger (2007). Modulation of gene expression and cytoskeletal dynamics of the amyloid precursor protein intracellular domain (AICD). Mol. Biol. Cell **18**: 201-210.

Munoz, D. G., D. Wang and B. D. Greenberg (1993). Hirano bodies accumulate C-terminal sequences of beta-amyloid precursor protein (beta-APP) epitopes. J Neuropathol Exp Neurol **52**(1): 14-21.

Ogata, J., G. N. Budzilovich and H. Cravioto (1972). A study of rod-like structures (Hirano bodies) in 240 normal and pathological brains. Acta Neuropathol **21**(1): 61-7.

Okamoto, K., S. Hirai and A. Hirano (1982). Hirano bodies in myelinated fibers of hepatic encephalopathy. Acta Neuropathol **58**(4): 307-10.

Perkinton, M. S., C. L. Standen, K. F. Lau, S. Kesavapany, H. L. Byers, M. Ward, D. M. McLoughlin and C. C. J. Miller (2004). The c-Abl tyrosine kinase phosphorylates the Fe65 adaptor protein to stimulate Fe65/amyloid precursor protein nuclear signaling. J. Biol. Chem. **279**: 22084-22091.

Peterson, C., Y. Kress, R. Vallee and J. E. Goldman (1988). High molecular weight microtubule-associated proteins bind to actin lattices (Hirano bodies). Acta Neuropathol **77**(2): 168-74.

Previll, L. A., M. E. Crosby, R. J. Castellani, R. Bowser, G. Perry, M. A. Smith and X. Zhu (2007). Increased expression of p130 in Alzheimer's disease. Neurochem. Res. **32**: 639-644.

Raychaudhuri, M. and D. Mukhopadhyay (2007). AICD and its adapters-In search of new players. J. Alzheimer's Dis. **11**: 343-358.

Sabo, S. L., A. F. Ikin, J. D. Buxbaum and P. Greengard (2003). The amyloid precursor protein and its regulatory protein FE65, in growth cones and synapses in vitro and in vivo. J. Neurosci. **23**: 5407-54151.

Saganich, M. J., B. E. Schroeder, V. Galvan, D. E. Bredesen, E. H. Koo and S. F. Heinemann (2006). Deficits in synaptic transmission and learning in amyloid precursor protein (APP) transgenic mice require c-terminal cleavage of APP. J. Neurosci. **26**: 13428-13436.

Sastre, M., R. Scott Turner and E. Levy (1998). X11 Interaction with b-amyloid precursor protein modulates its cellular stabilization and reduced amyloid b-protein secretion. J. Biol. Chem. **273**: 22351-22357.

Schmidt, M. L., V. M. Lee and J. Q. Trojanowski (1989). Analysis of epitopes shared by Hirano bodies and neurofilament proteins in normal and Alzheimer's disease hippocampus. Lab Invest **60**(4): 513-22.

Schochet, S. S., Jr. and W. F. McCormick (1972). Ultrastructure of Hirano bodies. Acta Neuropathol **21**(1): 50-60.

Shao, C. Y., J. F. Crary, C. Rao, T. C. Sacktor and S. S. Mirra (2006). Atypical protein kinase C in neurodegenerative disease II: PKC i/l in tauopathies and a-synucleinopathies. J. Neuropathol. Exp. Neurol. **65**: 327-335.

Stokin, G. B., C. Lillo, T. L. Falzone, R. G. Brusch, E. Rockenstein, S. L. Mount, R. Raman, P. Davies, E. Masliah, D. S. Williams and L. S. B. Goldstein (2005). Axonopathy and transport deficits early in the pathogenesis of Alzheimer's disease. Science **307**: 1282-1288.

Tu, H., O. Nelson, A. Bezprozvanny, Z. Wang, S. F. Lee, Y. H. Hao, L. Serneels, B. De Strooper, G. Yu and I. Bezprozvanny (2006). Presenilins form ER Ca2+ leak channels, a function disrupted by familial Alzheimer's disease-linked mutations. Cell **126**: 981-993.

von Rotz, R. C., B. M. Kohli, J. Bosset, M. Meier, T. Suzuki, R. M. Nitsch and U. Konietzko (2004). The APP intracellular domain forms nuclear multiprotein complexes and regulates the transcription of its own precursor. J. Cell Sci. **117**: 4435-48.

Xu, Y., H. S. Kim, Y. Joo, Y. Choi, K. A. Chang, C. H. Park, K. Y. Shin, S. Kim, Y. H. Cheon, T. K. Baik, J. H. Kim and Y. H. Suh (2007). Intracellular domains of amyloid precursor-like protein 2 interact with CP2 transcription factor in the nucleus and induce glycogen synthase kinase-3beta expression. Cell Death Diff. **14**: 79-91.

Yamamoto, T. and A. Hirano (1985). Hirano bodies in the perikaryon of the Purkinje cell in a case of Alzheimer's disease. Acta Neuropathol **67**(1-2): 167-169.

Zambrano, N., G. Minopoli, P. de Candia and T. Russo (1998). The Fe65 adaptor protein interacts through its PID1 domain with the transcription factor CP2/FSF/LBP1. J. Biol. Chem. **273**: 20128-20133.

Zhao, Q. and F. S. Lee (2003). The transcriptional activity of the APP intracellular domain-Fe65 complex is inhibited by activation of the NF-kappaB pathway. Biochemistry **42**: 3627-3634.

Figure 2.1. The C-terminal domain of the amyloid-β precursor protein is co-localized with Hirano bodies. H4 cells stably expressing GFP or CT-GFP were stained for the presence of endogenous forms of APP that include the C-terminus (APPx) (A) or Fe65 (B), and visualized by TRITC-conjugated secondary antibodies (red). DNA was stained with Hoechst dye (blue). (A) APPx strongly localized in the nucleus with limited diffuse cytoplasmic staining in GFP stable cells, and showed extensive co-localization with Hirano bodies in the cytoplasm in CT-GFP stable cells. Areas of co-localization appear yellow in the merged image. (B) Fe65 co-localized extensively with nuclei in GFP stable cells and is partitioned between the nucleus and Hirano bodies in CT-GFP stable cells. Scale bar = 20 μm.

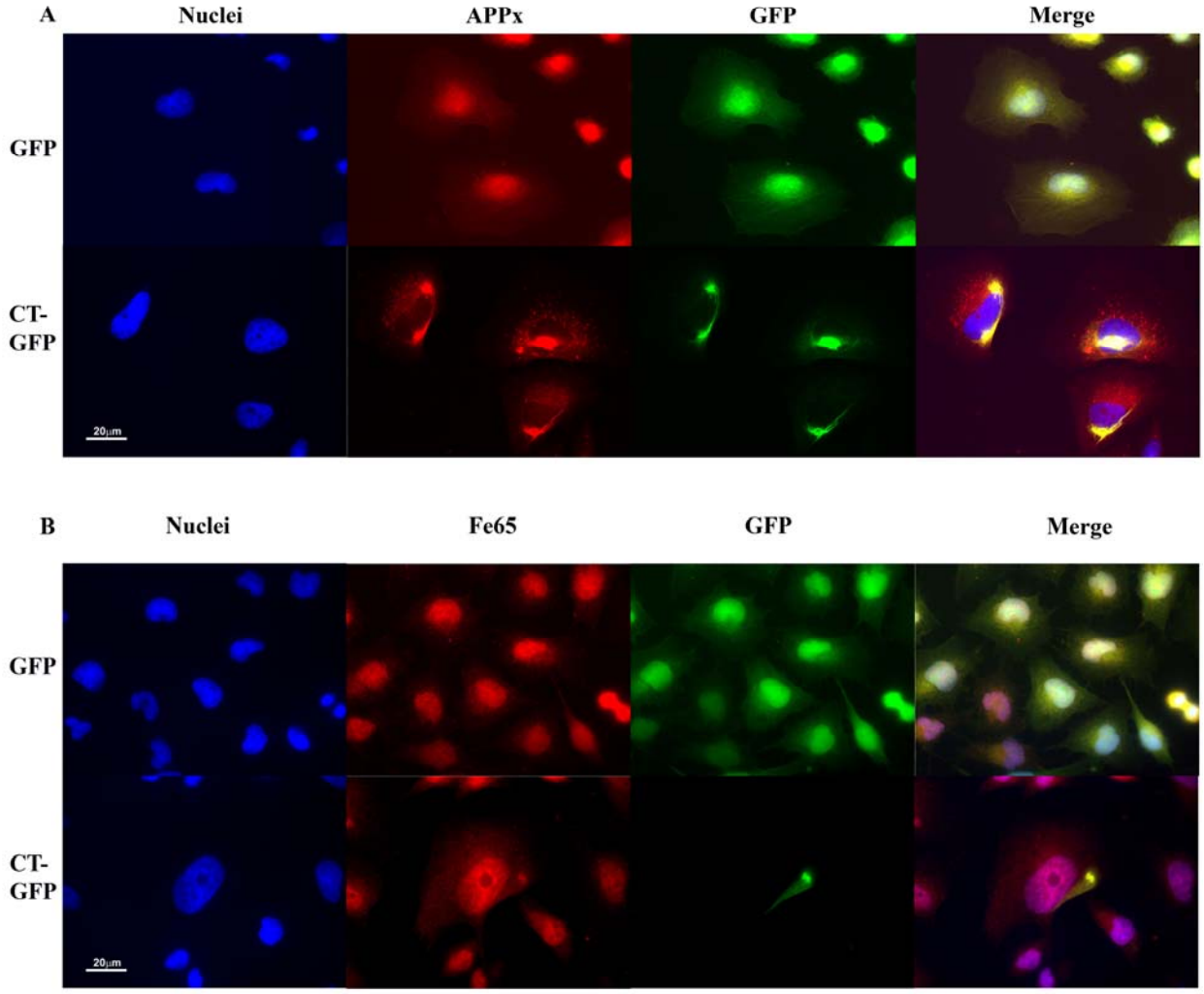
A
Nuclei
APPx
GFP
Merge
GFP
CT-GFP
20μm
B
Nuclei
Fe65
GFP
Merge
GFP
CT-GFP
20μm

Figure 2.2. Hirano bodies bind to C-terminal fragments of APP (APP695, APPC99/APPC83 and APPC57-59) and Fe65. (A) Cell lysates from wild type, GFP, and CT-GFP stable H4 cells were analyzed by western blot using antibody against GFP. To verify equal loading of the different cell lysates, α-tubulin was employed as a control. The 46 kDa CT-GFP fusion protein (arrow) and 27 kDa GFP protein (arrowhead) are detected as single bands. Marker proteins are 64.2, 48.8, 37.1, 25.9, and 19.4 kDa. (B and C) Cell lysates obtained from GFP and CT-GFP stable H4 cells were immunoprecipitated with an antibody against the C-terminal portion of APP (anti-APPx) or with anti-Fe65 antibody, respectively. Products were detected with either anti-GFP or B2C, a monoclonal antibody against 34 kDa protein. To verify equal loading of the different cell lysates, α-tubulin was employed as a control as well as APPx (panel B) and Fe65 (panel C). The input fraction in panel B contained full length APP (not shown) as well as C99/C83. The results show a specific interaction of APPx (B) and Fe65 (C) with CT-GFP in model Hirano bodies, but not with GFP.

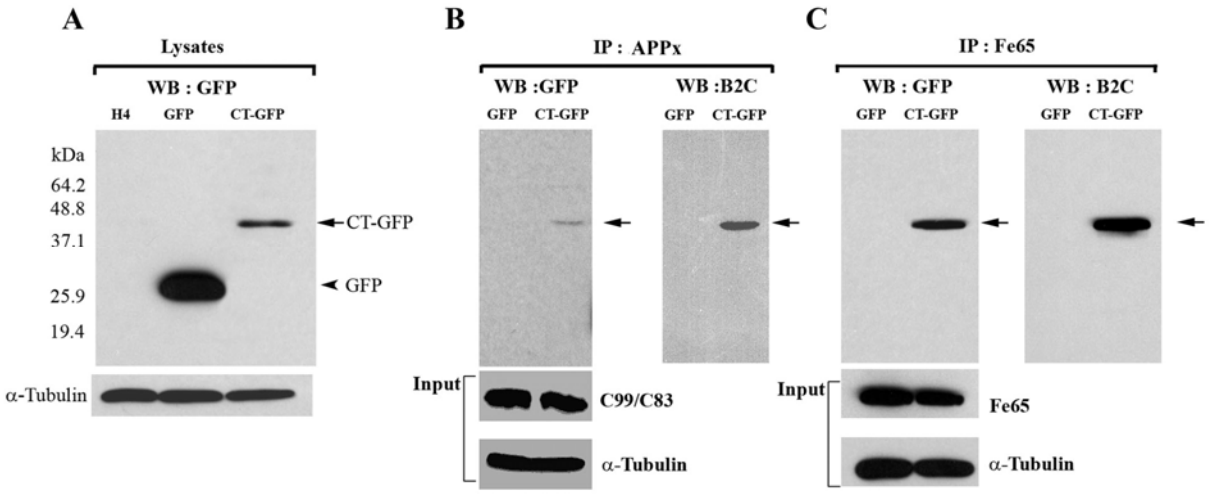
A
Lysates
WB : GFP
H4
GFP
CT-GFP
kDa
64.2
48.8
37.1
25.9
19.4
CT-GFP
GFP
α-Tubulin
B
IP : APPx
WB :GFP
WB :B2C
GFP
CT-GFP
GFP
CT-GFP
Input
C99/C83
α-Tubulin
C
IP : Fe65
WB : GFP
WB : B2C
GFP
CT-GFP
GFP
CT-GFP
Input
Fe65
α-Tubulin

Figure 2.3 The C-terminal domain of the amyloid-β precursor protein is co-localized with Hirano bodies. H4 stable cells expressing (A) CT-GFP or (B) GFP were transiently transfected with APPc58-myc and visualized by anti-myc, and TRITC-conjugated secondary antibody (red) for APPc58-myc. DNA was stained with Hoechst dye (blue). (A) Areas of specific co-localization of APPc58-myc with Hirano bodies in the cytoplasm in CT-GFP stable cells appear yellow in the merged images. (B) APPc58-myc is strongly localized in the nucleus in GFP stable cells. Scale bar = 20 μm.

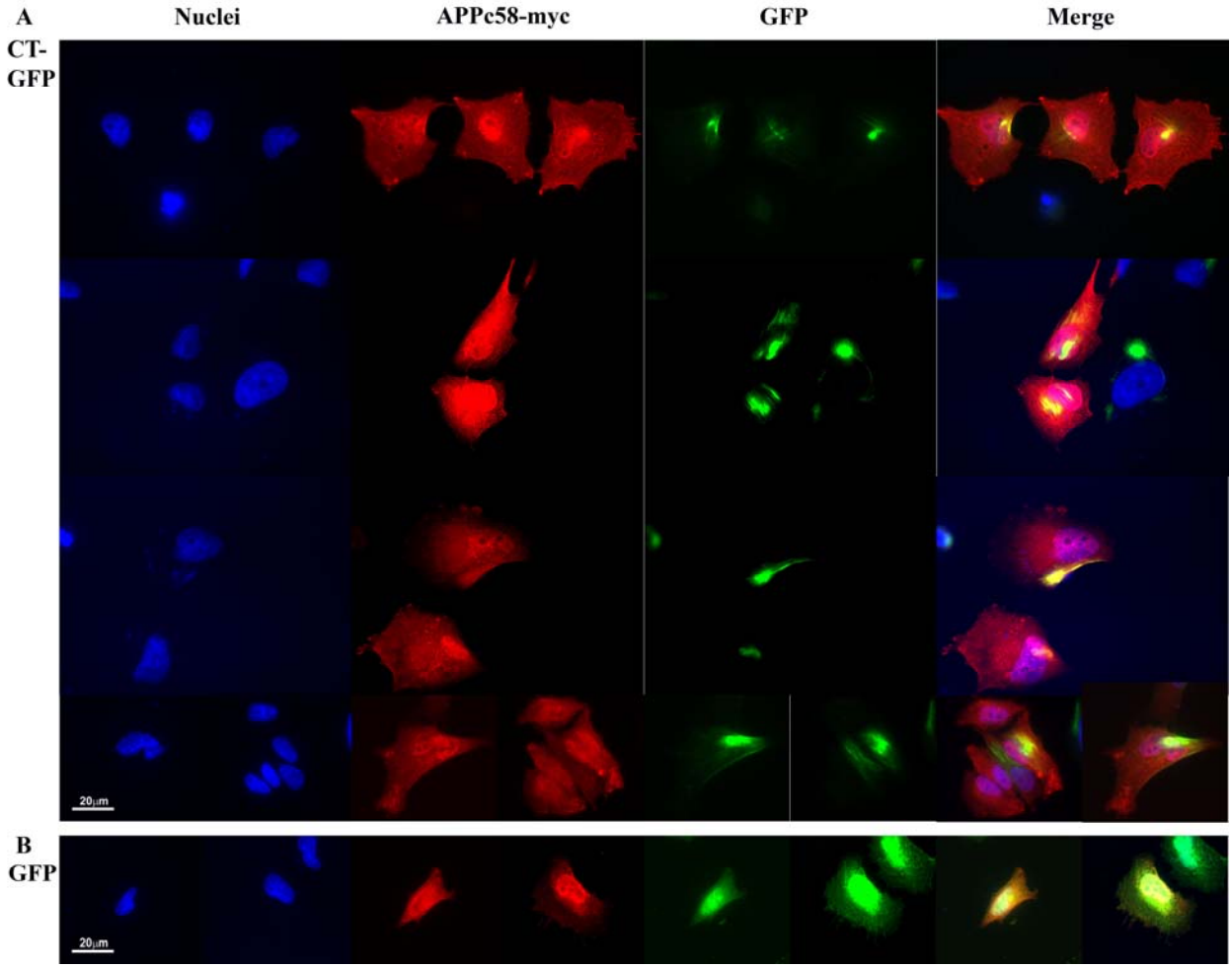
A
Nuclei
APPc58-myc
GFP
Merge
CT-GFP
20μm
B
GFP
20μm

Figure 2.4. Co-immunoprecipitation of AICD and Fe65 with Hirano bodies. The immunoprecipitated proteins were analyzed by western blot with either anti-GFP or anti-34 kDa (B2C) antibody. To verify equal loading of the different cell lysates, α-tubulin was employed as a control as well as APPc58-myc in A and HA-Fe65 in B. The results show a specific interaction of APPc58 (A) and Fe65 (B) with CT-GFP in model Hirano bodies, but not with GFP in control cells.

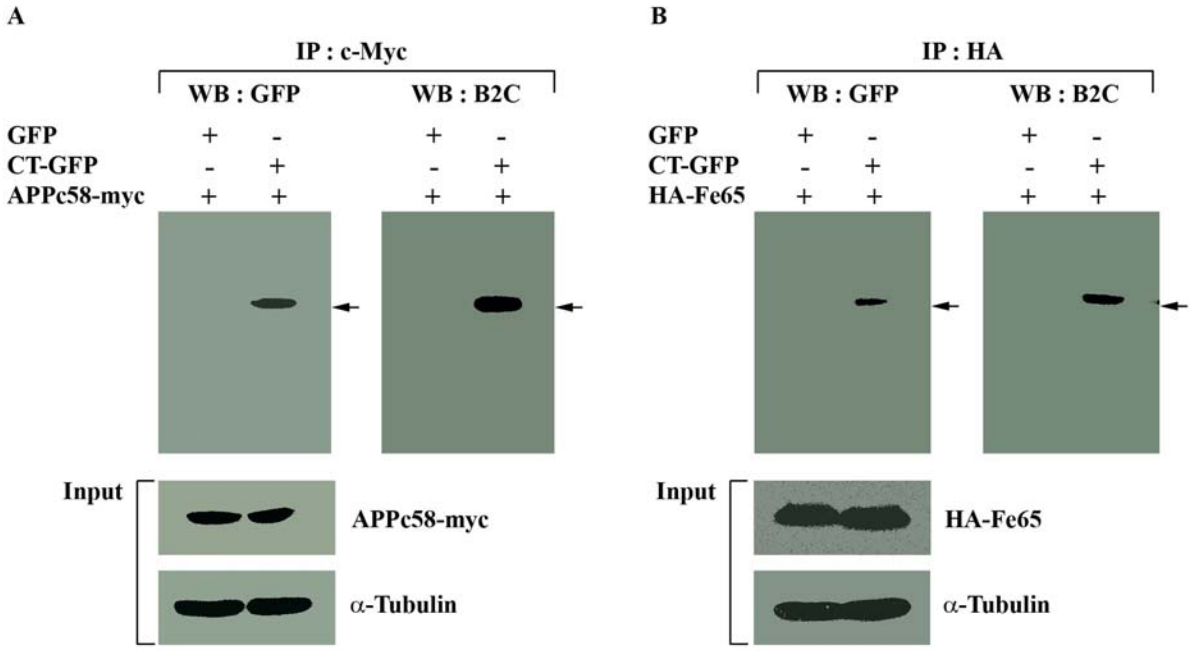
A
IP : c-Myc
WB : GFP
WB : B2C
GFP + - + -
CT-GFP - + - +
APPc58-myc + + + +
Input
APPc58-myc
α-Tubulin
B
IP : HA
WB : GFP
WB : B2C
GFP + - + -
CT-GFP - + - +
HA-Fe65 + + + +
Input
HA-Fe65
α-Tubulin

Figure 2.5. Hirano bodies significantly decrease AICD-induced apoptosis in H4 cells. H4 stable cells stably expressing GFP or CT-GFP were transiently transfected with APPc58-myc DNA (0, 0.5, or 1 μg DNA), and examined at 24 hours for cell viability (A) and caspase 3/7 activation (B). (A) Cells were stained with propidium iodide (PI) and Hoechst dye 33342 to assess cell viability. CT-GFP stable cells with Hirano bodies showed a lower percentage of cell death than GFP stable cells ($p < 0.001$). (B) Caspase-3 activity was measured using a fluorescence assay that was normalized to β-galactosidase activity as a control for transfection efficiency of APPc58-myc. Caspase-3 activity represented by relative fluorescence units (RFU) was significantly decreased in CT-GFP stable cells compared to GFP stable cells ($p < 0.001$). Data shown are mean ± S.E.M. of triplicate measurements, and repeated in three independent experiments. Cell lysates transiently transfected with various concentration of APPc58-myc DNA were examined by immunoblotting with anti-c-Myc antibodies (bottom panel) to verify that expression of APPc58-myc increased with the amount of DNA transfected.

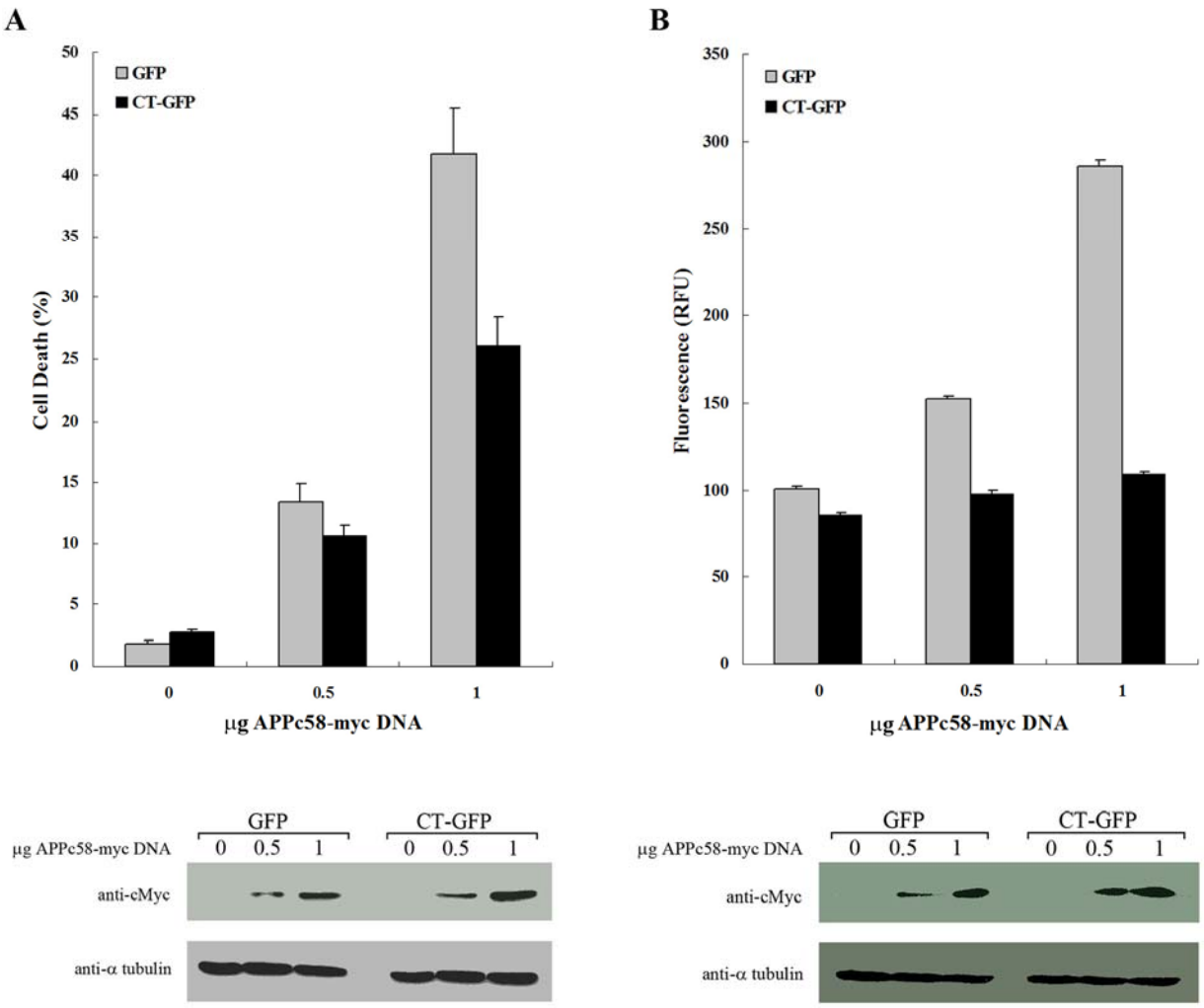
A
B
GFP
CT-GFP
Cell Death (%)
Fluorescence (RFU)
μg APPc58-myc DNA
0
0.5
1
anti-cMyc
anti-α tubulin

Figure 2.6. Fe65-dependent transcriptional activity of APP-Gal4 and APPct-Gal4 is down regulated in HEK293T stable cells with Hirano bodies. HEK293T stable cells ($1x10^4$ cells) expressing GFP or CT-GFP were co-transfected with 0.1 μg of pG5E1B-luc, 0.02 μg of pRL-TK and one of the following 5 different Gal4 constructs (C): 0.1 μg of pMst (Gal4), 0.1 μg of pMst-APP695 (APP-Gal4), 0.1 μg of pMst-APP695* (APP*-Gal4), 0.1 μg of pMst-APPct (APPct-Gal4), and 0.1 μg of pMst-APPct* (APPct*-Gal4) in the absence (A) or presence (B) of 0.1 μg of HA-Fe65. Plasmids with * contain the NATA mutation instead of NPTY in the C-terminal domain of APP that binds to Fe65. Transactivation activity was normalized to the level of transactivation of control Gal4. APP-Gal4 and APPct-Gal4 induced reporter expression was greatly enhanced by the presence of Fe65 (note the different scale bars in panels A and B). In the presence of Fe65, reporter expression was significantly lower in CT-GFP cells as compared to GFP cells ($p < 0.001$), and was significantly greater for APP-Gal4 and APPct-Gal4 than for the corresponding constructs with the NATA mutation (marked with *) in the Fe65 binding motif. Data shown are mean ± S.E.M. of triplicate measurements and repeated in three independent experiments.

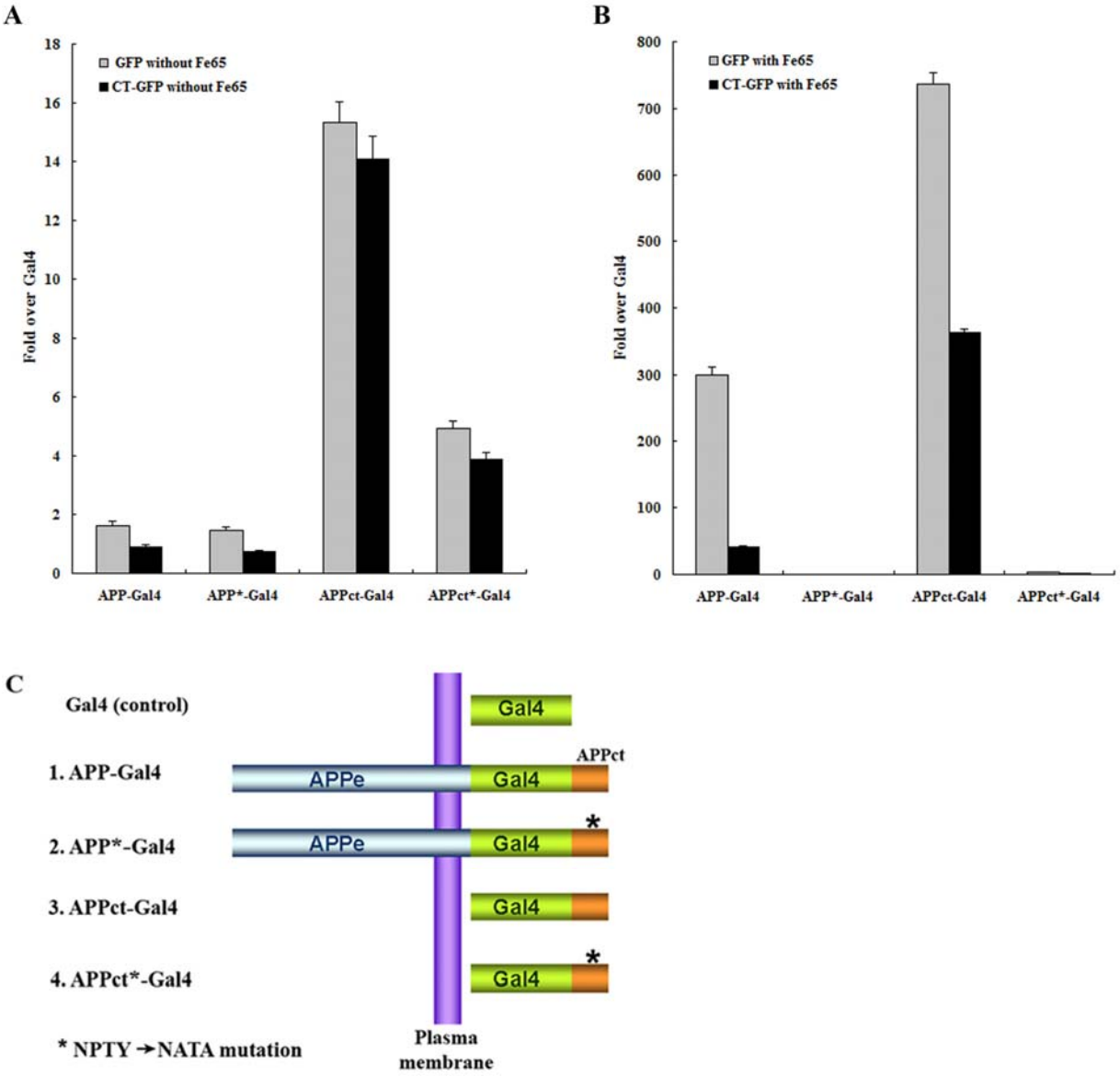
A
GFP without Fe65
CT-GFP without Fe65
Fold over Gal4
APP-Gal4
APP*-Gal4
APPct-Gal4
APPct*-Gal4
B
GFP with Fe65
CT-GFP with Fe65
Fold over Gal4
APP-Gal4
APP*-Gal4
APPct-Gal4
APPct*-Gal4
C
Gal4 (control)
1. APP-Gal4
2. APP*-Gal4
3. APPct-Gal4
4. APPct*-Gal4
APPe
Gal4
APPct
* NPTY → NATA mutation
Plasma membrane

Chapter 3

Transgenic mouse model for the formation of Hirano bodies[1]

[1] Sangdeuk Ha, Ruth Furukawa, Michael Stramiello, Lakshmi Kelamangalath, John Wagner. and Marcus Fechheimer. To be submitted to Acta Neuropathologica

Abstract

Hirano bodies are actin rich cytoplasmic inclusions found predominantly in the central nervous system in association with a variety of conditions including aging and Alzheimer's disease. Since most studies of Hirano bodies have been performed in post-mortem samples from patients, the physiological role of Hirano bodies has not been investigated. We have previously developed a cell culture model system for the formation of Hirano bodies in cells using a modified form of a 34 kD actin bundling protein named CT-GFP.

Herein, we report a transgenic mouse model of Hirano bodies. The murine Thy 1 promoter was used to drive Cre recombinase mediated excision to induce tissue-specific expression of Hirano bodies in a broad array of tissues including the brain and the hippocampus where Hirano bodies have been described most frequently. In accordance with Cre recombinase expression, CT-GFP was detected in the cerebral cortex and hippocampus, and was localized in discrete foci resembling Hirano bodies. Electron microscopy confirmed that these inclusions consist of paracrystalline F-actin. These structures were observed in the hippocampus in 6 month homozygous double transgenic mice ($R26CT^{+/+};Cre^{+}$), but not heterozygous double transgenic mice ($R26CT^{+/-};Cre^{+}$). These structures were small, and frequently enclosed by myelin sheath. In addition, spindle-shaped eosinophilic Hirano bodies were observed adjacent to pyramidal neurons primarily in the CA3 region of the hippocampus in $R26CT^{+/+};Cre^{+}$. Characterization of

these mice performed to date has not revealed any defects in histology of the brain, in cell density in the hippocampus, or in growth and fertility. Studies of long term potentiation (LTP) in hippocampal slice cultures revealed that mice with Hirano bodies ($R26CT^{+/+}$;Cre^{+}) show only minor (not significant) differences in synaptic plasticity compare to control mice ($R26CT^{+/+}$), consistent with the interpretation that Hirano bodies are not toxic or deleterious to neuronal function. In the future, this transgenic mouse model will allow us to study the physiological role of Hirano bodies *in vivo*, and to determine whether Hirano bodies may promote development of pathology or exert a protective effect during disease progression in the brain.

Introduction

Hirano bodies are cytoplasmic , eosinophilic, rod-shaped, paracrystalline inclusions that were initially described in patients with amyotrophic lateral sclerosis or parkinsonism-dementia complex on Guam (Hirano et al., 1968). Ultrastructually, Hirano bodies appear paracrystalline and are composed of 6-10 nm filaments with 10-12 nm spacing in longitudinal section, or a herringbone pattern in an oblique section (Schochet and McCormick, 1972; Tomonaga, 1974; Hirano, 1994). Hirano bodies contain F-actin, actin-associated proteins such as tropomyosin, vinculin, and cofilin (Goldman, 1983; Peterson et al., 1986; Galloway et al., 1987; Maciver and Harrington, 1995), as well as microtubule associated proteins including tau (Galloway et al., 1987;

Peterson et al., 1988). They also contain a number of other components including a wide variety of growth factors, enzymes, and transcriptional regulators including inducible nitric oxide synthase (Lee et al., 1999), FAC1 (Jordan-Sciutto et al., 1998), and the cytoplasmic fragment of the amyloid precursor protein (Munoz et al., 1993). These inclusions have been found predominantly in dendrites and cell bodies of hippocampal pyramidal neurons of the brain under various pathological conditions including Alzheimer's disease (AD), Amyotrophic Lateral Sclerosis (ALS), and Parkinson's disease (PD) as well as in normal aged individuals (Schochet et al., 1968; Gibson and Tomlinson, 1977). They have also been observed for human and animal pathological material in the cerebral cortex, cerebellum, Purkinje cells, peripheral nerve, oligodendroglia and Schwann cells, astrocytoma, and muscle cells. Some model APP transgenic mice showed cytoplasmic aggregations structurally similar to Hirano bodies in dystrophic neurites over 8 month of age (Masliah et al., 1996; Wegiel et al., 2001; Boutajangout et al., 2004), suggesting that Hirano bodies form during progression of neurodegenerative disease such as Alzheimer's disease. The physiological effect of Hirano bodies is not yet understood, since nearly all prior reports on Hirano bodies have been performed on post-mortem samples by immunohistochemistry and electron microscopy. Thus, we have recently developed cell models for the formation of Hirano bodies in cellular slime mold *Dictyostelium discoideum* as well as in a variety of cultured cell models such as fibroblasts, epithelial cells, glial cells, neuronal cell lines, and primary neurons

by expressing a truncated form (C-terminal amino acids 124-295) of the 34 kDa F-actin bundling protein (Maselli et al., 2002; Maselli et al., 2003). These model Hirano bodies in cultured mammalian cells closely match the features described for Hirano bodies in the brain (Davis et al., 2008). We reported that model Hirano bodies contain actin, actin binding protein, tau, and C-terminal fragment of amyloid precursor protein.

To understand the physiological function and effect of Hirano bodies in aging and on disease progression, we have used the Cre/loxP system to generate a transgenic mouse model expressing CT-GFP flanked by loxP sites at the Rosa26 locus (Zambrowicz et al., 1997; Sauer, 1998; Soriano, 1999). In this study, we confirmed that CT-GFP was expressed in the brain from embryonic day 14.5 following Thy1-Cre recombination as reported previously (Campsall et al., 2002). However, the formation of Hirano bodies in the hippocampus was first observed in 6 month homozygous double transgenic mice ($R26CT^{+/+}$;Cre^{+}). These inclusions revealed both eosinophilic rod-shape and paracrystalline F-actin structures consisting of 6-10 nm filaments with 10-12 nm spacing. This mouse model for Hirano bodies may provide a valuable tool to study the effects of Hirano bodies in human disease and aging.

Material and Methods

Mice

To generate inducible R26CT transgenic mouse expressing CT-GFP, a targeting vector was constructed by inserting a SA-loxP-βgeo-pA-STOP-loxP-CT-GFP-pA *CT-GFP* inducible cassette into the *Xba*I site of the vector pROSA26-1, which contains a 5-kb genomic fragment of Rosa26 locus for homologous recombination and a diphtheria toxin (DTA) expression cassette for negative selection (Soriano, 1999). The *CT-GFP* inducible cassette was generated from plasmid pSAβgeo (Friedrich and Soriano, 1991) by inserting a loxP site into *Hin*dIII site and ligating with STOP (Lakso et al., 1992) and a loxP-CT-GFP-pA fragment. A CT-GFP-pA fragment was generated by PCR in which the CT fragment (amino acids 124-295) encoding 34 kDa actin bundling protein from *Dictyostelium* was subcloned into the *Bam*HI site of the pEGFP-N1 (Clontech, Palo Alto, CA) at the carboxyl-terminus to express a fusion protein of CT with GFP (CT-GFP-pA). The targeting vector was linearized and introduced into a C57BL/6J mouse ES cell line by electroporation at the Medical College of Georgia Transgenic and Knockout Mouse Core Facility at Augusta, Georgia. Correctly targeted cell lines were screened with PCR and Southern Blot with a 5' flanking probe, both of which have been described previously (Soriano, 1999). For transgene genotyping in ES cells, we used the following primers (Fig 3.1): Pa (ROSA26 forward - 5' flanking) 5'-CCTAAAGAAGAGGCTGTGCTTTGG-3', Pb (Rosa SA

reverse) 5'-CATCAAGGAAACCC TGGACTACTG-3', Pc (GFP forward) 5'-GCACCATCTTCTTCAAGGACGAC -3', Pd (ROSA26 reverse - 3' flanking) 5'-CCGACAAAACCGAAAATCTGTG-3'. This genotyping PCR amplifies a 1.2 Kb band with Pa and Pb in 5' junction, as well as a 850 bp band with Pc and Pd in 3' junction to confirm homologous recombination in ROSA 26 locus using DNA isolated from ES cells. The targeted ES cells were microinjected into blastocysts to generate chimeric mice. The R26CT colony C57BL/6J genetic background was maintained by PCR genotyping, which can distinguish between the endogenous and transgenic Rosa26 allele.

To generate double transgenic mice for the formation of Hirano bodies in the brain, R26CT mice were mated to Thy1-Cre mice (line 703; Dr. Valerie Wallace, University of Ottawa) that express CRE recombinase broadly in neural and non-neural tissues under control of a modified Thy1 promoter (Campsall et al., 2002). For R26CT and Cre genotyping, we used the following primers (Fig 3.2). P1 (R26-1GTFOR) 5'-TTGGAGGCAGGAAGCACTTG -3', P2 (ROSASAREV) 5'-CATCAAGGAAACCC TGGACTACTG-3' and P3 (R26-1GTREV) 5'-CCGACAAAACCGAAAATCTGTG-3'. This genotyping PCR amplifies a 230 bp band from the R26CT allele and a 369 bp band from the wild-type Rosa26 allele. To check for Cre, the primers were; Cre forward 5'-CCAGGCCTTTTCTGAGCATACC-3' and Cre reverse 5'-CAACACCATTTTTTCTGACCCG-3'. The PCR product is 641 bp. The day of the vaginal plug

was designated as E0.5. All experiments were carried out with the approval of the UGA institutional animal care committee.

Immunofluorescence labeling

Immunofluorescence was performed roughly as described previously (Kim and Lauderdale, 2006). Mice from postnatal 0 to 9 month were anesthetized, and whole brains were dissected for immunostaining and histology. For cryosection, dissected whole brains were fixed with 4% paraformaldehyde overnight, followed by cryoprotection in 30% sucrose and embedding in OCT (Optical Cutting Temperature, Tissue-Tek 4583) and storage on liquid nitrogen. Sections (10μm) were cut from frozen tissue using a cryostat (Leica) and electrostatically attached to Super-frost glass slides (BDH). Sections were blocked for 1 hour in 4% milk/TST buffer (10 mM Tris–HCl, pH 7.4; 150 mM NaCl; 0.1% Tween20). They were incubated in primary antibody at room temperature overnight. The slides were washed three times in 4%/TST buffer for 5 min each, followed by 1 hour incubation with biotinylated secondary goat anti-rabbit antibody (Jackson, 1:100 dilution). After washing as above, they were incubated in Cy2 conjugated Streptavidin (Jackson, 1:200 dilution) for 30 min. Signal was detected by either standard fluorescence microscopy or laser scanning confocal microscopy. The following antibodies and dilution were used: polyclonal rabbit anti-GFP antibody (InVitrogen,

1:100 dilution) or polyclonal rabbit anti-34 kDa (B2C, 1:50 dilution) and Phalloidin-TRITC (Sigma, 1:40 dilution).

Histology

H&E staining was performed as previously described with slight modification (Moore-Scott and Manley, 2005). For paraffin sections, dissected brains were fixed with 4% paraformaldehyde at 4°C overnight, dehydrated in a graded series of 50, 75, 90, 96 and 100% ethanol, equilibrated with xylene, embedded in paraffin and sectioned on a sliding microtome at a thickness of 5-10 μm. After dewaxing with xylene, sections were stained with Mayer's hematoxylin (Sigma) and eosin (Sigma) solution and mounted on slides.

Transmission Electron Microscopy

TEM was performed as previously described with slight modification (Wegiel et al., 2001). Mice from postnatal 0 to 6 month were anesthetized, and whole brains were dissected to separate hippocampus from cortex and thalamus. Hippocampal tissue blocks were fixed by immersion with 4% paraformaldehyde/2% glutaraldehyde in 0.1 M cacodylate buffer, pH 7.4 overnight, and then postfixed in 1 % osmium tetroxide for 2 hours. After serial dehydration in ethyl alcohol, tissues were embedded in Epon (Embed-812; Electron Microscope science, PA, USA). Semithin sections were stained with 1 % toluidin blue in 1 % sodium tetraborate.

Ultrathin sections were collected on nickel grids, and counterstained with uranyl acetate for 30 min and lead citrate for 5min at room temperature to increase the signal. Samples were observed with a JEOL 100CX with an accelerating voltage of 80 kV.

Western blot analysis

Western analysis was performed by published protocols with slight modification (Boutajangout et al., 2004). The brains from transgenic mice were dissected and homogenized in 5 volumes of lysis buffer containing 1% triton-X 100, 0.1% SDS, 0.5% deoxycholic acid, 20 mM Tris-Cl pH 7.5, 10% glycerol, 0.5 M EDTA, 100 mM PMSF (phenylmethyl sulfonyl fluoride), leupeptin (1 μg/ml), pepstatin (1 μg/ml), and aprotinin (1 μg/ml). Cell debris was separated from total homogenate by centrifugation at 14,000g for 30 min at 4°C. Supernatant was stored at -80°C until used. Protein concentrations of the supernatants was determined by Bradford protein assay (Bio-Rad, Richmond, CA, USA) using BSA as a standard. For immunoblot analysis, tissue samples were loaded with 100 μg of protein per lane and separated on 12 % SDS-polyacrylamide gels. Blots were probed using anti-34 kDa (B2C) mouse monoclonal antibody at a 1:5000 dilution, anti-α Tubulin mouse antibody (Sigma) at a 1:1000 dilution, and anti-MAP LC3 (N-20) goat antibody (Santa Cruz Biotechnology, Inc.) at a 1:500 dilution. The signals were detected by chemiluminescence (Pierce Biotechnology, Rockford, IL).

Extracellular electrophysiology

This experiment is performed by the standard protocol of the Wagner laboratory (Swant and Wagner, 2006). Hippocampal slices were prepared from male homozygous transgenic mice at 7 month of age ($R26CT^{+/+}$ as a control and $R26CT^{+/+}$;Cre^{+} as a sample) using an experimental protocol performed in compliance with the University of Georgia Animal Care and Use guidelines. All mice were anesthetized with halothane prior to decapitation. The brain was removed and submerged in ice-cold, oxygenated (95% O_2/ 5% CO_2) dissection artificial cerebrospinal fluid (ACSF) containing 120 mM NaCl, 3 mM KCl, 4 mM $MgCl_2$, 1 mM NaH_2PO_4, 26 mM $NaHCO_3$, and 10 mM glucose. Horizontal brain slices were cut at a thickness of 400 μm, and the hippocampus dissected. Slices were then perfused with room-temperature, oxygenated (95% O_2 / 5% CO_2) standard ACSF containing 120 mM NaCl, 3 mM KCl, 1.5 mM $MgCl_2$, 1 mM NaH_2PO_4, 2.5 mM $CaCl_2$, 26 mM $NaHCO_3$, and 10 mM glucose at approximately 1 ml/min. Slices recovered for one hour at room temperature, and then a second hour at approximately 30°C, the temperature at which recordings were obtained. A bipolar stimulating electrode (Kopf Ins) was placed on the CA3-side of the CA1 region, in the stratum radiatum and an extracellular recording microelectrode (for LTP experiments: 1.0 MΩ tungsten recording

microelectrode, World Precision Ins; for LTD experiments: glass with ~1 μm tip, filled with standard ACSF was then positioned in the same layer in CA1.

Data were digitized at 10 kHz, low-pass filtered at 1 kHz, and analyzed with pCLAMP 9.2 software (Axon Instruments). The initial slope of the population fEPSP was measured by fitting a straight line to a 1 msec window immediately following the fiber volley. A stimulus-response curve was obtained at the beginning of each experiment, with stimulus pulses consisting of a single square wave of 270 μs duration delivered at 30, 40, 50, 60, 70, 85, 100, 120, 140, and 160 μA. To begin baseline recording, the stimulation intensity was adjusted to obtain a field EPSP of approximately 40-60 % of the maximum response, and fEPSPs were elicited by stimulation of either the Schaffer collateral-commissural pathway in stratum radiatum once every 60 s (.0167 Hz) for the duration of the experiment. Paired-pulse facilitation (PPF) was measured from an average of five pairs, each separated by 60 s, of two pulses delivered at a 50 msec interval. Synaptic responses were normalized by dividing all slopes by the average of the 5 fEPSP slopes obtained from the 5 min prior to tetanization. The tetanization protocol used to induce LTP in all experiments was a standard HFS (High Frequency stimulation) protocol consisting of 3 trains of 100 Hz/ 1 s administered at 20 s intertrain intervals. HFS is used to induce LTP, but not LTD. The tetanization protocol used to induce LTD in all experiments consisted two 15 min periods of 1 Hz stimulation, separated by 15 min of baseline recording

between these two periods. For all experiments, synaptic responses were normalized by dividing all slopes by the average of the 5 fEPSP slopes obtained from the final 5 minutes prior to initialization of tetanization. Planned comparisons with homozygous R26CT$^{+/+}$ transgenic mice as a control were made using unpaired *t*-tests. In our results, n-values indicate first the number of slices, and then number of animals tested.

Results

Generation of R26CT transgenic mice

To generate a transgenic (Tg) mouse model of Hirano bodies, we applied a gene targeting method. We prepared a targeting vector, in which the sequence encoding CT-GFP along with poly A was inserted downstream of a floxed βgeo-pA-STOP cassette, and introduced into the pROSA26-1 trap vector containing ROSA26 genomic sequences to permit homologous recombination and also a cassette containing a phosphoglycerate kinase-1 promoter and diphtheria toxin (PGK-DTA) for negative selection (Fig 3.1A) (Soriano, 1999). The targeting vector was electroporated into embryonic stem (ES) cells derived from strain C57BL/6 and the targeted alleles were screened by Southern blotting to determine homologous recombination (Fig 3.1A, B). To confirm homologous recombination of the CT-GFP transgene within the ROSA26 locus, 5' and 3' flanking regions were amplified by PCR using two primer sets at the same time

(Fig 3.1A, C). The targeted ES cell clones were injected into C57BL/6 blastocysts to generate chimeric mice. By targeting these chimeric animals for germ line transmission, we identified 4 founders (R26CT) out of 6 mice in which the CT-GFP transgene was targeted into the ROSA26 genomic region as determined by southern blot and PCR (Fig 3.1D, E). Homozygous R26CT ((R26CT$^{+/+}$) mice were generated through appropriate crosses between heterozygous R26CT (R26CT$^{+/-}$) to increase the expression level of the CT-GFP transgene. Transgene and Cre gene presence as well as copy number were determined by PCR genotyping (Fig 3.2 A-C).

Generation of R26CT$^{+/-}$;Thy1-Cre^{+} double transgenic (DTg) mice

To induce formation of Hirano bodies, we used the Cre/loxP site specific recombination system (Sauer, 1998; Soriano, 1999). Cre DNA recombinase is a powerful tool for the analysis of gene function in transgenic mice. The tissue specificity of expression for the recombinationally activated dormant transgene is determined by the promoter specificity of the Cre transgene. Thy1-Cre transgenic mice induce a transgene with tissue-specificity in the central and peripheral nerve systems including neuronal tissues of the cerebral cortex and hippocampus, and non-neuronal tissue (Campsall et al., 2002). R26CT allele carrying CT-GFP transgene were mated with Thy1-Cre (703 line) transgenic mice expressing the Cre recombinase under the control of

murine Thy1.2 regulatory elements. Double transgenic mice generated by Cre-mediated DNA recombinational activation were screened by PCR (Fig 3.2 A-C).

Expression of CT-GFP in the hippocampus at P0

As previously reported, Thy1-Cre reporter activity was shown in retina and hippocampus at postnatal day 0 (P0) in Thy1-Cre;ROSA transgenic mice (Campsall et al., 2002). We first asked whether double transgenic mice express CT-GFP transgene in the hippocampus at P0. To assess CT-GFP expression in hippocampus of the brain, frozen sections of the brain prepared from neonatal wild type, heterozygous, and homozygous transgenic mice were stained with anti-GFP antibody to intensify signal of transgene and visualized by fluorescence microscopy. CT-GFP was expressed in the hippocampus as previously reported (Campsall et al., 2002). Expression level of CT-GFP of homozygous DTg mice was higher than that of heterozygous DTg mice (Fig 3.3A). It has been reported that F-actin is a component of Hirano bodies (Goldman, 1983). To examine whether CT-GFP co-localizes with F-actin in the brain at P0, expression of CT-GFP in the hippocampus was examined by immunohistochemistry using either anti-GFP antibody (Fig 3.4) or anti-34 kDa (B2C) antibody (Fig 3.5) with phalloidin-TRITC to stain filamentous actin, respectively. We confirmed that CT-GFP was not only predominantly expressed in the hippocampus, but also co-localized with F-actin in the hippocampal pyramidal

layer including CA1, CA2, and CA3. In addition, the expression level of CT-GFP was higher in CA3 as compared to CA1 (Fig 3.4 and 3.5).

Both heterozygous and homozygous DTg mice were viable and fertile (data not shown). The Rosa26 promoter has been characterized to be a ubiquitous promoter which is relatively weak and displays a low level of transcription (Jullien et al., 2007). In order to test whether a high expression level of CT-GFP protein is required to induce formation of Hirano bodies, we compared expression levels of CT-GFP between heterozygous and homozygous double transgenic mice. Total lysates obtained from a whole brain of each mouse were examined by western blot analysis with anti-34 kDa (B2C) antibody (Fig 3.3B). Expression levels of the transgene in homozygous DTg mice were increased more than two times compared to that of heterozygous DTg mice. Therefore, the expression level of CT-GFP protein is consistent with transgene copy number.

Formation of Hirano bodies in the hippocampus of 6 month homozygous DTg mice

In various human disorders and experimental animal models, Hirano bodies have three major distinctive features; first, filamentous actin-rich inclusions (Goldman, 1983), second, eosinophilic rod-shaped cytoplasmic inclusions (Hirano et al., 1968), third, lattice-like aggregates of parallel filaments (Schochet and McCormick, 1972; Tomonaga, 1974). We have

already confirmed that R26CT transgenic mice accumulate punctate foci of actin filaments stained with phalloidin in the hippocampus of the brain after birth (Fig 3.4 and 3.5).

To see whether model Hirano bodies form eosinophic rod-like aggregates and paracrystalline structure, we performed H&E staining for histology, and electron microscopy, respectively. A whole brain was dissected at 6 month homozygous DTg mice, and each brain hemisphere was used to characterize the features of Hirano bodies. The results confirmed that cytoplasmic inclusions were formed adjacent to the perikaryon of pyramidal cells in the hippocampus (Fig 3.6O). There was no difference in cell density in the subfields CA1, CA2, and CA3 of the hippocampus between WT and R26CT allele (Fig 3.6 A-L). Ultrastructural study showed that Hirano bodies, under 1 μm in diameter, appeared to lie partially within myelinated sheath. These paracrystalline inclusions were composed of parallel filaments 8-10 nm in diameter with 10-12 nm interspacing between filaments consistent with previous study (Fig 3.7) (Ogata et al., 1972; Schochet and McCormick, 1972; Gibson, 1978). As a control, we used H4 cells expressing CT-GFP, and observed Hirano bodies in the cytoplasm without enclosed membrane (Fig 3.7A and B). Therefore, Hirano bodies were observed either by H&E or by electron microscopy in homozygous transgenic mice at 6 months of age. Hirano bodies were first seen in homozygous DTg mice prior to 6 month of age, but were not observed in heterozygous DTg mice. It was surprising to us that accumulation of Hirano bodies was not observed until 9

months for heterozygous DTg mice and 6 month for homozygous DTg mice, since we were able to detect expression of CT-GFP at P0. Since autophagy can contribute to degradation of Hirano bodies (Kim* et al.), we asked whether the delay in accumulation of Hirano bodies in our transgenic mouse model might be due to major induction of autophagy in the brain. We performed western blot analysis using whole brain lysate dissected from 1, 3, and 6 month homozygous DTg mice with anti-34 kDa (B2C) antibody to detect CT protein and anti-MAP LC3 antibody that recognize both cytosolic LC3-I and LC3-II (Fig 3.3C). Increased autophagic activity is reflected by the enhanced conversion of LC3-I to LC3-II (Hara et al., 2006). Whereas expression of CT-GFP protein stayed at similar levels up to 6 month, expression of LC3-II was not detected by 6 month (Fig 3.3C, arrow head). However, we found consistent expression of cytosolic LC3-I protein in the brain (Fig 3.3C, arrow). Thus, these results suggested that the low level of Hirano bodies prior to 6 months is not due to major induction of autophagy leading to clearance of the Hirano bodies as rapidly as they formed.

Effect of Hirano bodies on synaptic plasticity to test if Hirano bodies are toxic or deleterious to neuronal function, the field excitatory post-synaptic potential (fEPSP) was measured in the stratum radiatum layer of the CA1 region following LTP induction (Swant and Wagner, 2006). In early LTP induction at 30 min post-tetanus, the fEPSP slope appeared higher in the hippocampal slices of 7 month old control mice (homozygous $R26CT^{+/+}$) as compared to

transgenic mice (homozygous $R26CT^{+/+}$;Cre^{+}) (65 ± 17%, 37 ± 4% respectively), although the differences are not statistically significanct. Further, in late induction at180 min post-tetanus, the fEPSP slope was similar in transgenic mice compared to those of control mice (50 ± 11%, 37 ± 15% respectively) (Fig 3.8). Taken together, these initial results suggested that Hirano bodies are not toxic or deleterious to neuronal function in the hippocampus of brain.

Discussion

A mouse model of Hirano bodies was generated using the Cre/loxP system in this study. The formation of Hirano bodies was first observed in homozygous double transgenic mice ($R26CT^{+/+}$;Cre^{+}) at 6 month, and showed hallmarks of Hirano body consistent with reports in the literature regarding these inclusions. First, eosinophilic rod-shaped inclusions were seen in the pyramidal CA3 layer of hippocampus by hematoxylin and eosin staining (H&E) (Fig 3.6) (Hirano et al., 1968). Second, paracrystalline structure with a filament diameter 6-8 nm and a center to center spacing of 10-12 nm were observed inside of a myelin sheath and resemble the ultrastructural definition of Hirano bodies reported in the human hippocampus (Fig 3.7) (Ogata et al., 1972; Schochet and McCormick, 1972; Gibson, 1978). Third, immunohistochemistry study showed that CT protein was co-localized with actin filaments stained with phalloidin in the cytoplasm of hippocampal neurons in double transgenic mice (Fig 3.4 and 3.5) (Goldman, 1983).

Therefore, these results suggested that this mouse model of Hirano bodies has similar features to Hirano bodies found in humans and animal models.

We found that heterozygous double transgenic mice ($R26CT^{+/-}$;Cre^{+}) appeared healthy and are fertile without evidence of neurodegeneration or other histopathological changes for up to 9 month. In case of heterozygous DTg mice, although we were able to detect CT-GFP expression in the brain obtained from P0 to 9 month with immunohistochemisty, the formation of Hirano bodies was not detected by both H&E staining and electron microscopy (data not shown). Hirano bodies were first detected at 6 month in homozygous double transgenic mice ($R26CT^{+/+}$;Cre^{+}). There are three possible hypotheses to explain these results. First, the ROSA26 promoter is relatively weak and expresses a low level of transcription of transgene. From previous work, the transcription levels of the Dimerizable Cre (DiCre) constructs in adult or embryonic transgenic animals driven by the CAG promoter was significantly higher than that controlled by the Rosa26 promoter (Jullien et al., 2007). Second, one copy of transgene is not enough to induce the formation of Hirano bodies. We have reported the formation of Hirano bodies in slime mold *Dictyostelium* and in various cultured mammalian cells including fibroblasts, HeLa cells, HEK 293, COS7, astrocytes, neuronal cells and primary neurons (Maselli et al., 2002; Maselli et al., 2003; Davis et al., 2008). In all cases, CT protein driven by strong CMV promoter was expressed and induced the formation of Hirano bodies. However, in most

case of transfection, cells were harboring multiple copies of the gene. Thus, strong expression and multiple copies of transgene may be required to induce the formation of Hirano bodies *in vivo*. Third, time and/or other processes associated with aging may be required for the formation and accumulation of Hirano bodies. This explanation is consistent with the report that Hirano bodies are present not only in patients with specific disease conditions, but also in normal individuals who are middle aged and older (Ogata et al., 1972).

The precise mechanisms that induce formation of Hirano bodies in the brain remain unknown. Actin and actin associated proteins are the major components of Hirano bodies (Goldman, 1983; Galloway et al., 1987) as well as ADF/cofilin and tau (Munoz et al., 1993; Maciver and Harrington, 1995). Actin as a major cytoskeletal protein in neurons is involved in many aspects of cell motility, vesicle transport and membrane turnover. ADF/cofilin (AC) family regulates actin assembly, and ADF/cofilin rod inclusions are found in the hippocampus of AD brain (Maciver and Harrington, 1995). These rods disrupt distal neurite function (Bamburg, 1999; Kuhn et al., 2000; Minamide et al., 2000). Overexpression of human tau induces the formation of tau filamentous inclusions in neurons that result in cytoskeletal disruption and synaptic loss (Hall et al., 2000). Therefore, some reports suggested that defective function of the actin cytoskeleton in cells under stress, aging, and neurodegenerative disease results in neuronal cell death and synaptic loss. In our previous work, however, we reported that model Hirano

bodies down-regulate both AICD-dependent apoptosis and the transcriptional activity of the AICD/Fe65 complex. These results suggested that the association of AICD with Hirano bodies impedes its function in promoting apoptosis and modulating transcription. The relationship between cell death and cell survival by actin aggregation is controversial. Therefore, further research in this mouse model will help to understand the physiological function of Hirano bodies.

Whereas most reports of Hirano bodies in the brain of AD describe large structures (~2 μm) organized in a single ordered array (Gibson, 1978; Goldman, 1983), we saw not only smaller Hirano bodies (~1 μm) but also the fingerprint appearance in this mouse model (Fig 3.7). These findings suggested that Hirano bodies are formed by a process in which small ordered aggregates form, coalesce into larger structures, and then rearrange into a single large ordered array of the type most often reported in the literature . Studies of older mice (over 6 month of age) will reveal whether the brain and tissue distribution of Hirano bodies varies with age, and will permit comparison with Hirano bodies formed in cell cultures (Davis et al., 2008) and in the brain (Hirano et al., 1968; Hirano, 1994). One intriguing difference is that Hirano bodies are observed most frequently in the CA3 region of our double transgenic mice at 6 months of age, while they are reported most often in the CA1 region in elderly humans. The basis for this selectivity, and for the difference observed between our mouse model and studies of people will be an interesting topic for future studies.

Synaptic plasticity is the ability to change the strength of connections between neurons. Since memories are postulated to be represented by mostly interconnected networks of synapses in the brain, synapstic plasticity is one of the important neurochemical foundations of learning and memory (Martin et al., 2000). Neuronal and synaptic dysfunction are an early change that precedes the accumulation of the hallmark pathological lesions. Aβ induces alterations in synaptic function in the pathogenesis of AD (Selkoe, 2002). LTP is a form of plasticity thought to underlie learning and memory in the hippocampus region (Bliss and Collingridge, 1993). To understand the physiological roles of Hirano bodies in vivo, we measured long term potentiation (LTP) in hippocampal slices from 7 month old mice. Althought control mice (homozygous $R26CT^{+/+}$) appeared to be increased relative to transgenic mice (homozygous $R26CT^{+/+}$;Cre^{+}) in early LTP at 30 min post-tetanus (65 ± 17%, 37 ± 4% respectively), it was not significantly greater (Fig 3.8). Therefore, these initial results revealed only minor (not significant) differences in synaptic plasticity between Hirano body and littermate control mice, consistent with the interpretation that Hirano bodies are not toxic or deleterious to neuronal function.

A mouse model system will be of great value in future studies of the formation and degradation of Hirano bodies as well as their effects on disease progression. Additional investigations involving older mice and additional measures of normal neuronal function and synaptic plasticity will help to elucidate the physiological functions of Hirano bodies *in vivo*. It

may be especially fruitful to investigate the physiological effects of the interactions of AICD and tau with Hirano bodies *in vivo*, since the association of these components with Hirano bodies may either promote or impede their effects on disease progression. Although some APP transgenic mouse revealed Hirano-like bodies in the brain, physiological roles of Hirano bodies on AD progression are not clear (Masliah et al., 1996; Wegiel et al., 2001; Boutajangout et al., 2004). Until now, a variety of model APP transgenic mice have been generated and well characterized phenotypes include elevation of Abeta, progressive deposition of plaque, abnormal neuron morphology, abnormal spatial learning, and synaptic dysfunction as revealed by immunohistochemical, behavioral, and electrophysiological measures (Masliah et al., 1996; Tsien et al., 1996; Wegiel et al., 2001; Oddo et al., 2003; Boutajangout et al., 2004; Schindowski et al., 2006). Thus, we will generate multiply transgenic mice to study the effects of Hirano bodies on progression of Alzheimer's disease. Through such study, it could be possible to determine whether Hirano bodies have either a deleterious or adaptive effect on AD progression, and to discern their relation to the progress of the many different conditions with which they are associated.

Acknowledgements

We thank Philippe Soriano (Fred Hutchinson Cancer Research Center) for Rosa26 targeting vector, Southern blot probe vector and pβgeo vecotor. Thanks to Zhijie Liu (University of Georgia) for STOP vector and for helpful discussions on the experiments. Most of the microscopy was performed using the facilities of the University of Georgia Center for Advanced Ultrastructural Research. Many thanks to John P. Shields for helping with TEM. Thanks to both Michael Stramiello and Lakshmi Kelamangalath (University of Georgia) for performing electrophysiology expreiments. This work was supported by awards to RF and MF from NSF (MCB 98-08748), the Alzheimer's Association (IIRG-00-2436), and NIH (1R01-NS04645101).

References

Alves da Costa, C., C. Sunyach, R. Pardossi-Piquard, J. Sevalle, B. Vincent, N. Boyer, T. Kawarai, N. Girardot, P. St George-Hyslop and F. Checler (2006). Presenilin-dependent gamma-secretase-mediated control of p53-associated cell death in Alzheimer's disease. J. Neurosci. **26**(23): 6377-85.

Bamburg, J. R. (1999). Proteins of the ADF/cofilin family: essential regulators of actin dynamics. Annu. Rev. Cell Dev. Biol. **15**: 185-230.

Bliss, T. V. and G. L. Collingridge (1993). A synaptic model of memory: long-term potentiation in the hippocampus. Nature **361**(6407): 31-9.

Boutajangout, A., M. Authelet, V. Blanchard, N. Touchet, G. Tremp, L. Pradier and J. P. Brion (2004). Characterisation of cytoskeletal abnormalities in mice transgenic for wild-type human tau and familial Alzheimer's disease mutants of APP and presenilin-1. Neurobiol Dis **15**(1): 47-60.

Campsall, K. D., C. J. Mazerolle, Y. De Repentingy, R. Kothary and V. A. Wallace (2002). Characterization of transgene expression and Cre recombinase activity in a panel of Thy-1 promoter-Cre transgenic mice. Dev. Dyn. **224**(2): 135-43.

Davis, R. C., R. Furukawa and M. Fechheimer (2008). A cell culture model for investigation of Hirano bodies. Acta Neuropathol **115**(2): 205-17.

Friedrich, G. and P. Soriano (1991). Promoter traps in embryonic stem cells: a genetic screen to identify and mutate developmental genes in mice. Genes Dev **5**(9): 1513-23.

Galloway, P. G., G. Perry and P. Gambetti (1987). Hirano body filaments contain actin and actin-associated proteins. J. Neuropathol. Exp. Neurol. **46**(2): 185-99.

Galloway, P. G., G. Perry, K. S. Kosik and P. Gambetti (1987). Hirano bodies contain tau protein. Brain Res **403**(2): 337-40.

Gibson, P. H. (1978). Light and electron microscopic observations on the relationship between Hirano bodies, neuron and glial perikarya in the human hippocampus. Acta Neuropathol **42**(3): 165-71.

Gibson, P. H. and B. E. Tomlinson (1977). Numbers of Hirano bodies in the hippocampus of normal and demented people with Alzheimer's disease. J. Neurol. Sci. **33**(1-2): 199-206.

Goldman, J. E. (1983). The association of actin with Hirano bodies. J. Neuropathol. Exp. Neurol. **42**(2): 146-52.

Hall, G. F., B. Chu, G. Lee and J. Yao (2000). Human tau filaments induce microtubule and synapse loss in an in vivo model of neurofibrillary degenerative disease. J Cell Sci **113 (Pt 8)**: 1373-87.

Hara, T., K. Nakamura, M. Matsui, A. Yamamoto, Y. Nakahara, R. Suzuki-Migishima, M. Yokoyama, K. Mishima, I. Saito, H. Okano and N. Mizushima (2006). Suppression of basal autophagy in neural cells causes neurodegenerative disease in mice. Nature **441**(7095): 885-9.

Hirano, A. (1994). Hirano bodies and related neuronal inclusions. Neuropathol. Appl. Neurobiol. **20**(1): 3-11.

Hirano, A., H. M. Dembitzer, L. T. Kurland and H. M. Zimmerman (1968). The fine structure of some intraganglionic alterations. Neurofibrillary tangles, granulovacuolar bodies and "rod-like" structures as seen in Guam amyotrophic lateral sclerosis and parkinsonism-dementia complex. J. Neuropathol. Exp. Neurol. **27**(2): 167-82.

Jordan-Sciutto, K., J. Dragich, D. Walcott and R. Bowser (1998). The presence of FAC1 protein in Hirano bodies. Neuropathol. Appl. Neurobiol. **24**(5): 359-66.

Jullien, N., I. Goddard, S. Selmi-Ruby, J. L. Fina, H. Cremer and J. P. Herman (2007). Conditional transgenesis using Dimerizable Cre (DiCre). PLoS ONE **2**(12): e1355.

Kim, J. and J. D. Lauderdale (2006). Analysis of Pax6 expression using a BAC transgene reveals the presence of a paired-less isoform of Pax6 in the eye and olfactory bulb. Dev Biol **292**(2): 486-505.

Kim*, D.-H., R. C. Davis*, R. Furukawa and M. Fechheimer Degradation of Hirano Bodies by Autophagy. Submitted for publication.

Kuhn, T. B., P. J. Meberg, M. D. Brown, B. W. Bernstein, L. S. Minamide, J. R. Jensen, K. Okada, E. A. Soda and J. R. Bamburg (2000). Regulating actin dynamics in neuronal growth cones by ADF/cofilin and rho family GTPases. J Neurobiol **44**(2): 126-44.

Lakso, M., B. Sauer, B. Mosinger, Jr., E. J. Lee, R. W. Manning, S. H. Yu, K. L. Mulder and H. Westphal (1992). Targeted oncogene activation by site-specific recombination in transgenic mice. Proc Natl Acad Sci U S A **89**(14): 6232-6.

Lee, S. C., M. L. Zhao, A. Hirano and D. W. Dickson (1999). Inducible nitric oxide synthase immunoreactivity in the Alzheimer disease hippocampus: association with Hirano bodies, neurofibrillary tangles, and senile plaques. J. Neuropathol. Exp. Neurol. **58**(11): 1163-9.

Lim, R. W., R. Furukawa, S. Eagle, R. C. Cartwright and M. Fechheimer (1999). Three distinct F-actin binding sites in the Dictyostelium discoideum 34,000 dalton actin bundling protein. Biochemistry **38**(2): 800-12.

Maciver, S. K. and C. R. Harrington (1995). Two actin binding proteins, actin depolymerizing factor and cofilin, are associated with Hirano bodies. Neuroreport **6**(15): 1985-8.

Martin, S. J., P. D. Grimwood and R. G. Morris (2000). Synaptic plasticity and memory: an evaluation of the hypothesis. Annu Rev Neurosci **23**: 649-711.

Maselli, A., R. Furukawa, S. A. Thomson, R. C. Davis and M. Fechheimer (2003). Formation of Hirano bodies induced by expression of an actin cross-linking protein with a gain-of-function mutation. Eukaryot. Cell **2**(4): 778-87.

Maselli, A. G., R. Davis, R. Furukawa and M. Fechheimer (2002). Formation of Hirano bodies in Dictyostelium and mammalian cells induced by expression of a modified form of an actin-crosslinking protein. J. Cell Sci. **115**(Pt 9): 1939-49.

Masliah, E., A. Sisk, M. Mallory, L. Mucke, D. Schenk and D. Games (1996). Comparison of neurodegenerative pathology in transgenic mice overexpressing V717F beta-amyloid precursor protein and Alzheimer's disease. J Neurosci **16**(18): 5795-811.

Minamide, L. S., A. M. Striegl, J. A. Boyle, P. J. Meberg and J. R. Bamburg (2000). Neurodegenerative stimuli induce persistent ADF/cofilin-actin rods that disrupt distal neurite function. Nat. Cell Biol. **2**(9): 628-36.

Moore-Scott, B. A. and N. R. Manley (2005). Differential expression of Sonic hedgehog along the anterior-posterior axis regulates patterning of pharyngeal pouch endoderm and pharyngeal endoderm-derived organs. Dev Biol **278**(2): 323-35.

Munoz, D. G., D. Wang and B. D. Greenberg (1993). Hirano bodies accumulate C-terminal sequences of beta-amyloid precursor protein (beta-APP) epitopes. J. Neuropathol. Exp. Neurol. **52**(1): 14-21.

Oddo, S., A. Caccamo, J. D. Shepherd, M. P. Murphy, T. E. Golde, R. Kayed, R. Metherate, M. P. Mattson, Y. Akbari and F. M. LaFerla (2003). Triple-transgenic model of Alzheimer's disease with plaques and tangles: intracellular Abeta and synaptic dysfunction. Neuron **39**(3): 409-21.

Ogata, J., G. N. Budzilovich and H. Cravioto (1972). A study of rod-like structures (Hirano bodies) in 240 normal and pathological brains. Acta Neuropathol. (Berl) **21**(1): 61-7.

Peterson, C., Y. Kress, R. Vallee and J. E. Goldman (1988). High molecular weight microtubule-associated proteins bind to actin lattices (Hirano bodies). Acta Neuropathol. (Berl) **77**(2): 168-74.

Peterson, C., K. Suzuki, Y. Kress and J. E. Goldman (1986). Abnormalities of dendritic actin organization in the brindled mouse. Brain Res. **382**(2): 205-12.

Sauer, B. (1998). Inducible gene targeting in mice using the Cre/lox system. Methods **14**(4): 381-92.

Schindowski, K., A. Bretteville, K. Leroy, S. Begard, J. P. Brion, M. Hamdane and L. Buee (2006). Alzheimer's disease-like tau neuropathology leads to memory deficits and loss of functional synapses in a novel mutated tau transgenic mouse without any motor deficits. Am J Pathol **169**(2): 599-616.

Schochet, S. S., Jr., P. W. Lampert and R. Lindenberg (1968). Fine structure of the Pick and Hirano bodies in a case of Pick's disease. Acta Neuropathol. (Berl) **11**(4): 330-7.

Schochet, S. S., Jr. and W. F. McCormick (1972). Ultrastructure of Hirano bodies. Acta Neuropathol. (Berl) **21**(1): 50-60.

Selkoe, D. J. (2002). Alzheimer's disease is a synaptic failure. Science **298**(5594): 789-91.

Sergeant, N., J. P. David, D. Champain, A. Ghestem, A. Wattez and A. Delacourte (2002). Progressive decrease of amyloid precursor protein carboxy terminal fragments (APP-CTFs), associated with tau pathology stages, in Alzheimer's disease. J. Neurochem. **81**(4): 663-72.

Soriano, P. (1999). Generalized lacZ expression with the ROSA26 Cre reporter strain. Nat Genet **21**(1): 70-1.

Swant, J. and J. J. Wagner (2006). Dopamine transporter blockade increases LTP in the CA1 region of the rat hippocampus via activation of the D3 dopamine receptor. Learn Mem **13**(2): 161-7.

Tomonaga, M. (1974). Ultrastructure of Hirano bodies. Acta Neuropathol. (Berl) **28**(4): 365-6.

Tsien, J. Z., P. T. Huerta and S. Tonegawa (1996). The essential role of hippocampal CA1 NMDA receptor-dependent synaptic plasticity in spatial memory. Cell **87**(7): 1327-38.

Wegiel, J., K. C. Wang, H. Imaki, R. Rubenstein, A. Wronska, M. Osuchowski, W. J. Lipinski, L. C. Walker and H. LeVine (2001). The role of microglial cells and astrocytes in fibrillar plaque evolution in transgenic APP(SW) mice. Neurobiol Aging **22**(1): 49-61.

Zambrowicz, B. P., A. Imamoto, S. Fiering, L. A. Herzenberg, W. G. Kerr and P. Soriano (1997). Disruption of overlapping transcripts in the ROSA beta geo 26 gene trap strain leads to widespread expression of beta-galactosidase in mouse embryos and hematopoietic cells. Proc. Natl. Acad. Sci. U. S. A. **94**(8): 3789-94.

Figure 3.1. Targeting strategy of *CT-GFP* inducible R26CT mouse. (A) The targeting vector contains a loxP-flanked (βgeo/stop) cassette with CT-GFP pA target gene. The pROSA26-1 plasmid contains ROSA26 genomic sequences and a diphtheria toxin gene (PGK-DTA) to increase rate of homologous recombination and to permit negative selection in ES cells, respectively. The genomic organization of endogenous Rosa26 locus is shown, and the structure of the targeted Rosa26 allele named R26CT which expresses β-galactosidase and a neomycin resistance cassette fusion gene mRNA. Following Cre-mediated excision of the targeted R26CT allele, *CT-GFP* mRNA is transcribed. loxP, solid arrow head; βgeo, a fusion gene of β-galactosidase and Neomycin (Neo) resistant gene;. pA, polyA signal; STOP, a transcription termination sequence. (B) Southern Blot analysis of genomic DNA prepared from Neo resistant ES cell lines. DNA was digested with *Eco*RV and then hybridized with a 32P-labeled 5' probe indicated on the targeted locus in A. The 3.8kb *Eco*RV fragment indicates the targeted R26CT allele and the 11kb *Eco*RV fragment represents wild type Rosa26 allele. (C) PCR screening for the targeting event in ES cells. A set of primers shown in A were used to amplify 1.2 kb (Pa and Pb) and 0.85 kb (Pc and Pd) size fragments from the R26CT allele, but not wild-type Rosa26 allele. (D) Southern Blot analysis of genomic DNA prepared from heterozygous R26CT and wild-type mice. DNA was digested with *Eco*RV and analyzed using the 5' probe decribed above.

(E) PCR screening for the targeting event in transgenic mice. 1.2 kb band from the R26CT allele shows the presence of the transgene as described above for analyzing ES cells.

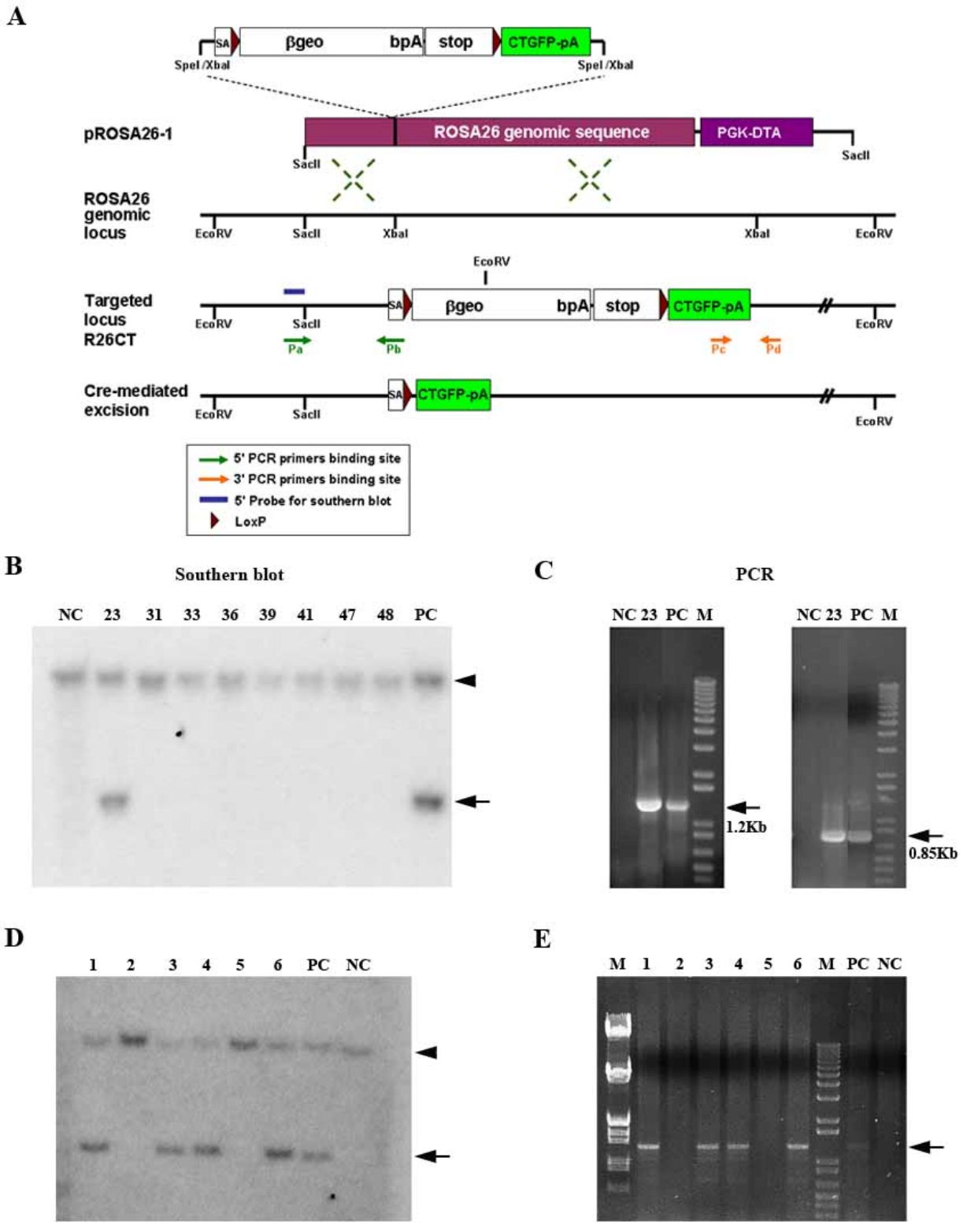
A
SA
βgeo
bpA
stop
CTGFP-pA
SpeI /XbaI
SpeI /XbaI
pROSA26-1
ROSA26 genomic sequence
PGK-DTA
SacII
SacII
ROSA26 genomic locus
EcoRV
SacII
XbaI
XbaI
EcoRV
EcoRV
Targeted locus R26CT
EcoRV
SacII
SA
βgeo
bpA
stop
CTGFP-pA
EcoRV
Pa
Pb
Pc
Pd
Cre-mediated excision
EcoRV
SacII
SA
CTGFP-pA
EcoRV
5' PCR primers binding site
3' PCR primers binding site
5' Probe for southern blot
LoxP
B
Southern blot
NC 23 31 33 36 39 41 47 48 PC
C
PCR
NC 23 PC M
1.2Kb
NC 23 PC M
0.85Kb
D
1 2 3 4 5 6 PC NC
E
M 1 2 3 4 5 6 M PC NC

Figure 3.2. Cre-mediated excision of targeted R26CT allele.

(A) PCR screen used to determine the genotype of mice in the R26CT colony. Genomic DNA made from tail biopsy of littermates obtained from mating of R26CT allele and Thy1-Cre (Cre^{+}) allele was genotyped to identify both Cre gene and trangene by PCR. (B) PCR primers for transgene were used to amplify 230 bp band (P1 and P3) from mutant allele and a 369 bp band (P1 and P2) from wild-type allele. (C) PCR primer for Cre gene is used to detect 641 bp band using same genomic DNA (material and methods). Lane 1, wild type. Lane 2, Thy1-Cre^{+}. Lane 3, $R26CT^{+/-}$. Lane 4, $R26CT^{+/-}$;Cre^{+}. Lane 5, $R26CT^{+/+}$. Lane 6, $R26CT^{+/+}$;Cre^{+}.

A

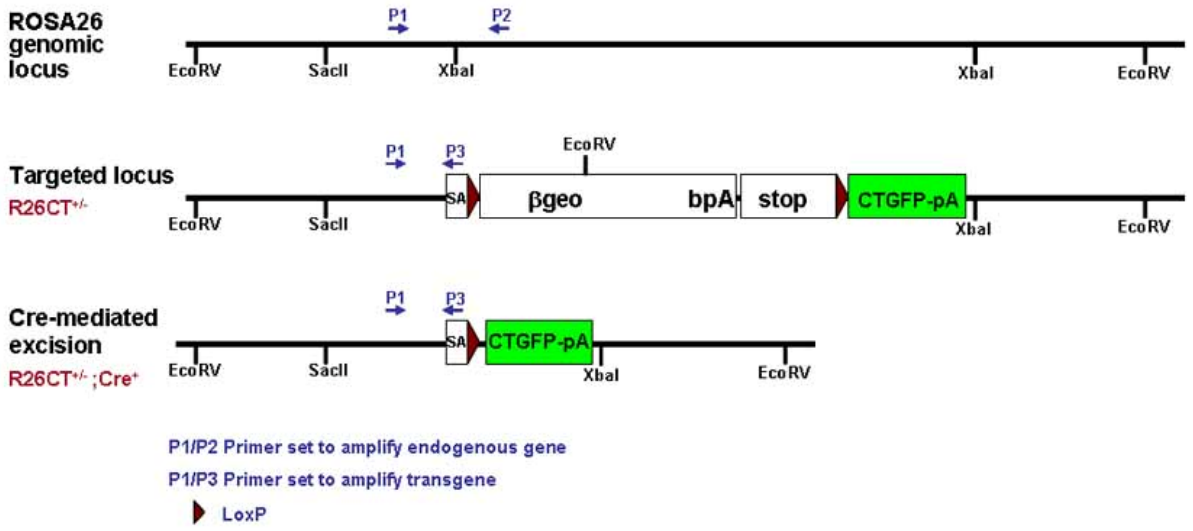
ROSA26 genomic locus
P1
P2
EcoRV
SacII
XbaI
XbaI
EcoRV
Targeted locus
R26CT+/-
P1
P3
EcoRV
SA
βgeo
bpA
stop
CTGFP-pA
EcoRV
SacII
XbaI
EcoRV
Cre-mediated excision
R26CT+/-;Cre+
P1
P3
SA
CTGFP-pA
EcoRV
SacII
XbaI
EcoRV
P1/P2 Primer set to amplify endogenous gene
P1/P3 Primer set to amplify transgene
LoxP

B

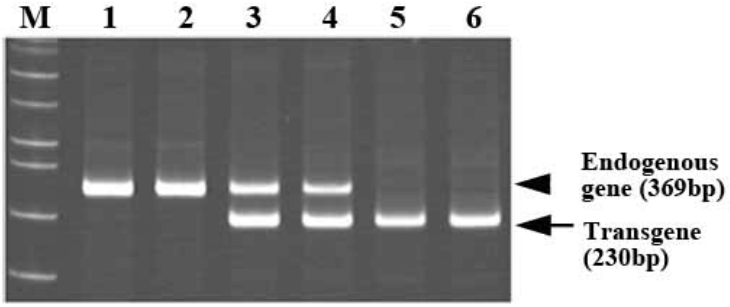
M 1 2 3 4 5 6
Endogenous gene (369bp)
Transgene (230bp)

C

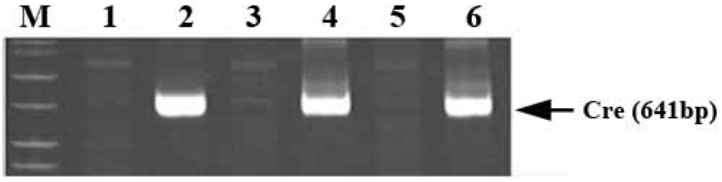
M 1 2 3 4 5 6
Cre (641bp)

Figure 3.3. Expression level of CT-GFP in the brain of double transgenic R26CT mice. (A) Transgene expression in the hippocampus of double transgenic R26CT allele and wild type (WT) at P0. Heterozygous and homozygous double transgenic mice were stained with anti-GFP antibody. (B) Brain homogenates of different double transgenic R26CT allele were analyzed by western blot using anti-34 kDa. Levels of CT-GFP were higher in the homozygous transgenic mice compare to heterozygous transgenic mice. A 46 kDa fusion protein from CT-GFP was detected by the anti-34 kDa (B2C) antibody. (C) Analysis of transgene expression over aging (6 month of age) in homozygous double transgenic mice. Total protein lysates obtained from homozygous double transgenic mice were examined by western blot analysis with the anti-34 kDa (B2C) antibody and the anti-MAP LC3. Expression level of CT-GFP fusion protein in the brain remained at the same level during this period. No evidence for induction of autophagy was observed, since virtually all of the LC3 remained in isoform LC3-I. Arrow indicate cytosolic LC3-I and arrow head represents an autophagosome-associating form, LC3-II.

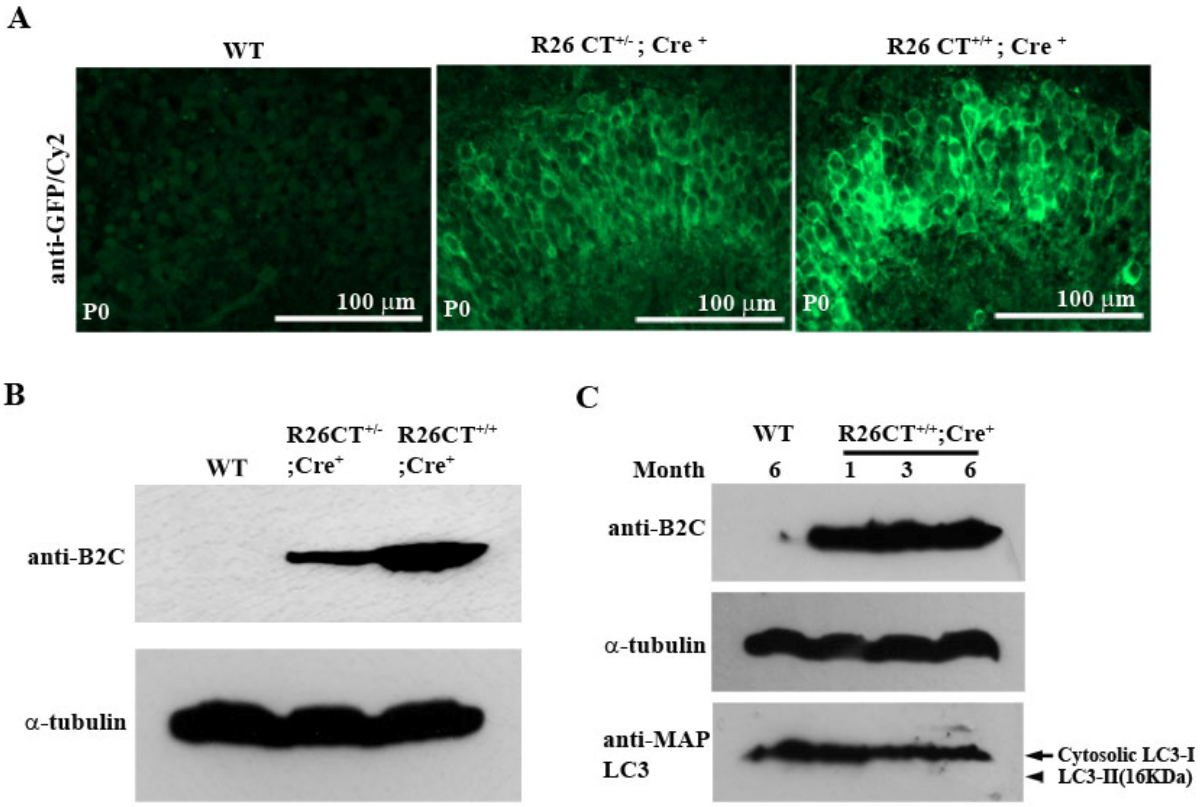
A
WT
R26 CT+/-; Cre +
R26 CT+/+; Cre +
anti-GFP/Cy2
P0
100 μm
P0
100 μm
P0
100 μm
B
WT
R26CT+/- ;Cre+
R26CT+/+ ;Cre+
anti-B2C
α-tubulin
C
WT
R26CT+/+;Cre+
Month
6
1
3
6
anti-B2C
α-tubulin
anti-MAP LC3
Cytosolic LC3-I
LC3-II(16KDa)

Figure 3.4. Expression of transgene CT-GFP in the hippocampus of newborn mice visualized with anti-GFP antibody. Sections cut through brain of wild type (A-D) and R26CT allele (E-P) were visualized by immunofluorescence at postnatal 0 (P0). Hirano bodies induced by CT-GFP protein are co-localized with phalloidin in the pyramidal layer of hippocampus. Panels show the section of brain labeled with anti-GFP (green; A, E, I, M) for staining CT-GFP protein, phalloidin conjugated TRITC (red; B, F, J, N) for staining F-actin, Hoechst 33342 (C, G, K, O) for staining nuclei, and merged images (D, H, L, P). (A-D), wild type; (E-H), heterozygous $R26CT^{+/-}$;Cre^{+}; (I-P), homozygous $R26CT^{+/+}$;Cre^{+}. (M-P), Higher magnification of hippocampal cells in homozygous double transgenic mice. Areas of co-localization appear yellow in the merged image. Scale bar = 100 μm.

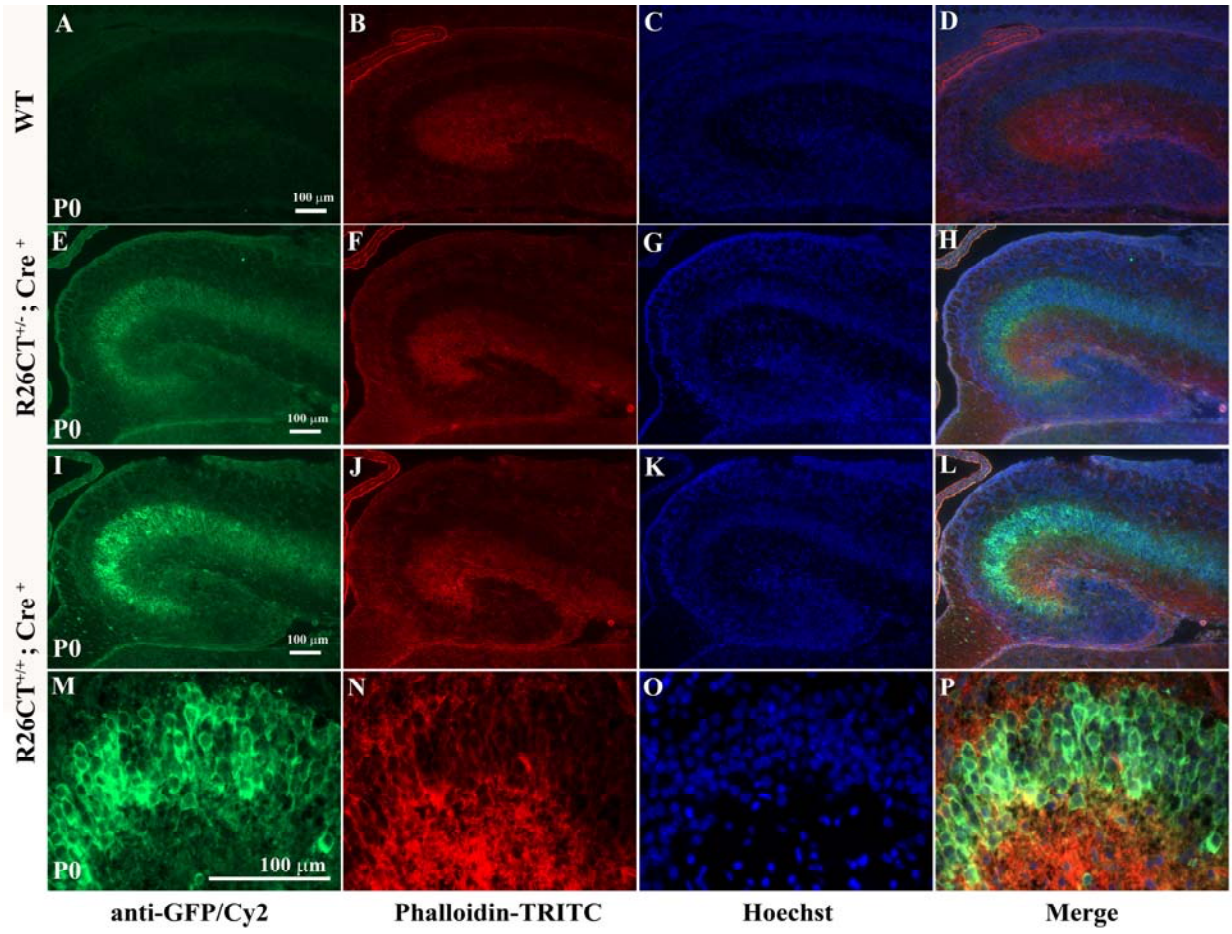
A
B
C
D
WT
P0
100 μm
E
F
G
H
R26CT+/- ; Cre +
P0
100 μm
I
J
K
L
R26CT+/+ ; Cre +
P0
100 μm
M
N
O
P
P0
100 μm
anti-GFP/Cy2
Phalloidin-TRITC
Hoechst
Merge

Figure 3.5. Expression of transgene CT in the hippocampus of newborn mice visualized with B2C antibody that recognizes the CT protein. Sections cut through brain of wild type (A-D) and R26CT allele (E-P) were visualized by immunofluorescence at postnatal 0 (P0). Hirano bodies induced by CT-GFP protein are co-localized with phalloidin in the pyramidal layer of hippocampus. Panels show the section of brain labeled with anti-GFP (green; A, E, I, M) for staining CT-GFP protein, phalloidin conjugated TRITC (red; B, F, J, N) for staining F-actin, Hoechst 33342 (C, G, K, O) for staining nuclei, and merged images (D, H, L, P). (A-D), wild type; (E-H), heterozygous $R26CT^{+/-}$;Cre^{+}; (I-P), homozygous $R26CT^{+/+}$;Cre^{+}; (M-P), Higher magnification of hippocampal cells in homozygous double transgenic mice. Areas of co-localization appear yellow in the merged image. Scale bar = 100 μm.

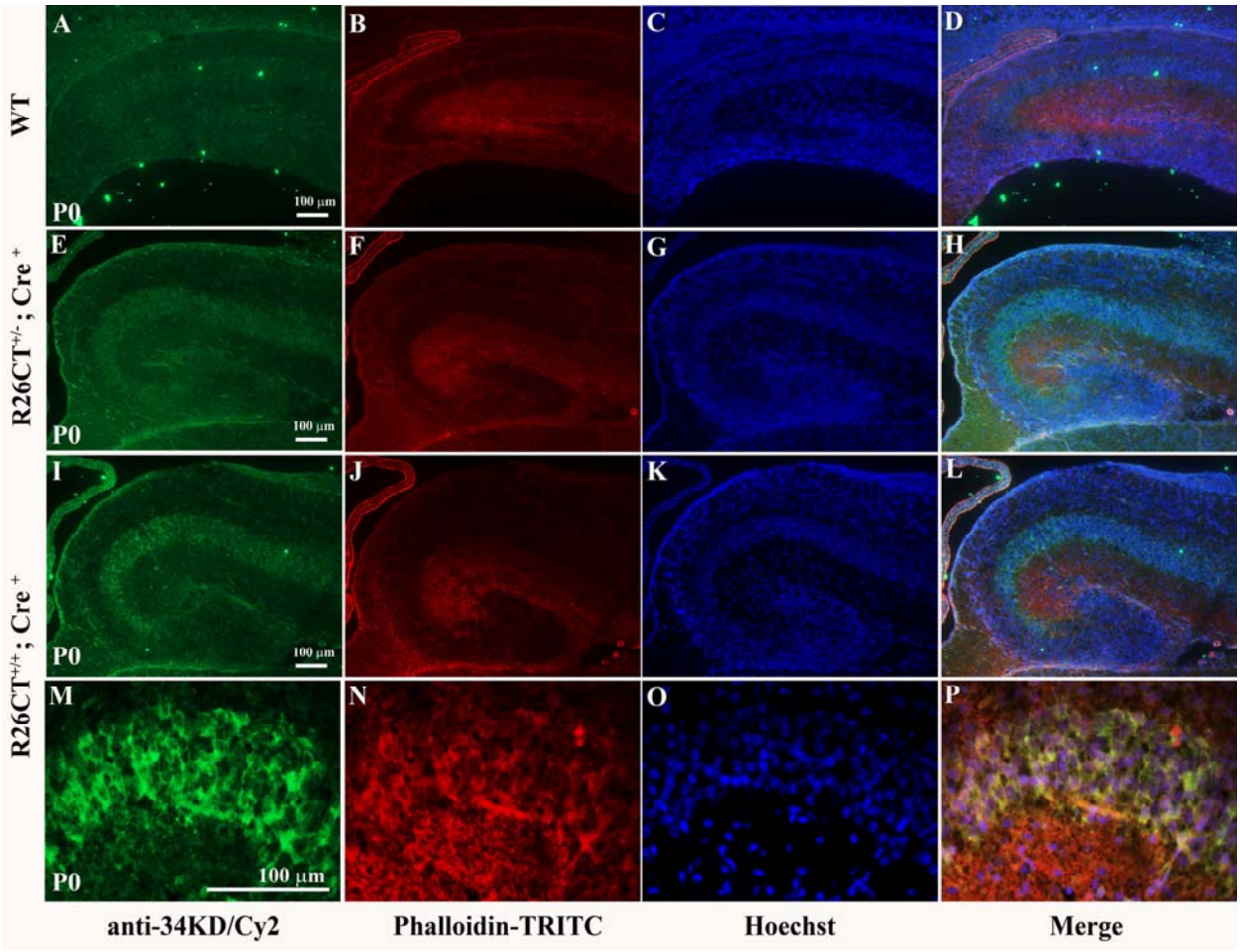
WT
R26CT+/-; Cre+
R26CT+/+; Cre+
A
B
C
D
E
F
G
H
I
J
K
L
M
N
O
P
P0
100 μm
anti-34KD/Cy2
Phalloidin-TRITC
Hoechst
Merge

Figure 3.6. Histological analysis of adult brain at 6 month.

Serial sagittal sections of brains from wild type and homozygous transgenic mice were analyzed by hematoxylin and eosin (H&E) staining. (A-L) No difference of pyramidal cell layer in the hippocampus (CA1, CA2, and CA3) between wild type (A-D), $R26CT^{+/+}$ (E-H), and $R26CT^{+/+}$;Cre^{+} (I-L) transgenic mice at 6 month of age. (M-O) Higher magnification of CA3 region of hippocampus. The rod-shaped eosinophilic inclusions were found in the vicinity of pyramidal cells of hippocampus in homozygous double transgenic mice. Arrow head indicates Hirano bodies. Scale bar: 200 μm (A, E, and I); 100 μm (B, C, D, F, G, H, J, K, and L); 20 μm (M, N, and O).

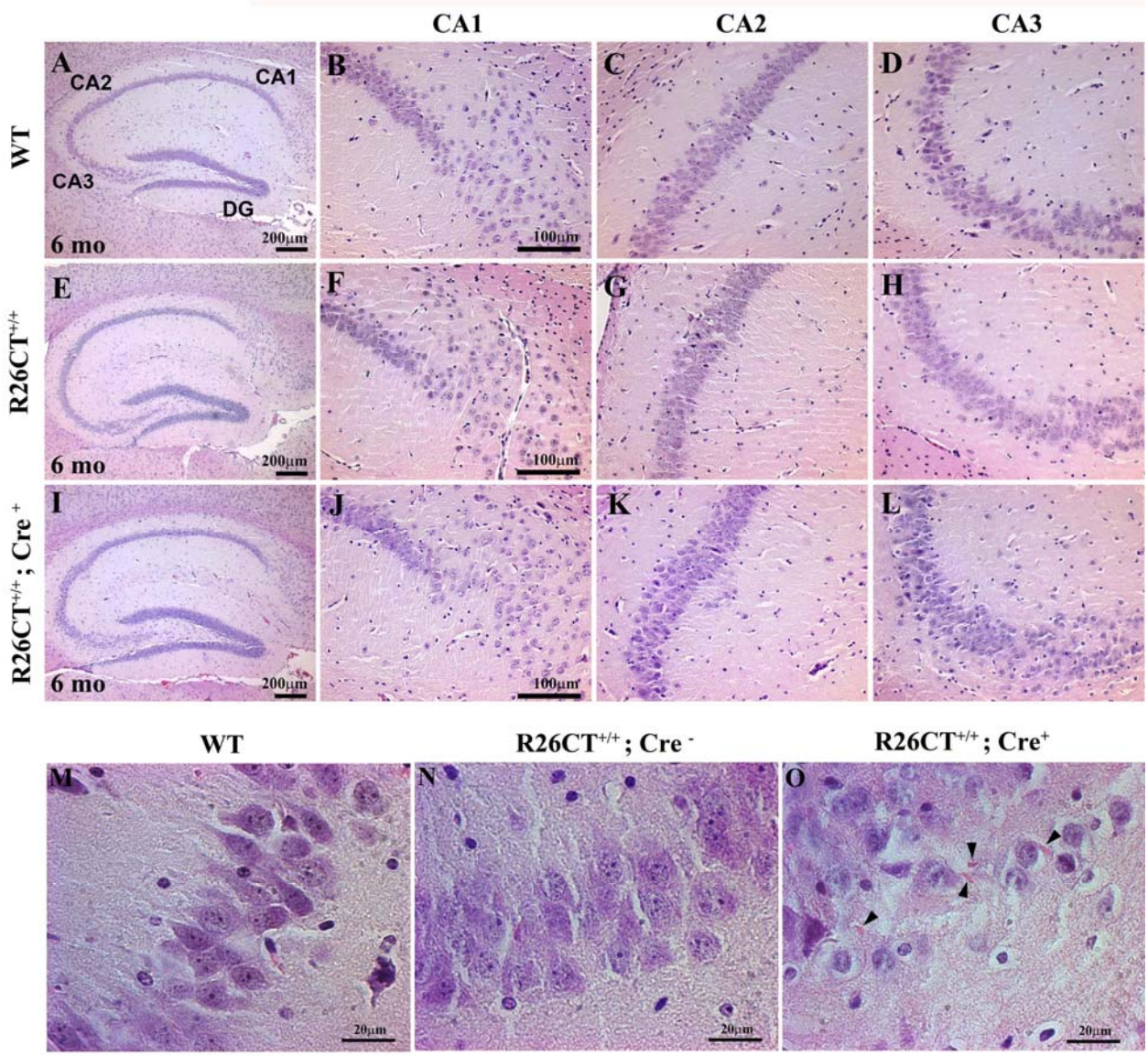
CA1
CA2
CA3
WT
R26CT+/+
R26CT+/+ ; Cre +
A
CA2
CA1
CA3
DG
6 mo
200µm
B
100µm
C
D
E
6 mo
200µm
F
100µm
G
H
I
6 mo
200µm
J
100µm
K
L
WT
R26CT+/+ ; Cre -
R26CT+/+ ; Cre+
M
20µm
N
20µm
O
20µm

Figure 3.7. Paracrystalline structure of mouse model Hirano bodies.

Hemisphere brain was dissected by separating hippocampus from cortex and thalamus. (A, B) Transmission electron microscope images of the electron dense region in CT-GFP stable H4 human neuroglioma cells show the composition, filamentous organization, and cross-hatched appearance of the inclusions. (C-H) TEM images of hippocampus in homozygous double transgenic mice at 6 month reveal model Hirano bodies with characteristic structure and periodicity. (I) The filamentous inclusions are enclosed by myelin sheath (left). (J) Mouse model Hirano bodies show paracrystalline structure which is similar to the ultrastructural definition of Hirano bodies reported in the human hippocampus. Scale bars: 500 nm (A, C, E, and G), 200 nm (B, D, F, and H), 50 nm (I) and 20 nm (J). White square box marks a filamentous array that is magnified in the inset (B, D, F and H).

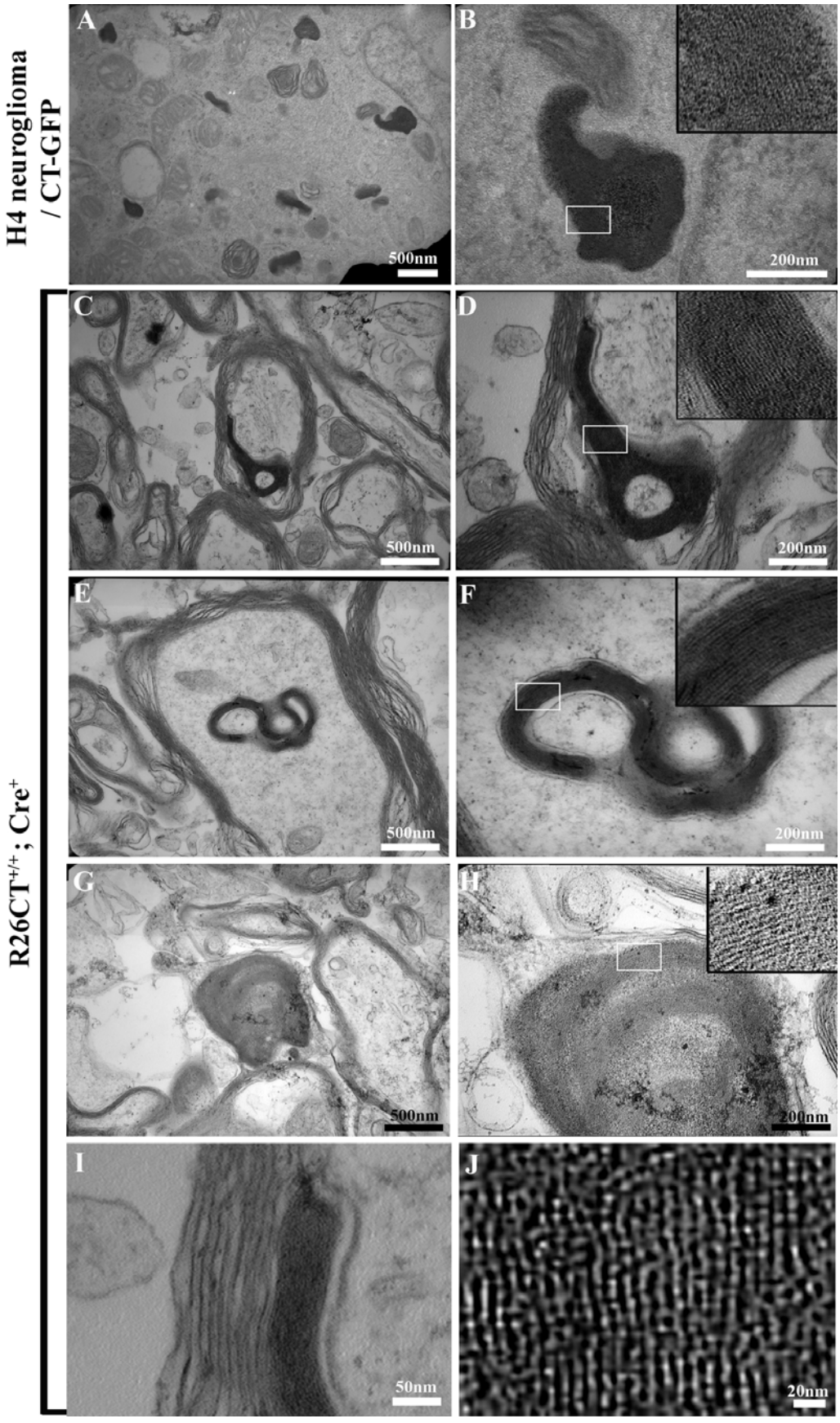
H4 neuroglioma / CT-GFP
R26CT+/+ ; Cre+
A
500nm
B
200nm
C
500nm
D
200nm
E
500nm
F
200nm
G
500nm
H
200nm
I
50nm
J
20nm

Figure 3.8. LTP in hippocampus of mouse model of Hirano bodies

Summary plot of normalized fEPSP slope measurements evoked and recorded in the stratum radiatum layer of the CA1 region. Field EPSP (fEPSP) responses were monitored in s. radiatum layer of the CA1 region and LTP was evoked with HFS using 3 x 100 Hz/1 s trains administered at 20 s intertrain intervals. Closed squares show responses from control slices (homozygous $R26CT^{+/+}$); open squares depict responses from transgenic slices (homozygous $R26CT^{+/+}$; $Thy1\text{-}Cre^{+}$). For a control set of slices (homozygous $R26CT^{+/+}$), the fEPSP slope was increased 65 ± 17% (n = 8 slices, 4 animals) 30 min following LTP induction and 37 ± 15% (n = 8, 4) 180 min following LTP induction. In a set of slices taken from transgenic mice (homozygous $R26CT^{+/+};Cre^{+}$**)**, the fEPSP slope was increased 37 ± 4% (n = 8, 4) 30 min following LTP induction and 50 ± 11% (n = 8, 4) 180 min following LTP induction. Error bars are the mean ± SEM. At both time points, the differences were not significantly different.

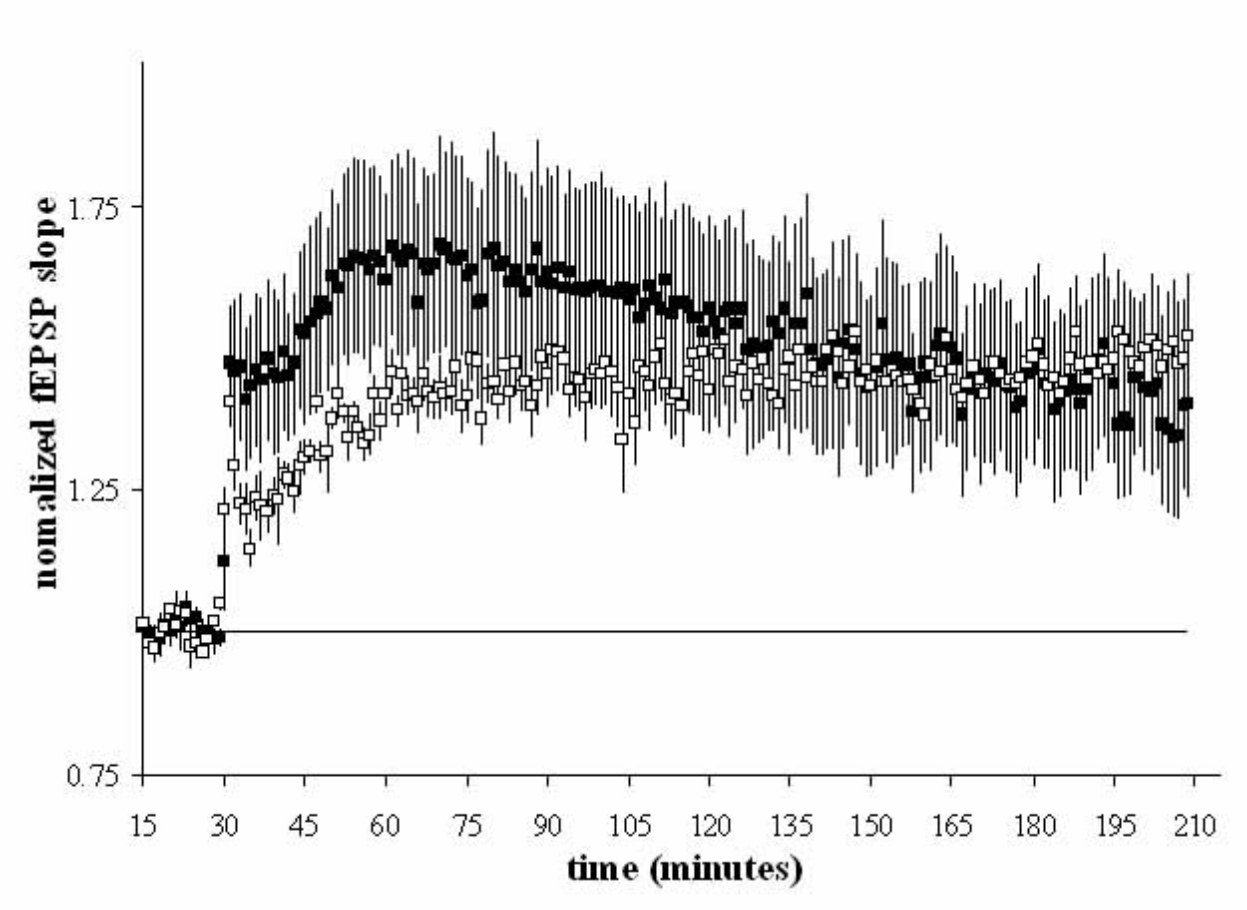
normalized fEPSP slope
1.75
1.25
0.75
15
30
45
60
75
90
105
120
135
150
165
180
195
210
time (minutes)

Chapter 4

Conclusion

Many reports suggest that neurodegenerative disorders result from mutations of genes related with neurodegerative disease and accumulation of the affected gene product which lead to progressive central nerve system disease (McMurray, 2000; Ross and Poirier, 2004; Skovronsky et al., 2006). Although the mechanism of amyloid accumulation is not clear, amyloid leads to neuronal death and dysfunction. In addition, many reports suggested that brain amyloidosis is related mechanically to impairments in axonal transport (Roy et al., 2005), inhibition of proteosomal activity (Tanaka et al., 2001), increased level of oxidative stress (Behl et al., 1994), and apoptosis (Nakagawa et al., 2000). There are three common amyloidgenic proteins: Aβ, tau, and α-synuclein. First, the most common form of dementia is Alzheimer's disease (AD) which is caused by mutations associated with amyloid precursor protein (APP), and the presenilins (Campsall et al., 2002; Campsall et al.). The extracellular senile plaques are generated by a deposition in the human brain of fibrils of the beta-amyloid peptide (Aβ), a fragment derived from the proteolytic processing of APP. The intracellular tau protein is the major component of paired helical filaments (PHFs), which form a compact filamentous network described as neurofibrillary tangles (NFTs) leading to massive loss of neurons and synapses (Maccioni et al.,

2001; Ross and Poirier, 2004; Muchowski and Wacker, 2005). Tau pathology is a prototypical intracellular amyloid and is seen in a variety of neurodegerative diseases such as Pick's disease and Fronto-temporal dementia with Parkinsonism. Second, tau mutations are caused by several distinctive mechanisms including alteration of tau splicing wnich impairs tau ability to promote microtubule assembly, and promotes tau aggregation (Hasegawa et al., 1998; Hong et al., 1998; D'Souza et al., 1999). Third, familial parkinson's disease (PD) is caused by mutation in the gene for α-synuclein and is characterized by the Lewy bodies composed of filamentous aggregates of the intracellular amyloid α-synuclein (Polymeropoulos et al., 1997; Spillantini et al., 1997). Abnormal accumulations of proteins related to microtubules and intermediate filaments are detected in a variety of neurodegerative diseases, but those of actin related proteins are rare. One of the actin cytosketon defects, actin/cofilin (AC) rods contains actin depolymerizing factor and cofilin. These rods are induced by oxidative stress and ATP depletion in hippocampal neurons which inhibit distal neurite functions (Minamide et al., 2000). Although actin and cofilin are constituents of both AC rods and Hirano bodies, AC rods lack the hallmark ultrastructural features of Hirano bodies and do not stain with phalloidin. Therefore, further work is needed to evaluate the possible relationship between AC rods and Hirano bodies.

Most research reported that Hirano bodies are actin rich aggregations that are associated with a variety of neurodegerative disorders. They are composed of several proteins such as actin,

actin associated proteins, MAPs, neurofilament, and c-terminal fragment of APP, but not microtubules. These inclusions have only been identified by ultrastructural and immunohistochemical studies. The physiological function and effect of Hirano bodies on neurodegerative diseases such as AD is not yet clear. In this study, my first goal was to understand the relationship of the C-terminal fragment of APP (AICD) and Hirano bodies. We used a mammalian cell model in which Hirano bodies are formed in human H4 neuroglioma cells. We found model Hirano bodies accumulate AICD consistent with a single previous report (Munoz et al., 1993). Recent studies have showed that AICD forms multimeric complexes with the nuclear adaptor protein Fe65, the histone acetyltransferase Tip60, or CP2/LSF/LBP1 transcription factor, and these complexes potently stimulate gene expression, induce apoptosis, and modulate level of ER calcium (Zambrano et al., 1998; Cao and Sudhof, 2001; Schneider et al., 2001; Kinoshita et al., 2002; Leissring et al., 2002; Kim et al., 2003). In addition, it has been reported that Hirano bodies are involved in transcriptional regulation and apoptosis. Cleavage of APP by caspase 3 facilitates the generation of Aβ peptide formation as well as the C-terminal fragments of APP including a cytotoxic peptide C31, resulting in generation of senile plaques and apoptotic death of neurons associated with Alzheimer's disease (Gervais et al., 1999; Lu et al., 2000). Since Fe65 interacts with a YENPTY binding motif of the C-terminal domain of APP, a variety of C-terminal fragments of APP released by proteolysis may form complexes with Fe65

and interact with Hirano bodies. In caspase 3 and dual luciferase reporter assays, model Hirano bodies down-regulate both AICD-dependent apoptosis and the transcriptional activity of the AICD/Fe65 complex. Therefore, we suggest that association of AICD with Hirano bodies in cells impedes its function in promoting apoptosis and modulating transcription.

In order to study why the C-terminal fragment of APP is accumulated in Hirano bodies, and what are roles of Hirano bodies on the progression of AD, a mammalian cell culture system is severely restricted. Generally, transgenic mouse strategies have allowed researchers to produce mice that recapitulate some, if not all, features of neurodegenerative disorders. Transgenic animals are very useful tools in testing hypotheses to define some of the *in vivo* events occurring in diseases as well as testing novel therapeutic strategies (Price et al., 1998; Hock and Lamb, 2001). Therefore, we generated transgenic mouse model Hirano bodies using the Cre/loxP system to understand their phyological roles in the progression of neurodegerative diseases and aging. These transgenic mice develop inclusions that share many features of model Hirano bodies. Mammalian cultured cell model Hirano bodies are composed of multiple aggregates that are smaller than large structures (~2 μm) organized in a single ordered array in AD, implying that Hirano bodies might form by coalescence of small aggregates into a large ordered structure (Davis et al., 2008). In this study, mouse model Hirano bodies showed aggregation in the hippocampus at 6 month of age and are not detected before 6 month. Ultrastructurally, Hirano

bodies are partially enclosed within myelin sheath and contain the filament diameter of 6-8 nm and the center to center spacing of 10-12 nm consistent with reports in the literature (Gibson, 1978).

Many reports suggested that the aggregates of misfolded protein are composed of amyloid fibrils through association of intermediate structures such as oligomeric or globular form by a hypothetical several step pathway (Ellis and Pinheiro, 2002; Ross and Poirier, 2004; Muchowski and Wacker, 2005). It is known that intermediate structures that form early in the aggregation process are more toxic to the cells than either amyloid fibrils or aggregates (Bucciantini et al., 2002; Walsh et al., 2002; Arrasate et al., 2004). Recently, we reported a variety of cultured cell models for formation of Hirano bodies, and also found that model Hirano bodies are non toxic to the cells and cells expressing Hirano bodies grow normally (Davis et al., 2008). I found that cells with model Hirano bodies are more viable compared to wild type when transiently transfected with AICD. Therefore, this finding suggests that Hirano bodies are not an intermediate form in terms of the general aggregation pathway mentioned above. Furthermore, Hirano bodies might be formed to protect cells from some conditions such as oxidative stress or energy depletion. This hypothesis may explain why Hirano bodies are not cytotoxic inclusions. Further, the basal level of caspase-3 activity in the brain may be decreased in mouse model of Hirano bodies as compared to wild type mouse since Hirano bodies associate with AICD in the cytoplasm

preventing its translocation to the nucleus and association with other proteins and factors such as Fe65, Tip60 and CP2/LSF/LBP1. Neuronal cell death is controlled by the activity of signaling pathways such as caspase-3 family, and proteins with a cross talk between various organelles such as mitochondria and endoplasmic reticulum. In order to test if Hirano bodies decrease the basal level of caspase-3 activity in a mouse model of Hirano bodies, the glutamate receptor analogue kainic acid (KA) could be added to hippocampal slices or neurons to induce seizures and excitotoxic cell death leading to cell body and dentritic swelling as well as to increases in intracellular calcium in the brain (Virgili et al., 1997; Puig and Ferrer, 2002; Savaskan et al., 2003; Xiang et al., 2004; Sokka et al., 2007). Therefore, the level of caspase-3 activity in hippocampal slices of a mouse model of Hirano bodies can be compared to that of a control mouse, under basal conditions on following kainite induced excitotoxicity.

Mouse model of Hirano bodies is viable and fertile and no major phenotype has been detected at this time. In addition, LTP in mouse model of Hirano bodies shows a small but not significant difference in synaptic plasticity compared to control mice. These results suggest that Hirano bodies have no toxic effects to neurons in the brain. Additional studies are needed to confirm or modify this finding. In addition, mouse model Hirano bodies are co-localized with APP in the hippocampal neurons of the brain. This is consistent with my observations in H4 neuroglioma cells stably expressing CT-GFP protein. Some APP transgenic mice reveal Hirano

body-like structures in the dystrophic neurites over 8 month of age (Masliah et al., 1996; Wegiel et al., 2001; Boutajangout et al., 2004). Recent studies suggested that APP-C31, generated by cleavage of APP intracellular domain at Asp664, induces synaptic deficits and neuronal damage in a major pathway of Aß dependent toxicity that affects synaptic strength, inhibits long-term potentiation (LTP) and induce long-term depression (LTD) as well as alterations in synaptic structure (Galvan et al., 2006). Both activated caspase-3 and APP-C31 are increased in an early stage of AD leading to synapse loss, dentate gyral atrophy, astrogliosis, and memory impairments (Zhao et al., 2003; Galvan et al., 2006; Banwait et al., 2008). In addition, the J20 mouse expressing human APP with the Swedish (K670N/M671L) and Indiana (V717F) FAD mutation have well characterized elevation of Abeta, progressive deposition of plaque, abnormal spatial learning, and synaptic dysfunction (Hsia et al., 1999; Mucke et al., 2000; Galvan et al., 2006; Saganich et al., 2006). Since C31 may play a major role in toxicity in AD, it will be informative to determine whether Hirano bodies can also sequester C31 and inhibit its harmful biological effects as predicted from the results of our studies with AICD. In addition, if we could generate APP;R26CT$^{+/+}$;Cre^{+} transgenic mice by crossing Hirano body model mice with AD model mice, we will be able to investigate the physiological roles of Hirano bodies on the progression of AD by measuring the levels of Aβ, deposition of senile plaques, and the density of pyramidal cell layers of hippocampus. Therefore, this study provides a foundation for investigation of the

physiological effects of Hirano bodies in the progression of AD and aging. First, one could determine whether the development of Alzheimer's disease is either promoted, impeded, or unaffected by Hirano bodies. Second, one could reveal whether selective death of specific types of neurons in AD may be either promoted or possibly prevented by Hirano bodies. Third, results showing that Hirano bodies promote or protect cells during the progression of AD would strongly support in development of drugs that affect formation of Hirano bodies as alternative targets for treatment of AD in the future.

References

Arrasate, M., S. Mitra, E. S. Schweitzer, M. R. Segal and S. Finkbeiner (2004). Inclusion body formation reduces levels of mutant huntingtin and the risk of neuronal death. Nature 431(7010): 805-10.

Banwait, S., V. Galvan, J. Zhang, O. F. Gorostiza, M. Ataie, W. Huang, D. Crippen, E. H. Koo and D. E. Bredesen (2008). C-terminal cleavage of the amyloid-beta protein precursor at Asp664: a switch associated with Alzheimer's disease. J Alzheimers Dis 13(1): 1-16.

Behl, C., J. B. Davis, R. Lesley and D. Schubert (1994). Hydrogen peroxide mediates amyloid beta protein toxicity. Cell 77(6): 817-27.

Boutajangout, A., M. Authelet, V. Blanchard, N. Touchet, G. Tremp, L. Pradier and J. P. Brion (2004). Characterisation of cytoskeletal abnormalities in mice transgenic for wild-type human tau and familial Alzheimer's disease mutants of APP and presenilin-1. Neurobiol Dis 15(1): 47-60.

Bucciantini, M., E. Giannoni, F. Chiti, F. Baroni, L. Formigli, J. Zurdo, N. Taddei, G. Ramponi, C. M. Dobson and M. Stefani (2002). Inherent toxicity of aggregates implies a common mechanism for protein misfolding diseases. Nature 416(6880): 507-11.

Campsall, K. D., C. J. Mazerolle, Y. De Repentingy, R. Kothary and V. A. Wallace (2002). Characterization of transgene expression and Cre recombinase activity in a panel of Thy-1 promoter-Cre transgenic mice. Dev Dyn 224(2): 135-43.

Campsall, K. D., C. J. Mazerolle, Y. De Repentingy, R. Kothary and V. A. Wallace (2002). Characterization of transgene expression and Cre recombinase activity in a panel of Thy-1 promoter-Cre transgenic mice. Dev. Dyn. 224(2): 135-43.

Cao, X. and T. C. Sudhof (2001). A transcriptionally [correction of transcriptively] active complex of APP with Fe65 and histone acetyltransferase Tip60. Science 293(5527): 115-20.

D'Souza, I., P. Poorkaj, M. Hong, D. Nochlin, V. M. Lee, T. D. Bird and G. D. Schellenberg (1999). Missense and silent tau gene mutations cause frontotemporal dementia with parkinsonism-chromosome 17 type, by affecting multiple alternative RNA splicing regulatory elements. Proc Natl Acad Sci U S A 96(10): 5598-603.

Davis, R. C., R. Furukawa and M. Fechheimer (2008). A cell culture model for investigation of Hirano bodies. Acta Neuropathol 115(2): 205-17.

Ellis, R. J. and T. J. Pinheiro (2002). Medicine: danger--misfolding proteins. Nature 416(6880): 483-4.

Galvan, V., O. F. Gorostiza, S. Banwait, M. Ataie, A. V. Logvinova, S. Sitaraman, E. Carlson, S. A. Sagi, N. Chevallier, K. Jin, D. A. Greenberg and D. E. Bredesen (2006). Reversal of Alzheimer's-like pathology and behavior in human APP transgenic mice by mutation of Asp664. Proc. Natl. Acad. Sci. U.S.A. 103(18): 7130-5.

Gervais, F. G., D. Xu, G. S. Robertson, J. P. Vaillancourt, Y. Zhu, J. Huang, A. LeBlanc, D. Smith, M. Rigby, M. S. Shearman, E. E. Clarke, H. Zheng, L. H. Van Der Ploeg, S. C. Ruffolo, N. A. Thornberry, S. Xanthoudakis, R. J. Zamboni, S. Roy and D. W. Nicholson (1999). Involvement of caspases in proteolytic cleavage of Alzheimer's amyloid-beta precursor protein and amyloidogenic A beta peptide formation. Cell 97(3): 395-406.

Gibson, P. H. (1978). Light and electron microscopic observations on the relationship between Hirano bodies, neuron and glial perikarya in the human hippocampus. Acta Neuropathol 42(3): 165-71.

Hasegawa, M., M. J. Smith and M. Goedert (1998). Tau proteins with FTDP-17 mutations have a reduced ability to promote microtubule assembly. FEBS Lett 437(3): 207-10.

Hock, B. J., Jr. and B. T. Lamb (2001). Transgenic mouse models of Alzheimer's disease. Trends Genet 17(10): S7-12.

Hong, M., V. Zhukareva, V. Vogelsberg-Ragaglia, Z. Wszolek, L. Reed, B. I. Miller, D. H. Geschwind, T. D. Bird, D. McKeel, A. Goate, J. C. Morris, K. C. Wilhelmsen, G. D. Schellenberg, J. Q. Trojanowski and V. M. Lee (1998). Mutation-specific functional impairments in distinct tau isoforms of hereditary FTDP-17. Science 282(5395): 1914-7.

Hsia, A. Y., E. Masliah, L. McConlogue, G. Q. Yu, G. Tatsuno, K. Hu, D. Kholodenko, R. C. Malenka, R. A. Nicoll and L. Mucke (1999). Plaque-independent disruption of neural

circuits in Alzheimer's disease mouse models. Proc Natl Acad Sci U S A 96(6): 3228-33.

Kim, H. S., E. M. Kim, J. P. Lee, C. H. Park, S. Kim, J. H. Seo, K. A. Chang, E. Yu, S. J. Jeong, Y. H. Chong and Y. H. Suh (2003). C-terminal fragments of amyloid precursor protein exert neurotoxicity by inducing glycogen synthase kinase-3beta expression. FASEB J. 17(13): 1951-3.

Kinoshita, A., C. M. Whelan, O. Berezovska and B. T. Hyman (2002). The gamma secretase-generated carboxyl-terminal domain of the amyloid precursor protein induces apoptosis via Tip60 in H4 cells. J. Biol. Chem. 277(32): 28530-6.

Leissring, M. A., M. P. Murphy, T. R. Mead, Y. Akbari, M. C. Sugarman, M. Jannatipour, B. Anliker, U. Muller, P. Saftig, B. De Strooper, M. S. Wolfe, T. E. Golde and F. M. LaFerla (2002). A physiologic signaling role for the gamma -secretase-derived intracellular fragment of APP. Proc Natl Acad Sci U S A 99(7): 4697-702.

Lu, D. C., S. Rabizadeh, S. Chandra, R. F. Shayya, L. M. Ellerby, X. Ye, G. S. Salvesen, E. H. Koo and D. E. Bredesen (2000). A second cytotoxic proteolytic peptide derived from amyloid beta-protein precursor. Nat Med 6(4): 397-404.

Maccioni, R. B., J. P. Munoz and L. Barbeito (2001). The molecular bases of Alzheimer's disease and other neurodegenerative disorders. Arch. Med. Res. 32(5): 367-81.

Masliah, E., A. Sisk, M. Mallory, L. Mucke, D. Schenk and D. Games (1996). Comparison of neurodegenerative pathology in transgenic mice overexpressing V717F beta-amyloid precursor protein and Alzheimer's disease. J Neurosci 16(18): 5795-811.

McMurray, C. T. (2000). Neurodegeneration: diseases of the cytoskeleton? Cell Death Differ 7(10): 861-5.

Minamide, L. S., A. M. Striegl, J. A. Boyle, P. J. Meberg and J. R. Bamburg (2000). Neurodegenerative stimuli induce persistent ADF/cofilin-actin rods that disrupt distal neurite function. Nat. Cell Biol. 2(9): 628-36.

Muchowski, P. J. and J. L. Wacker (2005). Modulation of neurodegeneration by molecular chaperones. Nat Rev Neurosci 6(1): 11-22.

Mucke, L., E. Masliah, G. Q. Yu, M. Mallory, E. M. Rockenstein, G. Tatsuno, K. Hu, D. Kholodenko, K. Johnson-Wood and L. McConlogue (2000). High-level neuronal expression of abeta 1-42 in wild-type human amyloid protein precursor transgenic mice: synaptotoxicity without plaque formation. J Neurosci 20(11): 4050-8.

Munoz, D. G., D. Wang and B. D. Greenberg (1993). Hirano bodies accumulate C-terminal sequences of beta-amyloid precursor protein (beta-APP) epitopes. J. Neuropathol. Exp. Neurol. 52(1): 14-21.

Nakagawa, T., H. Zhu, N. Morishima, E. Li, J. Xu, B. A. Yankner and J. Yuan (2000). Caspase-12 mediates endoplasmic-reticulum-specific apoptosis and cytotoxicity by amyloid-beta.

Nature 403(6765): 98-103.

Polymeropoulos, M. H., C. Lavedan, E. Leroy, S. E. Ide, A. Dehejia, A. Dutra, B. Pike, H. Root, J. Rubenstein, R. Boyer, E. S. Stenroos, S. Chandrasekharappa, A. Athanassiadou, T. Papapetropoulos, W. G. Johnson, A. M. Lazzarini, R. C. Duvoisin, G. Di Iorio, L. I. Golbe and R. L. Nussbaum (1997). Mutation in the alpha-synuclein gene identified in families with Parkinson's disease. Science 276(5321): 2045-7.

Price, D. L., R. E. Tanzi, D. R. Borchelt and S. S. Sisodia (1998). Alzheimer's disease: genetic studies and transgenic models. Annu Rev Genet 32: 461-93.

Puig, B. and I. Ferrer (2002). Caspase-3-associated apoptotic cell death in excitotoxic necrosis of the entorhinal cortex following intraperitoneal injection of kainic acid in the rat. Neurosci Lett 321(3): 182-6.

Ross, C. A. and M. A. Poirier (2004). Protein aggregation and neurodegenerative disease. Nat Med 10 Suppl: S10-7.

Roy, S., B. Zhang, V. M. Lee and J. Q. Trojanowski (2005). Axonal transport defects: a common theme in neurodegenerative diseases. Acta Neuropathol 109(1): 5-13.

Saganich, M. J., B. E. Schroeder, V. Galvan, D. E. Bredesen, E. H. Koo and S. F. Heinemann (2006). Deficits in synaptic transmission and learning in amyloid precursor protein (APP) transgenic mice require C-terminal cleavage of APP. J. Neurosci. 26(52): 13428-36.

Savaskan, N. E., A. U. Brauer, M. Kuhbacher, I. Y. Eyupoglu, A. Kyriakopoulos, O. Ninnemann, D. Behne and R. Nitsch (2003). Selenium deficiency increases susceptibility to glutamate-induced excitotoxicity. Faseb J 17(1): 112-4.

Schneider, I., D. Reverse, I. Dewachter, L. Ris, N. Caluwaerts, C. Kuiperi, M. Gilis, H. Geerts, H. Kretzschmar, E. Godaux, D. Moechars, F. Van Leuven and J. Herms (2001). Mutant presenilins disturb neuronal calcium homeostasis in the brain of transgenic mice, decreasing the threshold for excitotoxicity and facilitating long-term potentiation. J Biol Chem 276(15): 11539-44.

Skovronsky, D. M., V. M. Lee and J. Q. Trojanowski (2006). Neurodegenerative diseases: new concepts of pathogenesis and their therapeutic implications. Annu Rev Pathol 1: 151-70.

Sokka, A. L., N. Putkonen, G. Mudo, E. Pryazhnikov, S. Reijonen, L. Khiroug, N. Belluardo, D. Lindholm and L. Korhonen (2007). Endoplasmic reticulum stress inhibition protects against excitotoxic neuronal injury in the rat brain. J Neurosci 27(4): 901-8.

Spillantini, M. G., M. L. Schmidt, V. M. Lee, J. Q. Trojanowski, R. Jakes and M. Goedert (1997). Alpha-synuclein in Lewy bodies. Nature 388(6645): 839-40.

Tanaka, Y., S. Engelender, S. Igarashi, R. K. Rao, T. Wanner, R. E. Tanzi, A. Sawa, L. D. V, T. M. Dawson and C. A. Ross (2001). Inducible expression of mutant alpha-synuclein decreases proteasome activity and increases sensitivity to mitochondria-dependent apoptosis. Hum

Mol Genet 10(9): 919-26.

Virgili, M., M. Vandi and A. Contestabile (1997). Ischemic and excitotoxic damage to brain slices from normal and microencephalic rats. Neurosci Lett 233(1): 53-7.

Walsh, D. M., I. Klyubin, J. V. Fadeeva, W. K. Cullen, R. Anwyl, M. S. Wolfe, M. J. Rowan and D. J. Selkoe (2002). Naturally secreted oligomers of amyloid beta protein potently inhibit hippocampal long-term potentiation in vivo. Nature 416(6880): 535-9.

Wegiel, J., K. C. Wang, H. Imaki, R. Rubenstein, A. Wronska, M. Osuchowski, W. J. Lipinski, L. C. Walker and H. LeVine (2001). The role of microglial cells and astrocytes in fibrillar plaque evolution in transgenic APP(SW) mice. Neurobiol Aging 22(1): 49-61.

Xiang, Z., M. Yuan, G. W. Hassen, M. Gampel and P. J. Bergold (2004). Lactate induced excitotoxicity in hippocampal slice cultures. Exp Neurol 186(1): 70-7.

Zambrano, N., G. Minopoli, P. de Candia and T. Russo (1998). The Fe65 adaptor protein interacts through its PID1 domain with the transcription factor CP2/LSF/LBP1. J Biol Chem 273(32): 20128-33.

Zhao, M., J. Su, E. Head and C. W. Cotman (2003). Accumulation of caspase cleaved amyloid precursor protein represents an early neurodegenerative event in aging and in Alzheimer's disease. Neurobiol Dis 14(3): 391-403.